ANL-77-42

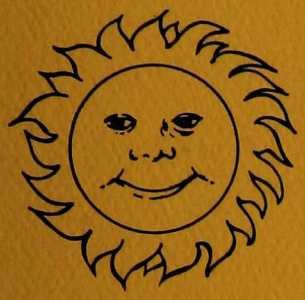

APPLICATION OF COMPOUND PARABOLIC CONCENTRATORS TO SOLAR PHOTOVOLTAIC CONVERSION

Final Report

by

R. L. Cole, A. J. Gorski, R. M. Graven,
W. R. McIntire, W. W. Schertz,
R. Winston, and S. Zwerdling

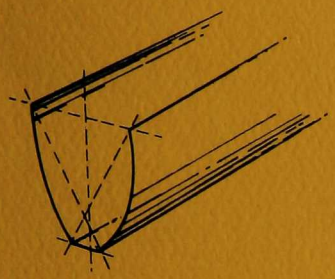

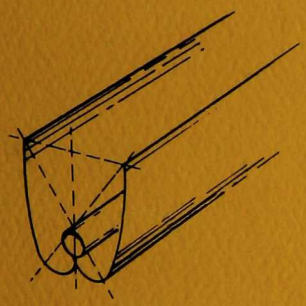

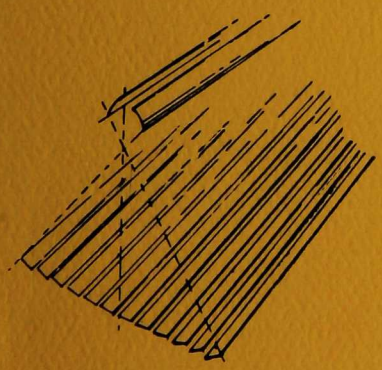

ARGONNE NATIONAL LABORATORY, ARGONNE, ILLINOIS
Prepared for the Division of Solar Energy
U.S. Energy Research and Development Administration
under Contract W-31-109-Eng-38

Printed in the United States of America
Available from
National Technical Information Service
U. S. Department of Commerce
5285 Port Royal Road
Springfield, Virginia 22161
Price: Printed Copy $5.50; Microfiche $3.00

Distribution Category:
Photovoltaic Conversion
(UC-63)

ANL-77-42

ARGONNE NATIONAL LABORATORY
9700 South Cass Avenue
Argonne, Illinois 60439

APPLICATION OF COMPOUND PARABOLIC CONCENTRATORS TO SOLAR PHOTOVOLTAIC CONVERSION

Final Report

by

R. L. Cole, A. J. Gorski, R. M. Graven,
W. R. McIntire, W. W. Schertz,
R. Winston, and S. Zwerdling

Solar Energy Group

Work Performed under Contract
to Sandia Laboratories

Contract Number 02-7918

February 1977

TABLE OF CONTENTS

TABLE OF CONTENTS (contd)

LIST OF FIGURES

LIST OF FIGURES (contd)

LIST OF TABLES

APPLICATION OF COMPOUND PARABOLIC CONCENTRATORS TO SOLAR PHOTOVOLTAIC CONVERSION

FINAL REPORT

February 1977

by

R. L. Cole, A. J. Gorski, R. M. Graven,
W. R. McIntire, W. W. Schertz, R. Winston, S. Zwerdling

EXECUTIVE SUMMARY

This project was an analytical and experimental study of the application of the Compound Parabolic Concentrator (CPC) and the Dielectric Compound Parabolic Concentrator (DCPC) to solar photovoltaic conversion. The objectives of the program included:

- Determination of the design requirements for using a CPC or DCPC for concentrating solar energy onto photovoltaic cells.
- Analyses of the design requirements imposed by the CPC or DCPC optical characteristics on the photovoltaic cells.
- Development of fabrication techniques suitable for making CPC or DCPC components in mass production.
- Design of a CPC panel and a DCPC panel that meet the essential requirements of JPL Specification 5-342-1.
- Construction and testing of a 1.2 m x 1.2 m (nominal) passively cooled panel incorporating the CPC.
- Construction and testing of a 1.2 m x 1.2 m (nominal) passively cooled panel incorporating the DCPC.
- Determination of the cost-effectiveness potential if panels of this type were mass produced.

These objectives were all met. The results of the first four above objectives were used in constructing the DCPC and CPC panels. Panels were delivered to Sandia on December 21, 1976 (DCPC), and on February 5, 1977 (CPC). The detailed results of this project are contained in this, the final report, "Application of Compound Parabolic Concentrators to Solar Photovoltaic Conversion."

The basic DCPC concentrator elements were injection-molded from acrylic (polymethylmethacrylate). These were bonded to silicon photovoltaic cells whose dimensions are 0.28 cm by 2.67 cm. The basic DCPC element is 4.45 cm high by 1.91 cm wide by 3.1 cm long. The complete DCPC panel contained 20 modules, each module consisting of 108 DCPC/cell units. Because the DCPC design uses the mechanism of Total-Internal-Reflection (TIR), no metallization is necessary on the concentrator elements.

A major design constraint imposed on both of these panels is that only passive cooling would be used. To avoid loss of conversion efficiency due to too high temperature of the solar cells, the cells were thermally coupled to an extended-surface heat sink. The complete DCPC panel, consisting of 20 separate modules, contained 2160 concentrator/cell units and weighed approximately 111 kg (244 lb).

The completed DCPC panel was tested in sunlight on December 13, 1976. The total insolation was 900 W/m^2, of which 818 W/m^2 was direct. The insolation within the acceptance angle of a DCPC unit was calculated to be 831 W/m^2; the measured peak output power of 114 W (4.85 A at 23.6 V) would scale up to 138 W for 1 kW/m^2 direct insolation. The panel fill factor is 0.74. The measured output power of the DCPC panel indicates a conversion efficiency of 10.7% of the light incident upon the acrylic module faces within the angular acceptance of the DCPC units. The large packing factor of 0.96 for the acrylic modules in the panel frame leads to a conversion efficiency of 10.3% over the total panel area, including the panel walls. An experimental measurement of the angular acceptance of the panel was also made; results show that 75% of the incident solar radiation is accepted over an angular range of 16°.

The basic CPC concentrator elements were injection-molded from acrylonitrile-butadiene-styrene copolymer (ABS). These CPC substrates were then treated with an undercoat polymer, evaporated aluminum, and a protective overcoat. A single CPC substrate is 5.1 cm high by 27.2 cm long. Two substrates--separated by 0.25 cm--form a reflective CPC trough. The basic design of the hollow (reflective) CPC panel is modular, similarly to the DCPC panel. Ten solar cells are positioned at the exit aperture of each CPC trough. Twelve rows of cells comprise one module; hence there are 120 cells/module or 1920 cells/panel (16 modules/panel). The cells are soldered to a

printed circuit sheet which provides alignment as well as electrical insulation from the aluminum extended-surface heat sink below. To protect the cells from the atmosphere, the cells as well as the substrates are potted in two-component RTV silicone rubber. Finally, an acrylic cover box is used to protect both the cells and the reflecting surfaces of the module. The completed CPC panel contains 16 modules and weighs approximately 76.5 kg (168.5 lb).

The completed CPC panel was tested in sunlight on January 31, 1977. The peak output power was 81 W (3.2 A at 25.6 V). This represents a conversion efficiency of 7.1% of the 844 W/m^2 within the acceptance angle of the panel, which is larger by a factor of 5.7 than the power output of cells having no concentration. The array efficiency could be increased by design modifications that would increase the packing factor. If the insolation within the acceptance angle is scaled up to 1 kW/m^2, the peak power scales up to 97 W. The hollow CPC panel has an efficiency of 7.1% over the panel area, but an efficiency of 9.6% over its active area. The packing factor of the panel could be increased by as much as 30% by design changes. Calculating the active area efficiency for a 0.96 packing factor would give a 9.25% panel efficiency. The angular acceptance of the CPC panel was also measured experimentally; the response curve is flat for approximately ±4° from the normal ($\geq$95% of peak) and has a full width at half maximum of approximately 14°.

The construction of these panels shows that the Compound Parabolic Concentrator concept offers several important advantages for a concentrator/photovoltaic system:

- Modern plastic molding techniques can be used to produce DCPC and CPC units at relatively low cost.
- Total Internal Reflection (used in the DCPC design) offers high light efficiency and simplicity.
- The elimination of metallization in a concentration system improves efficiency.
- For some terrestrial applications, the elimination of diurnal tracking of the sun (in both designs) is of considerable importance and should not be underestimated.

- Based on an efficiency model that has been confirmed by two prototype panels and on material and component cost data, photovoltaic CPC's can produce electricity at significantly lower cost than do flat photovoltaic arrays. The cost reductions are significant in comparison to the cost of a flat array even if the cost of silicon decreases by an order of magnitude.

Calculations show that the cost effectiveness of cone-type concentrators would be better to that of trough-type concentrators.

APPLICATION OF COMPOUND PARABOLIC CONCENTRATORS TO SOLAR PHOTOVOLTAIC CONVERSION

FINAL REPORT

February 1977

by

R. L. Cole, A. J. Gorski, R. M. Graven,
W. R. McIntire, W. W. Schertz, R. Winston

ABSTRACT

This report presents the final results of an analytical and experimental study of the application of nonimaging concentrators to solar photovoltaic conversion. Two versions of the Compound Parabolic Concentrator (CPC) were considered, the Dielectric Compound Parabolic Concentrator (DCPC) in which the concentrator is filled with a dielectric material that satisfies requirements for Total Internal Reflection (TIR), and a conventional CPC in which metallic reflection is used for the mirror surfaces.

Two working prototype panels were constructed and tested during the course of the program. The first was a 1.22 m by 1.22 m DCPC panel that requires only ten adjustments/year, has a panel utilization factor (packing factor) of 96%, and delivered the equivalent of 138 W (peak) under 1 kW/m^2 direct insolation. The net energy conversion efficiency was 10.3% over the entire panel area. The second panel was a conventional CPC panel measuring 1.22 m by 1.22 m. This panel requires thirty-six adjustments per year, and delivers the equivalent of 97 W when under 1 kW/m^2 direct insolation.

The results of a cost-effectiveness analysis of the concept of using nonimaging concentrators for photovoltaic conversion are also presented. The concentrator panels show a decided savings in comparison to the cost of flat plate photovoltaic panels, both at present-day silicon costs ($\$2000/m^2$) and projected lower silicon costs ($\$200/m^2$). At a silicon cost of $\$200/m^2$, a two-dimensional (cone) version of the collector has the potential for achieving from \$0.60-2.00 per average watt (about \$0.15-0.50 per peak watt) while requiring only crude (±4.5°) tracking.

I. INTRODUCTION

A. Background

The Compound Parabolic Concentrator (CPC) has been under development at Argonne National Laboratory since July 1974. The initial applications considered for the collector were for photothermal conversion of solar energy. The family of nonimaging concentrators (which includes the CPC) has demonstrated unique advantages for solar energy collection, since these collectors have the widest possible acceptance angle for any factor of concentration. This feature allows stationary collectors or collectors that require only periodic adjustments to achieve much better performance than flat plate collectors.[1-3]

In 1975, ANL subcontracted two studies of the use of the CPC concept for photovoltaic energy conversion. The first, awarded to Mobil-Tyco, analyzed the potential of CPC's as primary concentrators, with photovoltaic cells as the receiver.[4] The report concluded that with concentration ratios of 6-10, the concept offered good potential for a substantial reduction in cost for direct energy conversion. The second, a Spectrolab study, was of the use of a nonimaging concentrator as a second stage to a primary, focusing system.[5] The study showed significant advantages for a two-stage system including: flux smoothing of the radiation, a larger acceptance angle that reduces the overall accuracy requirements for the primary reflector, and/or a greater concentration ratio.

In October/November 1975, the concept of the Dielectric Compound Parabolic Concentrator (DCPC) was conceived and developed.[6] This study showed that a broadened acceptance angle could be achieved by filling the collector shape with a clear material that has an index of refraction greater than 1.4 and that if the concentrator wall shape is appropriately designed for the chosen value of index of refraction and desired acceptance characteristics, total internal reflection will occur at the medium-air interface.

A proposal to develop the CPC and DCPC concepts for photovoltaic energy conversion was submitted to the United States Energy Research and Development Administration (ERDA) in December 1975, and the program was initiated in February 1976, as a contract monitored by Sandia Laboratories.

The CPC (and DCPC) concept allows the construction of a concentrating photovoltaic panel that physically resembles a flat plate collector but uses less silicon. It has an advantage over other concentrating systems in that a nontracking flat plate collector can be replaced with a nontracking concentrating collector (which, however, requires periodic tilt adjustments). The performance can, therefore, be directly compared with the flat panel systems being developed by ERDA under the Low Cost Silicon Solar Array Project. These array specifications have been set to obtain nominal 1.2 m by 1.2 m panels for evaluation and demonstration.

B. Program Scope

This project included the design and analysis of the CPC and DCPC concept as applied to photovoltaic systems and the construction of two full-scale (1.2 m by 1.2 m) panels, one using the DCPC and the other using the CPC. A cost-effectiveness analysis was also performed to determine the potential of nonimaging concentrators for photovoltaic conversion.

C. Program Objectives

The objectives of the program included:

- Determination of the design requirements for using a CPC or DCPC for concentrating solar energy onto photovoltaic cells.
- Analysis of the design requirements imposed by the CPC or DCPC optical characteristics on the photovoltaic cells.
- Development of fabrication techniques suitable for making CPC or DCPC components in mass production.
- Design of a CPC and DCPC panel that meets the essential requirements of JPL Specification 5-342-1, including mechanical, electrical, and thermal integrity.
- Construction and testing of a 1.2 m x 1.2 m (nominal) passively cooled panel using the CPC.
- Construction and testing of a 1.2 m x 1.2 m (nominal) passively cooled panel using the DCPC.
- Determination of the cost-effectiveness potential if panels of this general type should be mass produced.

These objectives were all met, and the results are presented in Sections II, III, and IV of this report.

The DCPC panel was delivered to Sandia on December 21, 1976, for long-term testing and evaluation and the CPC panel was delivered on February 5, 1977.

During the course of the project, a technical paper was presented at the 12th IEEE Photovoltaic Specialists Conference in Baton Rouge, Louisiana describing the collector concept and the panel under consideration.[7]

II. DCPC PANEL

A. General Design Constraints

The design of the Dielectric Compound Parabolic Concentrator (DCPC) panel used the specifications outlined in JPL Document 5-342-1 for guidance.[8] This JPL specification outlined the requirements and objectives for the terrestrial silicon solar cell panels for a 130-kW procurement phase of the Large Scale Production Task. Since these specifications were specifically directed to nonconcentrating panels, variations of some of the design constraints were necessary.

The DCPC panel was designed to meet the JPL demonstration requirements for mounting into 1.2 m by 1.2 m subarrays, including a 2.54 cm border for handling. In addition, it was designed to meet the general packing requirements in regard to mechanical integrity, electrical integrity, and module interchangeability and replacement. The panel is also capable of withstanding the loads associated with normal handling and manipulation during field installation, operation, and repair. The panel is a rigid assembly with sufficient strength to withstand environmental loadings due to wind, rain, snow, and ice. Design loading values of ±2394 pascals (Pa) were assumed for these loads. The load is carried by the panel support structure, which consists of four aluminum (6061-T6) channels simply supported at the ends. Additional stiffness is provided by aluminum angles perpendicular to the channels. The support frame geometry and construction are described in greater detail below and can be seen in still greater detail by referring to the set of mechanical drawings in Appendix A.

To ensure the specifications' requirements for electrical integrity, redundant circuitry is used extensively. The DCPC panel consists of 20 modular subunits. Each such module contains 108 separate silicon solar cells wired in a series-parallel matrix for maximum redundancy. In addition, redundant outputs from each module are used to electrically couple modules to form the complete panel. In the DCPC panel, the outputs from each of the modules are routed to a common junction box in back of one of the aluminum channel units. This interconnection method allows the user the flexibility of wiring the modules in any manner necessary without removing them from the panel support structure. For example, the 20 modules could be wired in a

single series or parallel string, or in any combination thereof. The panel, as delivered, is arranged in four rows in series, each row containing five modules connected in parallel. The junction box also provides a convenient location for electrically checking the performance of each module in the panel. The flexibility of being able to change the operating voltage of the finished photovoltaic panel is not usually afforded by conventional panel designs.

The thermal characteristics of the panel are such as to minimize solar cell temperature to an extent consistent with minimizing panel cost per unit of power produced at the panel equilibrium temperature in a normal terrestrial thermal environment. The panel environment for thermal design was assumed to be 100 mW/cm^2, AM1 solar irradiance, and convective and radiant cooling from both front and rear module surfaces to 60°C still air.

B. Concentrators

The DCPC units that concentrate sunlight onto the solar cells have a trough geometry. They obey the optical relationship

$$C = n/\sin \theta$$

where C is the optical concentration ratio, n is the index of refraction of the medium in the collector, and θ is the angular acceptance (half angle). As stated above, each module of the panel consists of 108 separate solar cells so that 108 DCPC units are required per module. Because the DCPC design uses the mechanism of Total Internal Reflection (TIR), a necessary requirement is that the concentrator must be constructed from an optically clear material with a dielectric refractive index $n > 1$. For optimum performance, it is desirable to have $n > \sqrt{2.9}$ Two general classes of materials which could be used to fabricate DCPC units are glass and plastics.

Plastic materials have a number of advantages over glass. They are lower in fabrication cost, have higher impact resistance, are lower in weight, and may be fabricated in a greater variety of configurations. For a refractive type reflector such as the DCPC, the optical properties are of the utmost importance. As mentioned above, the design of the concentrator requires that the refractive index be greater than the square root of two for optimum performance. Acrylic has a value of 1.491, polystyrene 1.590, polycarbonate 1.586, and methyl methacrylate styrene copolymer (NAS) a value of 1.562. All

optical plastics degrade when exposed to ultraviolet radiation. Acrylic (polymethylmethacrylate), however, has the highest resistance to degradation. For a solar concentrator, this is important. Other candidate plastic materials can be stabilized for ultraviolet resistance, but long-lifetime data on the optical properties of these materials in the solar spectrum are not as well documented as for acrylic; therefore, acrylic was chosen as the DCPC material. It is more transparent than most glasses for the spectrum corresponding to a silicon solar cell response, withstands UV, has a refractive index of 1.491, and has good mechanical stability. In addition, the coating techniques used on optical glass elements can be applied to acrylic plastic elements. These include an anti-abrasive coating and antireflective and antistatic coatings. Another important feature of plastic DCPC units is that they can be mass-fabricated by injection-molding, casting, or pressing techniques.

For the 108 single DCPC units that compose a modular unit, three levels of fabrication were considered. The first is to mold all 108 units together in one piece. The second is to mold a number of DCPC units together to form a strip of concentrators and then to bond these together to form the complete module face. The third method is to mold each DCPC unit separately and then to bond all 108 together to form the array. Of these three methods, the first would seem to be the most desirable for mass production. The second method was actually used to construct concentrator module faces. This was dictated by the methods available to mold the plastic DCPC units. Three methods of fabricating DCPC units were considered: casting, heat and pressure forming, and injection molding.

To investigate casting as a fabrication method, two commercial plastic casting companies were contacted. In general, these firms stated that plastic parts coming out of the mold would not be clear and that it would be necessary to polish each piece to obtain the desired optical surface. The surfaces of the concentrator, which are quite complex, do not lend themselves to belt or disk sanding or polishing. Some examples of polyester cast by ANL personnel were obtained; they were observed to yellow under solar UV radiation. At that time, this method did not appear to be promising. However, later samples of usable optically clear aromatic epoxy casting resins have been obtained. Polishing of these materials after they come out of the mold is not necessary. An example of such an epoxy is Stycast 126A (bisphenol-A based epoxy resin).

Another method explored was that of using heat and pressure to form DCPC units from a sheet of solid acrylic. The Arrem Plastic, Inc. Company of Addison, Illinois, contracted to do some preliminary studies of this fabrication method. A die mold to produce a 3 x 3 "V" trough array was designed and fabricated for these studies, as shown schematically in Fig. II-1. This mold was used by the Arrem Company, but the results were inconclusive. Due to the proprietary nature of some of the molding techniques used, supervision by ANL was not allowed. This method may have promise for forming large sheet arrays for small concentrators.

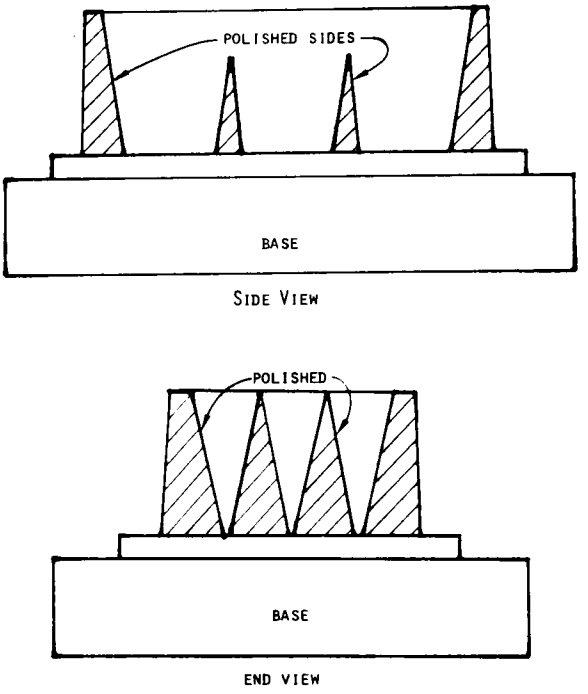

Fig. II-1. Pressure Forming Mold

The most promising method, which was the method used, was injection molding. To investigate this method, approximately 30 injection-molding companies were contacted. The first result of this search was a consensus of opinion that injection-molding of the complete module face (108 units) would be extremely difficult and that the mold costs would be of the order of $10,000 to $20,000. Molding of DCPC strips would be easier, and molding of a single DCPC should be no problem. The second result of this search is the finding that the plastic molding industry is generally reluctant to work on a research and development type project. The industry is, in general, geared to the mass production of thousands if not hundreds of thousands of identical

plastic items. Notable exceptions are the three plastic companies mentioned below. U.S. Precision Lens of Cincinnati, Ohio, is a plastic injection-molding company which specializes in the production of high-quality precision plastic optical lenses. This company was chosen as a backup source for the fabrication of DCPC strips. W. M. Plastics of Rolling Meadows, Illinois, contracted to machine a mold and to fabricate single DCPC units for evaluation. The mold for this single unit cavity cost approximately $2,000, and usable DCPC units were prepared by injection molding. The primary injection-molding effort was made by Plastic Tooling Aids Laboratory, Inc. (PTA) of Skokie, Illinois. PTA has had considerable experience in working with research and development organizations and has contributed significantly to the successful completion of this project.

A temporary injection cavity was made by PTA to fabricate a strip of nine DCPC units. After this mold was completed in Illinois, it was flown to their Boulder, Colorado, plant and used in a 75-oz. injection-molding machine. Examination of the first prototype strips revealed two major problems--sinks and warpage. The general configuration of the DCPC strip is shown in Fig. II-2. The injection-molding cycle consists of the injection of molten acrylic into the hot mold cavity, release of pressure, rapid cooldown, and ejection of the molded part. The cycle is then repeated. Typical cycle times are normally of the order of one to ten seconds. Due to the thickness of the acrylic DCPC strips, the parts after ejection actually had liquid, molten acrylic in their interiors after ejection from the mold. Internal solidification then caused the parabolic walls to sink in, resulting in severe optical distortions.

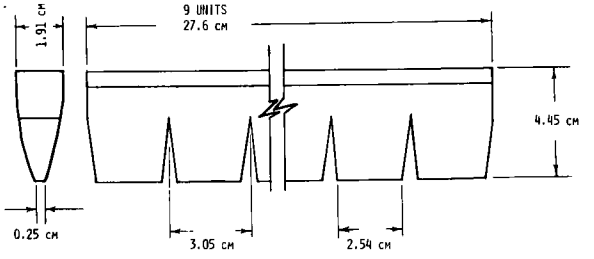

Fig. II-2. Injection Molded Plastic Strip
(Dielectric Compound Parabolic Concentrators)

The sink problem was solved by increasing the cycle time. The molten acrylic was maintained under pressure until cooldown, resulting in a cycle time of approximately 5 min. (In the plastics industry, this is an extremely long cycle time.) The DCPC strips produced in this way conformed so well to the contours of the mold that they could not be easily ejected.

To obtain conditions that gave molded parts with acceptable profiles and allowed ejection of the finished parts, a complete new mold was constructed. Following a molding cycle, this new mold actually split into two parts, forcing the plastic parts out. The DCPC strips produced by this mold were adequate and could be produced in large numbers if required. As a result of the experience described above, injection-molding of complete module faces is much closer to feasibility.

Due to the nonsymmetrical shape of the strips, a general warpage was observed in the strips, with the concave side warped in the direction of the exit apertures. The warping problem was solved by annealing the parts at 140°F for 24 hrs. This annealing operation would be necessary even in the absence of warpage, being required before any bonding operations are performed to prevent stress crazing.

Each DCPC strip contains nine single DCPC units, and twelve strips must be bonded together to form a complete module face. Two monomer-type cements were evaluated for this bonding operation, namely, Rohm and Haas PS-30 and PS-18. The cement PS-18 is a three-component system having the advantage that "spills" can be cleaned up with component "C." This cement system has two decided disadvantages: (1) if components are mixed in the wrong order, there is a potential explosive hazard and (2) it ends its pot life with the evolution of excessive heat and fumes. PS-30 is a two-component system with 15 to 20 min working time. The bonds obtained with PS-30 are extremely strong and clear. A DCPC module face bonded with PS-30 and consisting of 12 strips is a strong and durable structure and is shown in Fig. II-3.

C. Photovoltaic Cells

The design of photovoltaic cells for use with CPC's must take into consideration the nonuniform light intensity distribution across the exit aperture of the concentrator. The distribution depends upon the specific CPC shape, as well as the position of the sun, but in general one can describe it as shown in Fig. II-4. When the sun is at the acceptance angle, the intensity

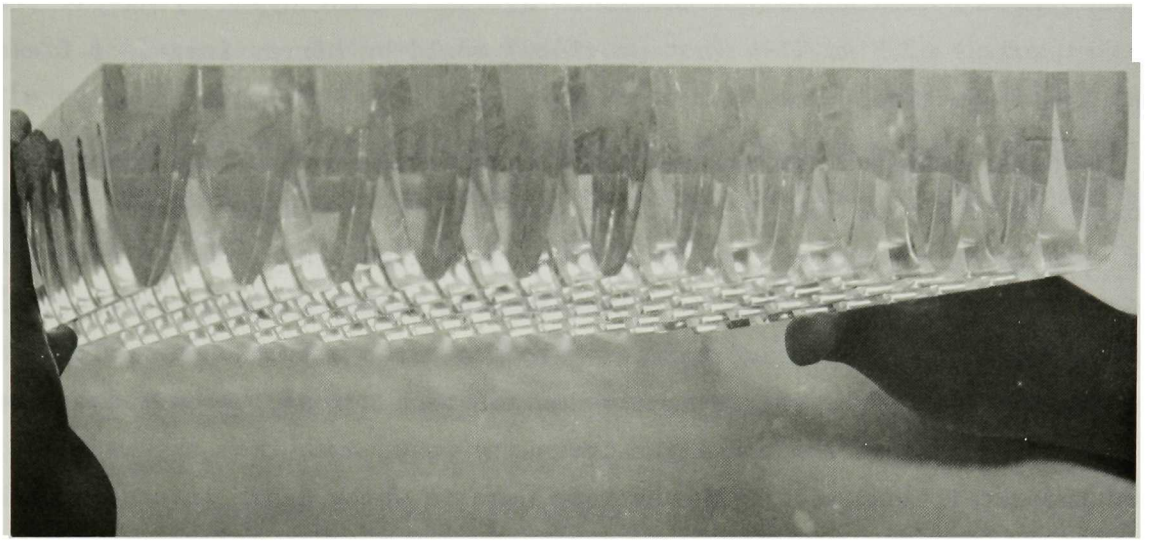

Fig. II-3. DCPC Module Face

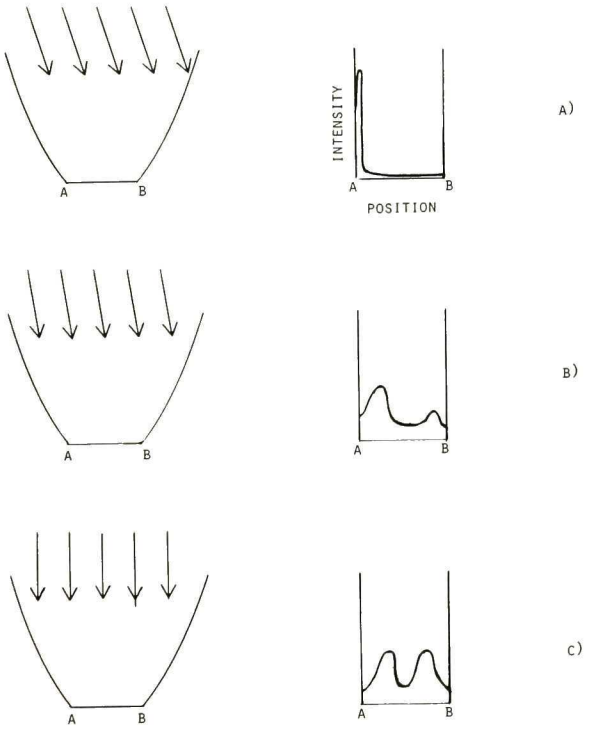

Fig. II-4.

Light Intensity Distribution in CPC Collectors

peaks at one edge of the exit aperture, as shown in A). Rays at angles closer to the optic axis of the CPC are concentrated into two broad bands of unequal intensities, as illustrated in B). With the rays parallel to the optic axis of the CPC, the bands are equal in intensity, and have moved toward (but not to the center of) the exit aperture. Case C) occurs whenever

the panel is oriented normal to the sun. Because of the symmetry of the CPC, frames D) and E) of Fig. II-4 (not provided) would be mirror images of frames B) and A), respectively.

The cells designed for the two photovoltaic panels take this light intensity distribution into account. Figure II-5 is a diagram of one of the cells. It is a long narrow cell with heavy metallization along the sides and at one end where the lead wire is soldered. The narrow shape is particularly suited to the CPC. All charge carriers are generated within about 0.13 cm of the metallization. From the intensity distribution across the exit aperture (Fig. II-4), one notes how the light intensity peaks away from the center toward the metallization. In the extreme case in which light intensity peaks at one edge, the charge carriers are still generated close to the metallization. Current is easily taken out of the cell and into the wires.

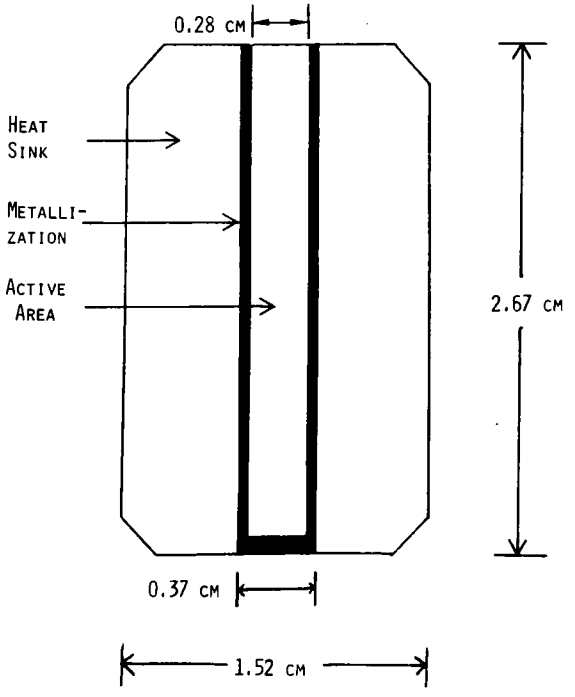

Fig. II-5.

Photovoltaic Cell on Heat Sink

About 26% of the silicon area is covered by metallization. However, the CPC does not concentrate light on the metallization along the sides. The DCPC does not even concentrate light onto the metallization strip at the end, but uses total internal reflection to concentrate light slightly in the east-west directions away from the metallization at the end. With the energy of "six suns" concentrated only on the cell's active area, the effect of

metallization drops to less than 6%, in comparison to the effect of metallization in a flat-plate photovoltaic panel (where it is ∿10-15%). In comparing CPC's to other concentrators, one should note that when cells are aligned properly with the CPC, no light is wasted on the metallization. This represents a gain of at least 15% in comparison with conventional concentrators which require cells with special metallization patterns.

The above general design considerations of photovoltaic cells for CPC use were formulated into a detailed set of specifications. These were then sent to six commercial cell manufacturers for competitive bids. The manufacturers were:

- Spectrolab, Sylmer, California
- Sensor Technology, Chatsworth, California
- M-7 International, Arlington Heights, Illinois
- Solarex, Rockville, Maryland
- Solar Power Corporation, Wakefield, Massachusetts
- OCLI, Santa Rosa, California

The general specifications that the cells were to meet were:

1. The diffused surface layer was to be n-type, and the base layer p-type.
2. The silicon photovoltaic cells were to have an area suitable for interfacing with a DCPC or CPC trough configuration. The nominal dimensions are 0.284 cm width, 2.570 cm length, and 0.0305 cm thickness.
3. Whether grid fingers were added to reduce series resistance loss was left as an option to the supplier.
4. The cell performance specification was to be at least 12% solar power conversion efficiency at 28°C when illuminated at 1 W/cm^2 (equivalent to ten suns), with an AM1 (or equivalent) solar spectrum. In determining the efficiency, the area of any grid fingers that penetrate the interface area region could not be substracted from the active area.

5. The use of an interference antireflection (AR) coating was allowed for obtaining 12% efficiency.

6. Each cell used for the DCPC panel was to be soldered to a Kovar heat sink to provide for cooling; the cells used for the CPC panel were not to be attached until a later specification.

7. The heat sink was to be made from Kovar, 0.025 cm thick, plated with 0.0025 cm silver followed by 0.005 cm of solder.

The cells for the DCPC panel, obtained from two sources, are shown schematically in Fig. II-6. Sensor Technology cells have thirteen grid fingers that cross the active area and an active area (including finger area) of approximately 0.7620 cm^2. Spectrolab cells have no collection grid fingers and have an active area of approximately 0.719 cm^2, still within the dimensional specifications. Both types of cells have an antireflection (AR) coating applied to the silicon surface. The manufacturers' specifications for each cell are shown in Table II-1.

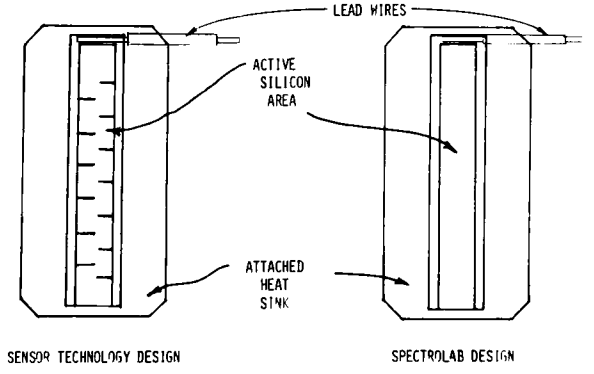

Fig. II-6.

Cells Supplied for Panels

TABLE II-1

Manufacturers' Data for Photovoltaic Cells

	Spectrolab	Sensor Technology
Base Material	Boron-Doped Si	Boron-Doped Si
Base Resistivity	0.5-1.5 Ω-cm	Up to 5 Ω-cm
Diffusion Depth	0.5 Micron Range	Less than 0.65 Micron
Sheet Resistance	∿22.5 Ω/sq.	30-50 Ω/sq.
Metallization	Ti, Pd, Ag Sintered at 600°C, Solder-Dipped, and Pressed (Sn-62)	Solder on Electrodeless Ni Plating
AR Coating	Ta_2O_5	SiO

Upon receipt, each solar cell was subjected to several mechanical and electrical functional tests. In addition, test cells were selected and subjected to Auger spectroscopy for verification of plating materials and thickness. The tests performed on each cell and on selected test cells were as follows:

1. Verification that the photovoltaic cell and heat sink obeyed the dimensional constraints and were of the required construction. Auger spectroscopy was used to examine the various plating layers and materials.

2. Verification that the heat sink was mounted to the cell in conformance with the dimensional constraints given above.

3. Verification of AR coating uniformity and general observation of cell cleanliness. Cleanliness is required to minimize contamination and to maximize solar energy collection and conversion efficiency.

4. Verification that the cell had at least a 12% solar power conversion efficiency.

5. Electrical measurements of open circuit voltage, short circuit current, and I-V curves at unconcentrated (one sun) and concentrated (ten suns) conditions.

Since the number of photovoltaic cells is of the order of 2000 for each panel, the labor involved in cell performance verification testing was considerable. M-7 International of Arlington Heights, Illinois, was awarded a subcontract to aid in the solar cell performance testing and in the wiring of cells into module arrays. The electrical tests performed by M-7 included measurement of cell efficiency under one-sun illumination, and the forward and backward leakage currents. The cells were sorted into performance categories before being wired into module arrays.

Individual solar cells were then wired into a 108-element matrix to be coupled to the DCPC concentrator module face. Before the actual coupling operation, the performance of the completed array was measured under one-sun conditions. After satisfactory operation of the array, it was optically coupled to the concentrator assembly.

Mechanical alignment of 108 wired, but still physically separate, solar cells to the 108 exit apertures of the concentrator module face required the

development of a holding fixture. The alignment problem is illustrated in Fig. II-7. The alignment fixture devised for this operation consisted of a mounting board, to which are fastened 12 thin strips of G-10 material that correspond to the 12 rows of solar cells in each module. These strips are mounted to the base plate by small screws through holes at each end. The holes in the G-10 strips are oversized to allow adjustment of the strips in a vertical or horizontal plane. (This movement is adequate to compensate for any possible variation in the spacings between DCPC strips resulting from the PS-30 bond joint.) To hold the solar cells down onto the nonmetallic G-10 strips, magnetic rubber strips from the Methods Research Corporation, Farmingdale, New Jersey, were bonded to the G-10 strips. This magnetic strip material is similar to the material used to close and seal refrigerator doors. It has a hard rubber-like composition, is magnetic so that the Kovar heat sinks are attracted to it, and comes in strips of various dimensions. This one simple fixture served as both a soldering fixture and an optical alignment fixture for the final bonding of the cell matrix to the DCPC module

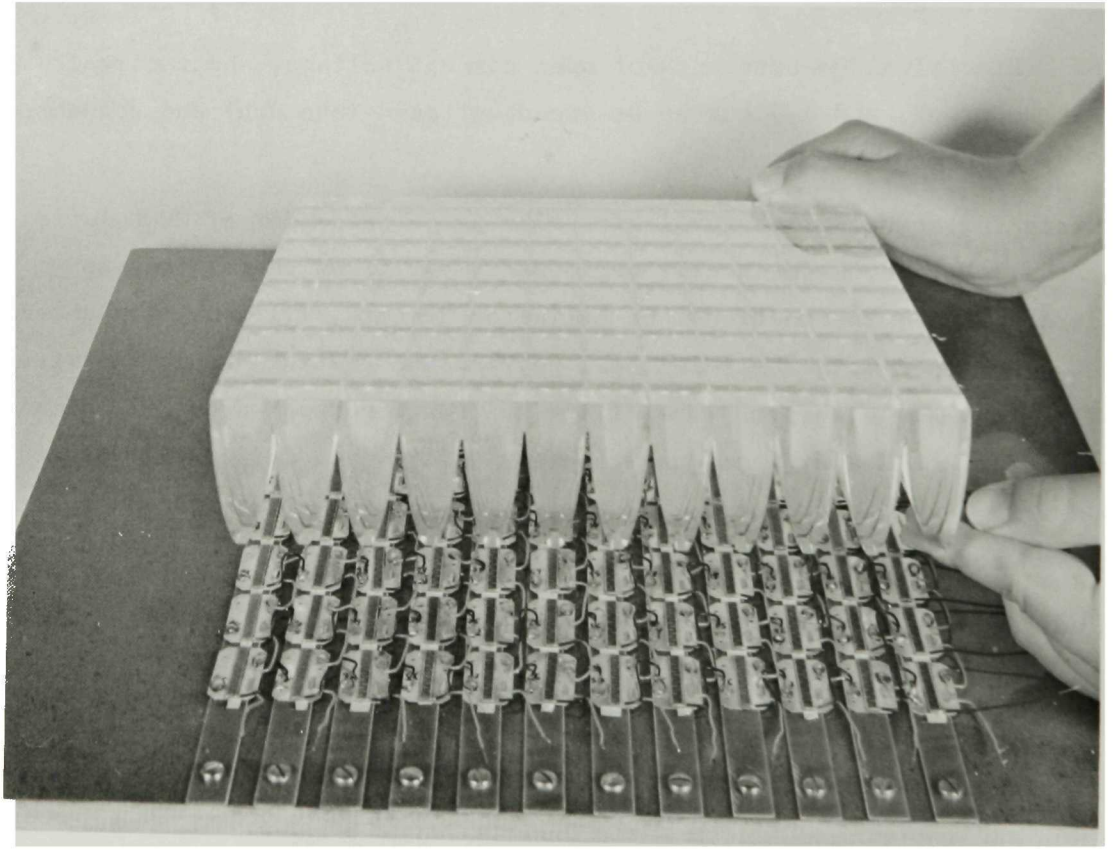

Fig. II-7. Cell Matrix Being Aligned to Concentrator Module Face

face. The magnetic force between the Kovar heat sinks and the magnetic strips was such that it allowed readjustments of cell position, yet was strong enough for easy transportation and storage of solar cell assemblies.

D. Optical Coupling--Cells to Concentrator

The silicon solar cells had to be optically coupled to the acrylic DCPC concentrators. Several types of adhesive were considered for this purpose. These included:

1. General Electric and Dow Corning single-component silicone rubber adhesive.
2. Cadco acrylic adhesive PS-30.
3. Nuclear Engineering 580 optical epoxy.
4. Ablestik 342-3A.
5. General Electric and Dow Corning two-component silicone rubbers such as RTV 615A and R-63-489.

In addition, several technical reports such as JPL-32-1528 were consulted as to previous space and terrestrial research in this area.[10] The successful application of an adhesive depends on many factors--not only adhesion of materials by surface attachment, but also compatibility with the desired assembly process. The proper adhesive and the correct time-temperature-pressure relationship that allows it to cure must be determined. A determination must also be made of the substrate-surface treatment which will yield an acceptable degree of permanence and bond strength. A most important consideration in this case is that the joint must be correctly designed to avoid stresses that could cause premature failure, and the adhesive must remain clear upon curing.

After extensive experimentation and testing, the adhesive and substrate-surface treatments selected were as follows: The acrylic exit-apertures were cleaned with 2-propanol and air-dried. Dow Corning 03-6060 primer was applied and allowed to dry. Over this, Dow Corning 1205 was applied and allowed to dry. The 1205 primer improved the adhesion of the final room temperature vulcanizing (RTV) adhesive. The adhesive used to actually bond the solar cells to the acrylic concentrators was a single-component RTV adhesive. RTV adhesive is a clear silicone rubber which forms a flexible bond with high

peel-strength. These materials cure by reacting with atmospheric moisture and can withstand exposure to 232°C for extended periods. No notable difference was observed between General Electric and Dow Corning products for this application.

Measurements were also taken to observe the effects of any possible bonding problems upon the electrical power concentration factor. Figure II-8 shows the results (as current-voltage curves) for a well-coupled contact, a noncoupled contact (dry contact), a one-half coupled contact, and a contact with extensive bubbles. It can be seen that even when the cell was half-coupled to the concentrator, the short-circuit current remained at approximately 85% of that of the well-coupled short-circuit current. It was determined that it is possible to bond DCPC module faces to cell matrices in which all cells are optically well coupled; any partial loss of coupling is not extremely detrimental to panel performance.

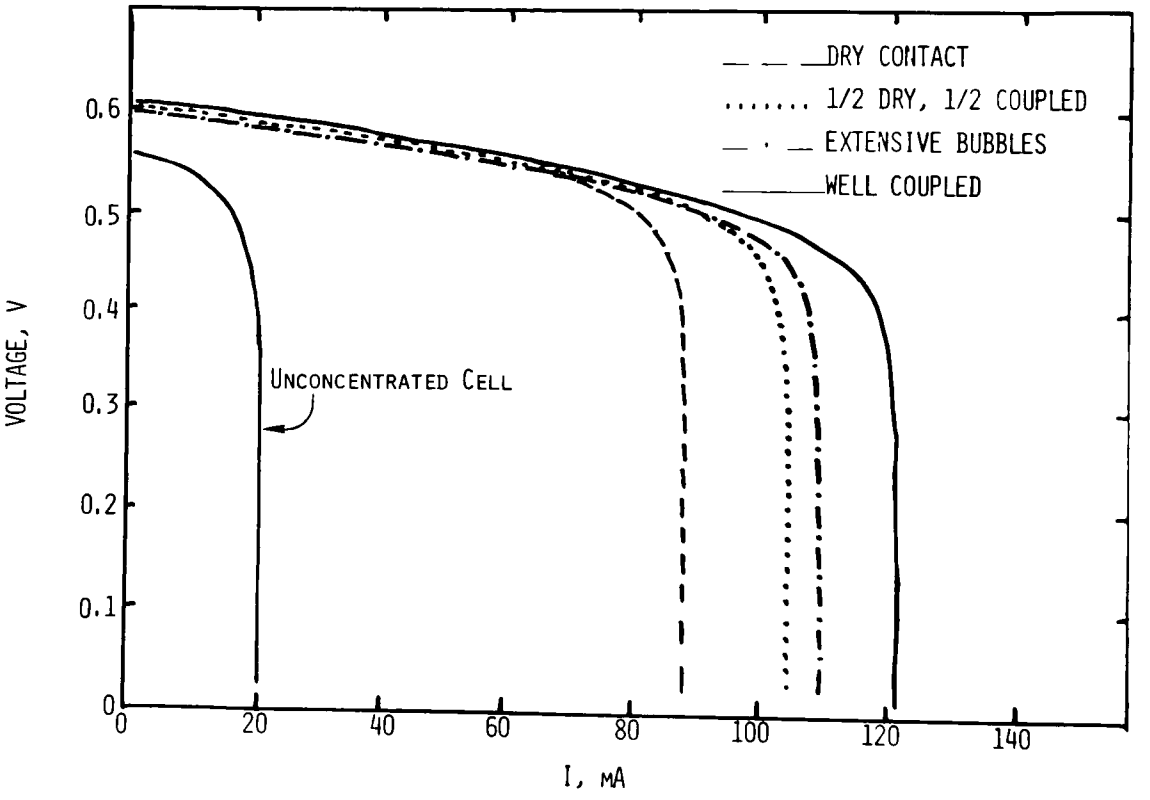

Fig. II-8. Effect on Performance of Optical Coupling

E. Thermal Design

A concentrator design must provide for the removal of the additional heat to avoid conversion efficiency loss due to temperature rise of the solar cells. A major design constraint imposed on these panels is that only passive cooling would be used. Concepts of fabricating the systems for active cooling by means of a recirculating fluid and using the low-grade heat derived thereby for other applications were not considered in this program but would be of considerable importance in future terrestrial applications.

As a basis for the thermal design, the incident peak solar radiation was assumed to be 1 kW/m^2 and the ambient temperature was assumed to be 60°C. An additional constraint of ≷6°C between cell and heat sink was also imposed. For a DCPC panel composed of 20 modules of dimensions 27.4 cm by 22.9 cm each, this corresponds to a total incident energy of 1,254 W or 4270 Btu/hr. Heat rejection must be by radiation and natural convection. A detailed analysis showed that for the above operating conditions, an overall heat transfer coefficient of 1.88 $Btu/(hr)(ft^2)(°F)$ from the heat sink to surroundings through the back of the solar panel is obtained. Taking into consideration heat transfer through the acrylic DCPC units to the surroundings, one obtains a combined heat transfer coefficient of 1.315 $Btu/(hr)(ft^2)(°F)$. From the above considerations, one calculates a heat loss of 800 Btu/hr from the front of the DCPC panel and 3470 Btu/hr from the rear. A heat loss of this magnitude at the rear of the concentrator requires an area that is a factor of three larger than the frontal area and thus implies an extended-surface heat sink.

As stated previously, a Kovar heat sink was soldered to each solar cell by the suppliers. This attached heat sink served as one of the cell contacts and as an intermediate heat sink for thermally coupling the cell to the main extended-surface heat sink. To provide electrical insulation between the Kovar and the extended-surface heat sink, a layer of electrical insulation (Mylar) is positioned between them. Calculations indicate that heat flow from the photovoltaic cells to the extended-surface heat sink results in only a few degrees of temperature drop if the thicknesses of the insulation and air gaps are kept low. For example, 0.008 cm of Mylar results in a ΔT of 0.6°C, and 0.013 cm of air results in a ΔT of 4.7°C. Air gaps are eliminated by the use of a heat-conductive silicone grease. The extended-surface heat

sink serves the additional function of providing a flat surface upon which the concentrator-cell elements can be mounted. A considerable savings in machining costs for the prototype panel was obtained by using standard aluminum extrusions for these extended-surface heat sinks. These extrusions can be obtained in various configurations and require only the machining of the top surface as a concentrator-mounting surface. Figure II-9 shows the general configuration of the DCPC photovoltaic module with the acrylic DCPC module face, the integral solar cell-heat sink assembly, and the extended-surface heat sink.

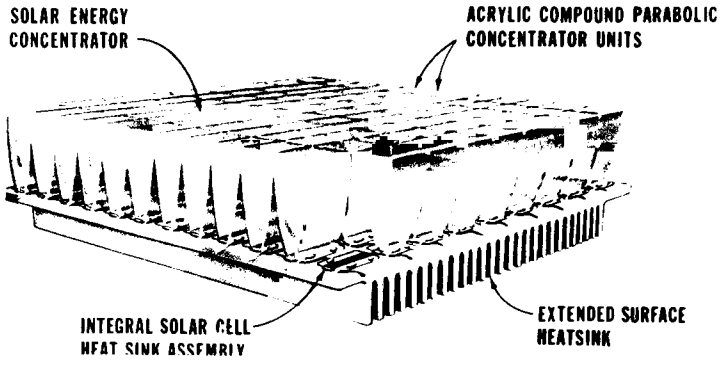

Fig. II-9. DCPC Photovoltaic Module

F. Module Support Structure

The general configuration of the DCPC support structure is similar to a window-frame type configuration. The load of 2394 pascals (Pa) is carried by four channels supported at the ends. Additional stiffness is provided by T sections positioned perpendicularly to the four channels. Both structures were fabricated from standard aluminum extrusions, type 6061-T1. Calculations indicate a deflection of 0.30 cm in the center of the 1.16-m span under maximum loading. The support structure for the DCPC panel contains the 20 DCPC modules. Figure II-10 shows the DCPC panel assembly with the 20 DCPC modules in place. The details of the frame are shown in the mechanical drawings, Appendix A.

G. Module Performance

I-V curves were measured for each modular array of photovoltaic cells before the cells were bonded to the acrylic DCPC's. These measurements were made under controlled 1 kW/m^2 AM1 conditions. The xenon light source used

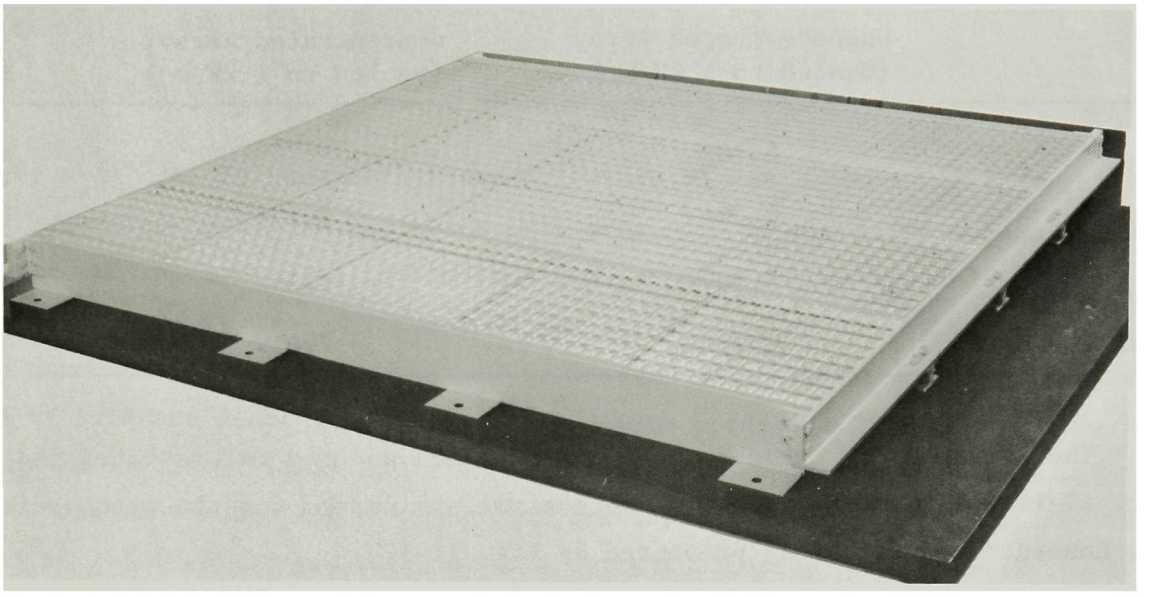

Fig. II-10. DCPC Panel Assembly

for these measurements could illuminate the module area evenly, but the angular dispersion of the light prevented use of the light source for measurements of the completed module performance. Measurements of I-V curves for all completed modules were made in sunlight, and the results may be scaled to 1 kW/m^2 direct insolation for comparison with the results for unconcentrated modules. Total-normal and direct-normal insolation were measured using a tracking Eppley pyranometer and pyrheliometer to determine the insolation within the acceptance angle of the DCPC units. If n is the index of refraction of the concentrator unit (1.00 for CPC, 1.49 for DCPC) and C is the concentration factor of the unit, the accepted insolation is equal to the direct component plus $\frac{n}{C}$ times the diffuse component. Although the completed modules were tested under varying insolation conditions on different days, one module was tested each day and its scaled output varied by less than 1.5%. The averaged results for the 20 modules are given below. The short-circuit current, I_{sc}, the open circuit voltage, V_{oc}, and the peak power values for the averaged concentrated array are scaled to 1 kW/m^2 direct beam. The following table shows that the actual peak power concentration ratio is approximately 6.4.

	Unconcentrated Array (Scaled to 1 kW/m^2)	Concentrated Array, (Scaled to 1 kW/m^2)	Ratio
V_{oc}	6.76V	7.76V	1.15
I_{sc}	0.22A	1.21A	5.50
$V_{max\ power}$	5.40V	6.14V	1.14
Peak Power	1.10W	7.01W	6.37

The averaged I-V curve for the concentrated modules is presented in Fig. II-11. The average power vs output voltage curves for the unconcentrated and concentrated arrays is presented as Fig. II-12.

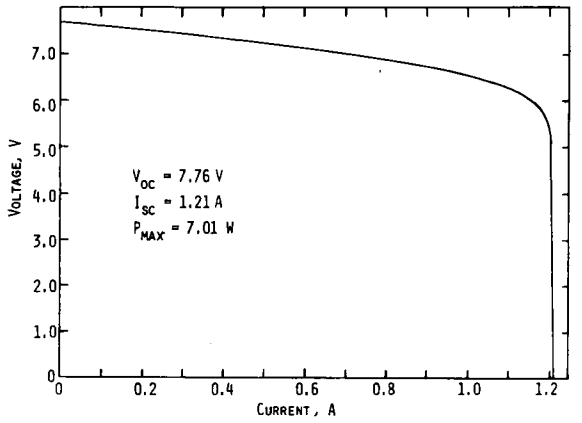

Fig. II-11.

Average DCPC Module Performance (Scaled to 1 kW/m^2 Direct)

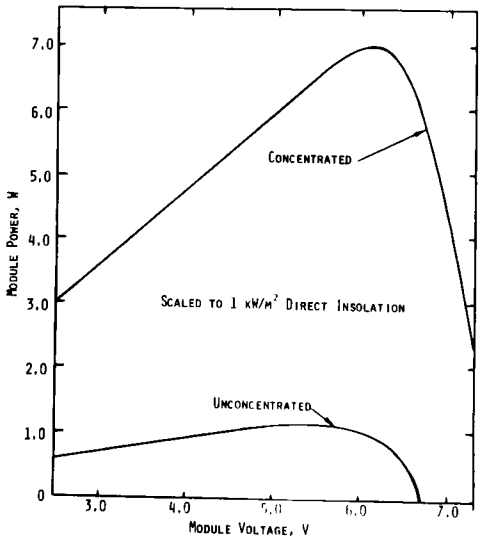

Fig. II-12.

Average DCPC Module Power Curves

Burgess[11] defined the actual concentration ratio, ACR, at a solar cell to be

$$ACR = \eta_o \, A_o/A_c.$$

where A_o/A_c is the geometrical concentration factor, when A_o is the incident aperture area and A_c is the solar cell area. η_o is the total optical efficiency of the concentrator-cell combination and includes reflection and transmission losses of the optics. For the DCPC design, $A_o/A_c \approx 7.45$. After correcting the power ratio by the factor 1.17 to account for improved cell performance due to increase light intensity,[4] the average optical efficiency (η_o) is about 73%. Measurements indicate an unavoidable loss of 8.4% due to light transmission through clear acrylic of similar thickness; therefore, an average loss of 18% from the maximum possible concentration ratio was due to imperfections such as sinks in the acrylic walls, nonperfect bond joints, cell surface reflections, etc. It is felt that with additional effort, these losses could be reduced.

Consider now the energy balance for the typical module. For 100 mW/cm^2 incident, the average module produces 7.01 W for a DCPC module of incident area 27.6 cm by 23.3 cm. This is equivalent to the power output of a hypothetical single solar cell of the same dimensions as the module, but of 10.9% efficiency. The average output from the unconcentrated arrays was only 1.10 W. We note that in terms of silicon, we are using only one-sixth the amount necessary to make a single equivalent cell. This savings of expensive silicon can be of considerable importance in large-scale terrestrial applications.

H. Panel Test Equipment

Testing of the completed panel required an accurate method of varying the current through the panel. A current amplifier circuit designed by Dr. K. Reed of Argonne National Laboratory is shown in Fig. II-13.

The "current amplifier" circuit acts as a high-power, high-resolution variable resistor. The level of forward bias at the base of the 2N3055 driver determines the amount of current which can be forced through the collector-emitter leads of the 2N3791 transistor by the photovoltaic panel, and hence determines the operating point of the panel. The X-Y recorder monitors the voltage across the panel directly and monitors the current by means of a calibrated, low-resistance shunt. Since the voltage drop across a

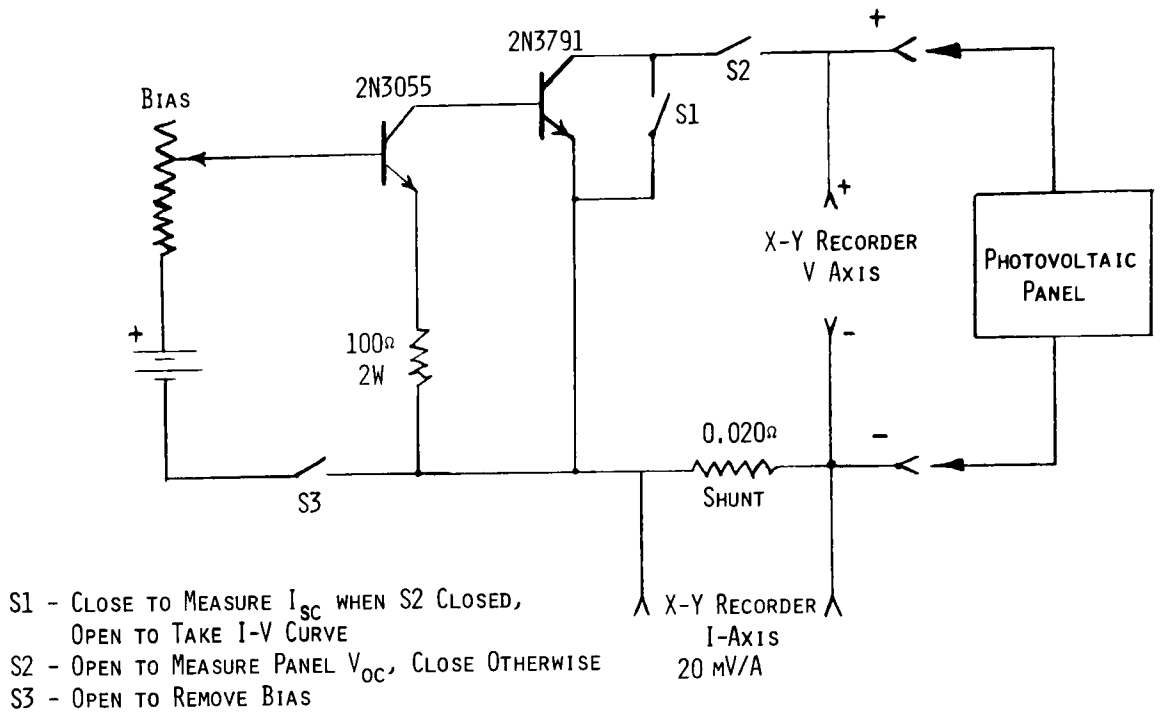

Fig. II-13. Current Amplifier Circuit for Panel Tests

silicon transistor in saturation can be considerable ($V_{CE(SAT)} \geq 1$ V), a switch is provided to bypass the transistor for short-circuit current measurements. Likewise, a switch is provided to isolate the panel for open-circuit voltage measurements. The circuit can sink 150 W continuously at a maximum of 30 A.

I. Panel Performance

The completed DCPC panel was tested in sunlight on December 13, 1976. The total insolation was 900 W/m^2 of which 818 W/m^2 was direct. The insolation within the acceptance angle of a DCPC unit was calculated to be 831 W/m^2, and so the measured peak output power of 114 W (4.85 A at 23.6 V) would scale up to 138 W for 1 kW/m^2 direct insolation. The I-V curve is presented in Fig. II-14, and the power curve is shown in Fig. II-15.

The measured output power of the DCPC panel indicates a conversion efficiency of 10.7% of the light incident on the acrylic module faces within the angular acceptance of the DCPC units. The large packing factor of 0.96 for the acrylic modules in the panel frame leads to a conversion efficiency of 10.3% over the total panel area, including the panel walls.

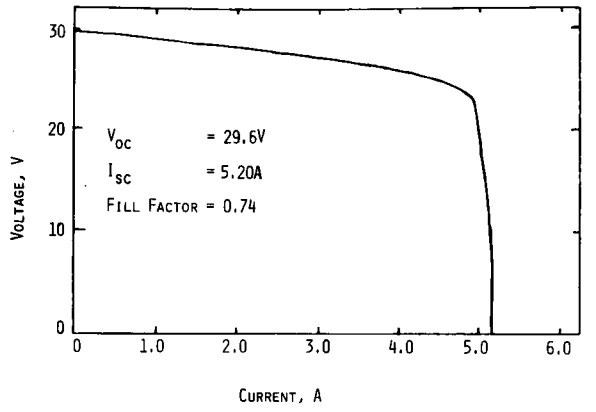

Fig. II-14.

Performance Curve for DCPC Panel

Insolation: 900 W/m^2 Total
818 W/m^2 Direct

Power Output: 114.4 W
(138 W When Scaled to 1 kW/m^2 Direct)

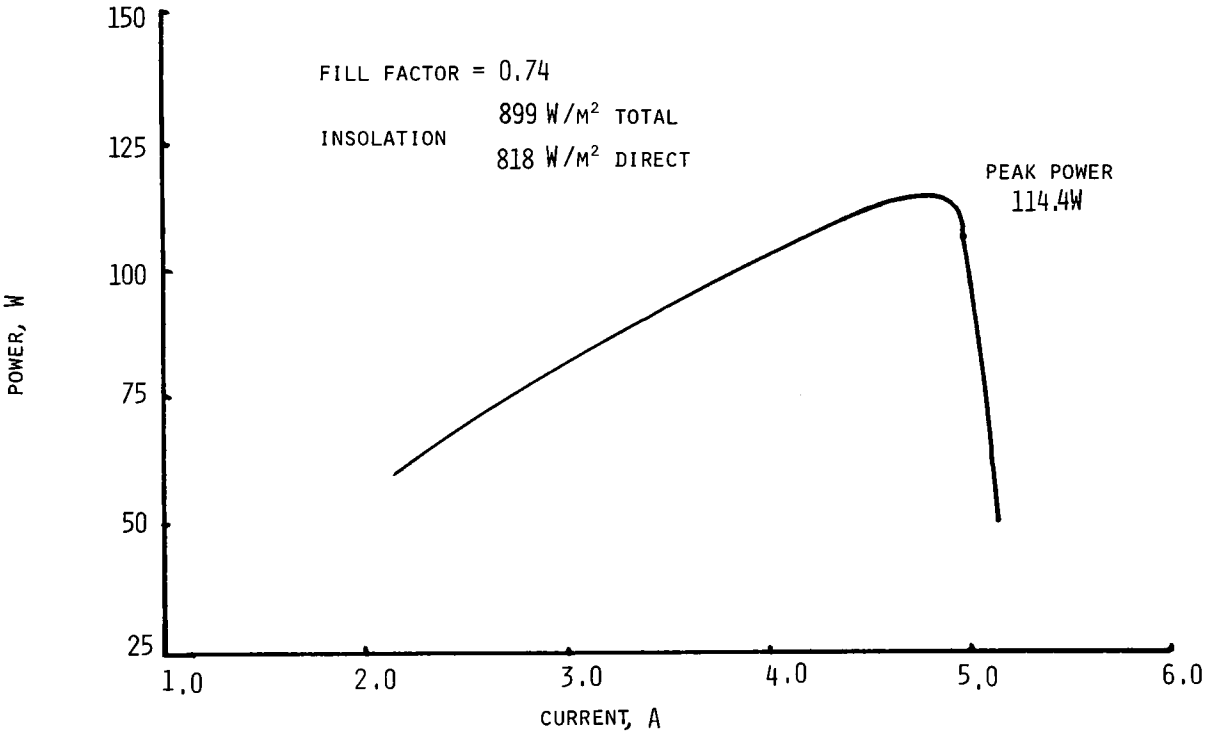

Fig. II-15. DCPC Panel Power Curve

A comparison of the panel performance and module performance is important to indicate the effects of the series-parallel wiring used in the panel. The average of the 20 modules' individual peak output powers scaled up to 1 kW/m^2 was 7.01 W; the sum of the peak powers was 140.2 W. The scaled peak output power of the panel was 138 W (an average of 6.9 W/module) or 98.7% of the sum for the individual modules. This agreement indicates that the series-parallel wiring was not a detriment to the panel performance. An experimental measurement of the angular acceptance of the panel was also taken and shows that 75%

of the incident solar radiation is accepted over an angular range of 16°. These measurements are shown in Fig. II-16. The tilt adjustment schedule for this panel is presented in Appendix C.

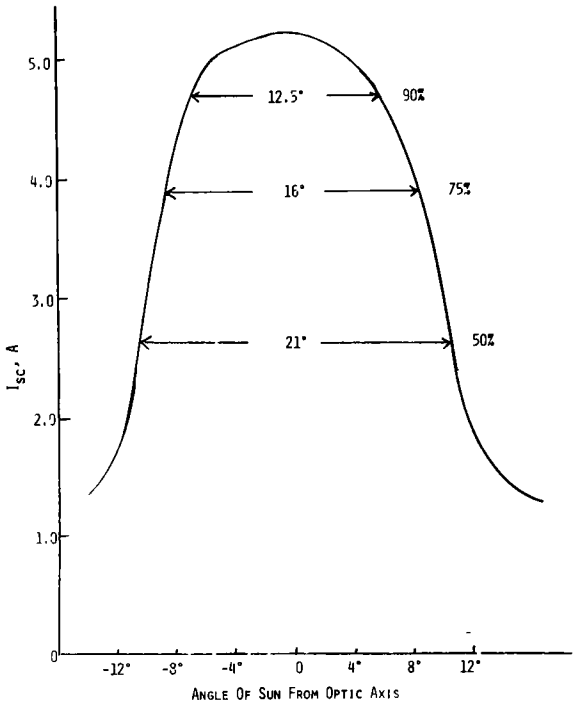

Fig. II-16.

Variation of Short Circuit Current with Orientation of Reflector to Sun

The construction of these panels shows that the compound parabolic concentrator concept offers several important advantages for a concentrator/photovoltaic system.

- Modern plastic molding techniques can be used to produce DCPC and CPC units at relatively low cost.
- Total Internal Reflection (used in the DCPC design) offers high light collection efficiency and simplicity.
- The elimination of metallization in a concentration system improves efficiency.
- Elimination of diurnal tracking of the sun in both designs is of considerable importance in some terrestrial applications and should not be underestimated.

The modular design philosophy as used here allows the scaling-up or -down of the DCPC concept; this scaling feature was found to be of considerable

importance. Prototype DCPC strips and modules have been used to power small solid-state radios and television sets, and such units can be incorporated into many types of small appliances used today. Of course, the weight of the solid acrylic concentrator becomes a disadvantage as one scales up the DCPC concept to larger areas. For larger configurations, the lightweight CPC design described in the next section has an advantage.

The cost-effectiveness of these systems is estimated in Section IV.

III. REFLECTIVE HOLLOW CPC PANEL

A. Design

The basic design considerations for the hollow CPC photovoltaic panel were the same as those for the DCPC panel. The CPC is a nontracking panel with moderate concentration, requiring only occasional north-south tilt adjustments. The panel size and the frame's mechanical specifications are the same as those for the DCPC panel (described in Section II). The detailed mechanical drawings are included as Appendix B.

An early decision was made to use the same cell design for both panels to reduce costs for cells by increasing the quantity of cells obtained from each manufacturer. The interchangeability of cells from the two panels allowed cell testing procedures to be standardized and provided an ample supply of cells for evaluating procedures of construction for both panels. The final reflective CPC panel design used the same cell-heat sink combination as the DCPC panel, which was permissible because the cell design had been standardized.

Figure III-1 is a photograph of early prototype components of a reflective CPC photovoltaic module. Six aluminized plastic reflector substrates are shown, as well as solar cells having grid fingers. The Argonne logo rests on the circuit sheet used for interconnecting the solar cells. An extruded aluminum heat sink forms the base, and provides alignment notches for the circuit sheet and CPC bars. A protective plastic cover shields the cells and reflectors from dust and dirt. A second extruded aluminum heat sink is also shown (upside down) to illustrate the extended surface and the mounting standoffs.

Figure III-2 is a closeup photograph of the six CPC reflectors. Solar cells having grid fingers have been placed between alternate rows to illustrate the contrast between troughs with and without cells. The 0.28-cm-wide cells at the base of the reflectors appear to completely fill the reflective trough. The alignment notches, positioning shoulders, and cover groove are also clearly shown.

The basic design of the hollow (reflective) CPC panel is modular, similar to the DCPC panel. A complete set of mechanical drawings of the module is in Appendix B. In each module, aluminized plastic CPC trough reflectors were

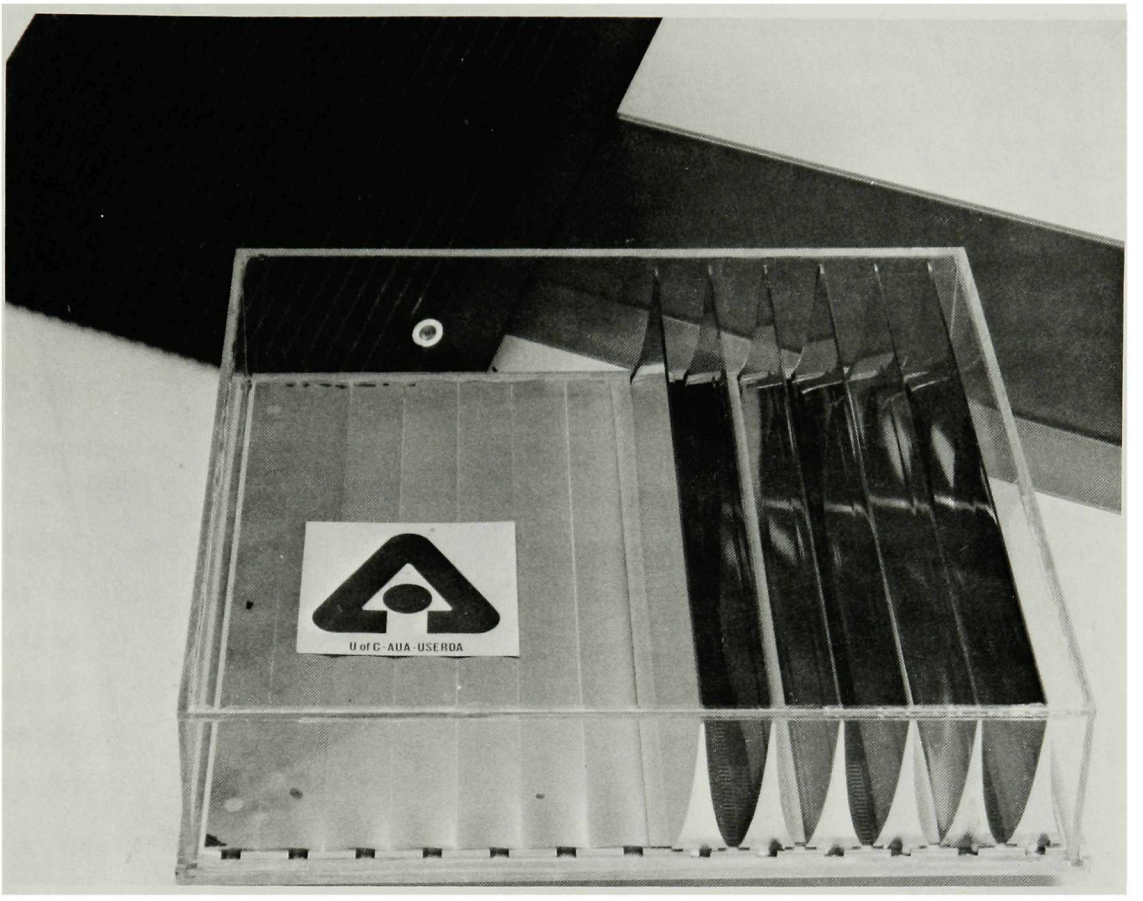

Fig. III-1. CPC Module Components

positioned above rows of 0.28-cm-wide photovoltaic cells. The ten cells in each row were soldered to a common copper strip on the circuit sheet, providing redundant parallel wiring of the row. The top lead wire from each cell was soldered to the next row, providing redundant series connections between rows. Twelve rows of cells comprised one module; hence 120 cells/module or 1920 cells/panel were required. After a completed, tested circuit sheet was aligned and epoxied to the module heat sink (with Shell Epon 815 epoxy resin, using Celanese 855 curing agent), the entire circuit sheet was coated with a two-component RTV (G.E. No. 615A), and the reflectors were installed before the silicone rubber cured. Tabs on the ends of the reflectors were press-fit into the positioning slots in the heat sink, and the cured RTV secured the reflectors. Finally, an acrylic cover box was used to protect both the cells and the reflecting surfaces of the module. To prevent displacement of the covers during barometric pressure changes, the boxes were not hermetically

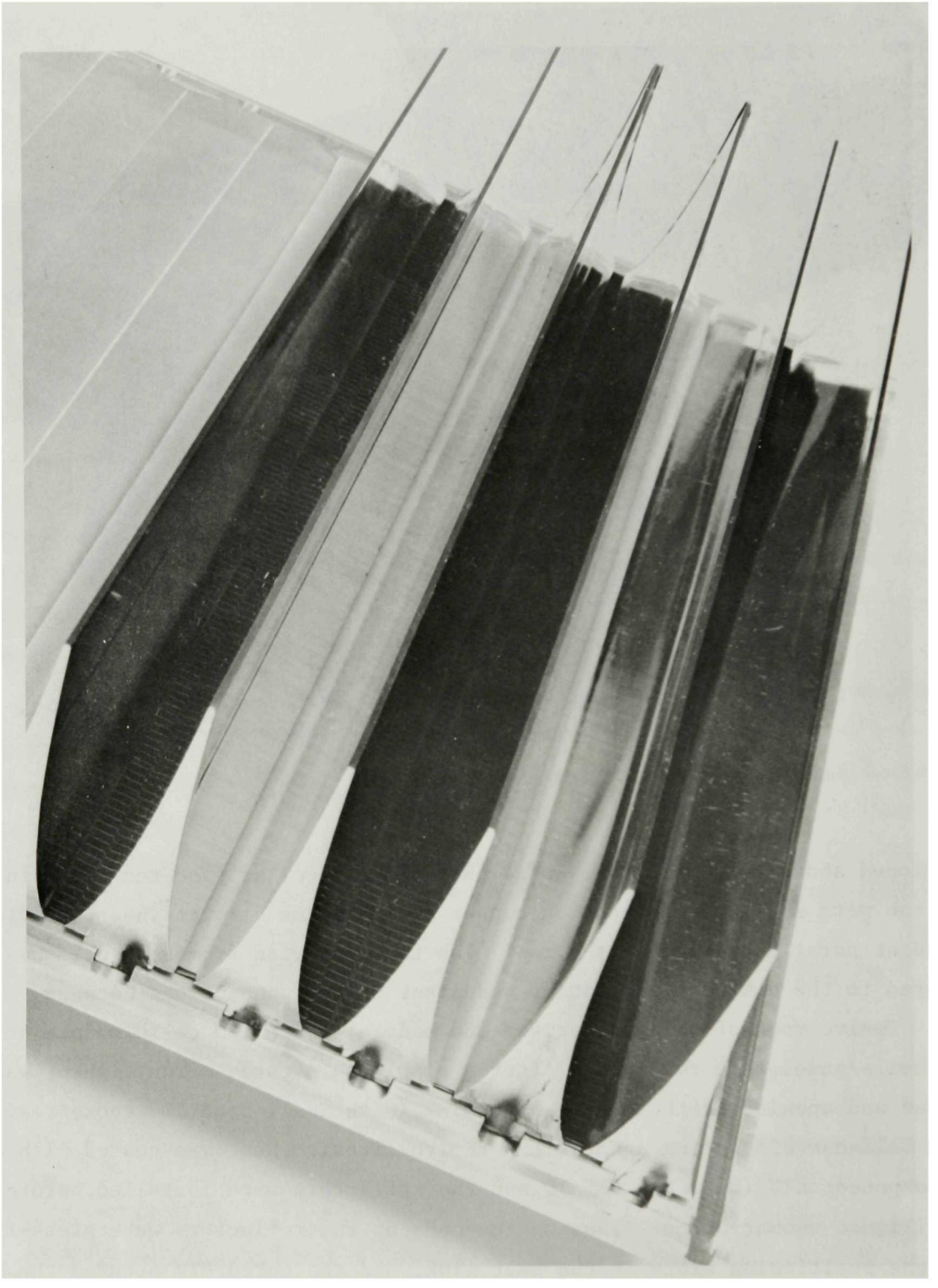

Fig. III-2. Closeup of CPC Reflectors

sealed. Each module was vented through long, partially crimped copper tubes running from north to south and protected between the fins of the heat sink.

The modular design of the panel has several advantages--both for prototype construction and for a production model panel. For the prototype panel, the modular design allowed small sections of the panel to be constructed and tested separately, which was particularly important since various assembly techniques could be evaluated on a small scale without committing a whole panel. For a production model with automated assembly, a modular design has advantages, especially with regard to tooling limitations. The module size in production might be substantially different from the size of the present prototype.

Modules are also interchangeable, and a damaged one can be replaced easily. By altering the wiring on the terminal strips housed in a protective aluminum box beneath the frame (as discussed for the DCPC panel), various output voltages are possible. For example, with 1 kW/m^2 direct insolation, the sixteen modules in the hollow (reflective) CPC panel could be wired in different series-parallel combinations to give peak output voltages of approximately 7.5, 15, 30, and 60 V with corresponding short circuit currents of approximately 8, 4, 2, and 1 A.

A penalty paid for the particular type of modular construction in the hollow CPC panel is a decrease in packing factor. Alternative designs for the panel could minimize this loss of packing factor.

B. Aluminized Plastic Reflectors

The design of the CPC shape (shown in Fig. III-3) narrowed the field of candidate materials and fabrication processes for producing reflectors. The materials considered for reflector substrates included polished sheet aluminum, plastic, and super-plastic zinc. The four processes evaluated were: extrusion of plastic, thermoforming of plastic sheets, thermoforming of the super-plastic zinc alloy, and injection-molding of plastics. Thin sheet metal reflectors were not selected for the first prototype panel because of schedule limitations.

Extrusion of plastic would be a high-speed method for the production of reflector substrates. However, long extrusions having non-uniform wall thicknesses were not considered to be precise enough for the small CPC units dictated by the cell size. If larger cells and correspondingly larger reflectors were used, extrusions would have to be reevaluated because the ability to maintain the CPC shape with extrusions has not been demonstrated.

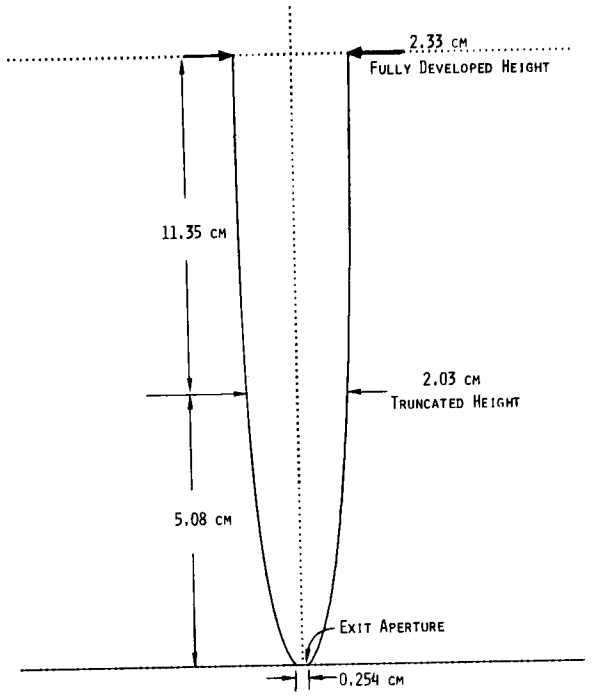

Fig. III-3.

CPC Shape for Reflective Panel

Thermoforming of plastics has demonstrated good potential for large CPC reflectors. Thin-walled, accurately-shaped reflectors have been made for the photothermal program. If cells of 1 to 2 cm width or larger were used, thermoforming would be a good candidate process for producing lightweight CPC reflectors. However, the prototype photovoltaic panel design required small, precise CPC units with sharp angles and too deep a draw for thermoforming.

Thermoforming of super-plastic zinc was also evaluated as a method of making a substrate that would be compatible with silver metallization for obtaining higher reflectivity than that of evaporated aluminum on plastic substrates. This process was judged to not be cost-effective for the prototype panel because of high tooling and development costs--or for production model panels because of high materials costs.

The plastic reflector substrates for the prototype panel were made by injection-molding. Sample acrylonitrile-butadiene-styrene copolymer (ABS) and polysulfone substrates were molded and treated with an undercoat polymer, evaporated aluminum, and a protective over-coat for evaluation. The more expensive polysulfone material ($4.41/kg) tolerates higher temperatures in the coating steps and was used as a backup for the ABS. Since there were no problems with the ABS substrates, this less expensive material ($1.10/kg) was used in the panel. Both the ABS and polysulfone substrates were undercoated

with SM1954 base coat resin mixed 1:1 with SV-1981 solvent.* After vapor deposition of an aluminum reflecting surface, the substrates were given a protective over coat of ET-4.* Lower drying temperatures and correspondingly longer drying times were required for the ABS substrates.

The aluminized reflectors were assumed to be electrically shorted to the heat sinks; therefore, 0.013-cm-thick Mylar sheets were attached to the bottom of the reflectors to insulate them from the top contact of the photovoltaic cells.

Several mold changes were required to produce acceptable reflector substrates. The final design used is shown in Fig. III-4. The tabs provided positioning in slots in the heat sinks and the shoulders provided vertical alignment. It should be noted that the packing factor of each module could be increased by molding special "half reflectors" for each end of the module. This option would have required tooling and development costs for a second mold, and was deemed unnecessary for the prototype panel. It should be clear that the packing factor for this panel could be improved significantly by such minor design changes in a second-generation panel. Figure III-5 is a photograph of reflector bars before and after aluminum evaporation.

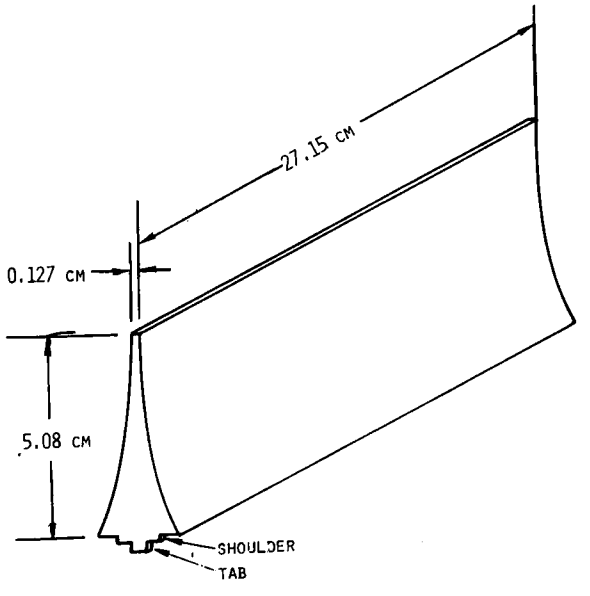

Fig. III-4.

CPC Reflector Substrate

*Red Spot Paint and Varnish Co., Inc., 110 Main Street, Evansville, Indiana 47703.

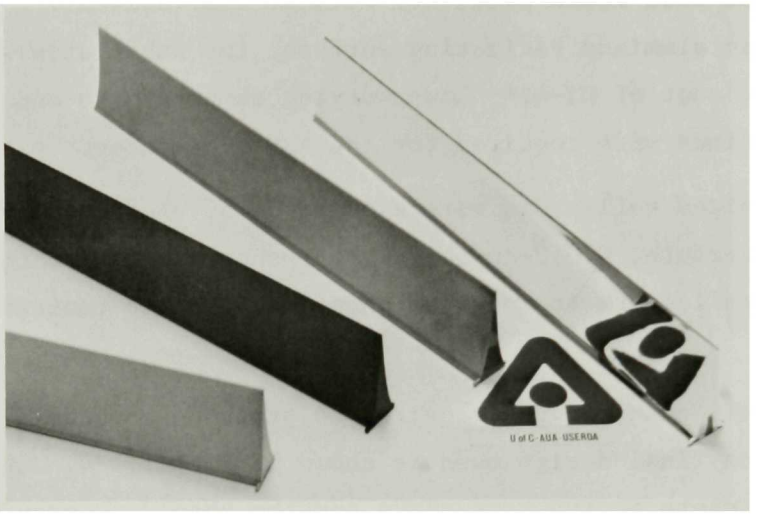

Fig. III-5. CPC Reflectors

C. Photovoltaic Cells and Circuit Sheets

The specifications for the photovoltaic cells used in both panels have been discussed in Section II. The original concept for the hollow CPC panel was that the cells would be mounted directly on an etched circuit sheet in a series-parallel circuit. A design change was made to make the units more durable--the cells would be soldered end-to-end on Kovar strips. After a given strip was completed and tested, it would then be soldered or epoxied to a circuit sheet. One cell manufacturer provided completed prototype strips, but problems developed with the technique, and delivery of the strips was delayed.

A decision was made to begin construction of the panel using cells on individual Kovar heat sinks as in the DCPC panel, while having the manufacturer continue some developmental work on the strips. Copper-on-Mylar circuit sheets were designed to provide the parallel wiring of rows, and the alignment holes in the Kovar heat sinks were used for positioning the cells on the sheet. The cells were held in position by magnetic strips beneath the circuit sheets. A thin aluminum sheet between the circuit sheet and the magnetic strips helped protect the Mylar from the soldering heat and also kept the circuit sheet flat.

The entire panel was completed using the cells on individual heat sinks; the development effort to make cells on Kovar strips was stopped after successful delivery of 60 strips and completion of the program.

D. Module Support Frame

The frames for both panels were designed to meet the dimensional and mechanical specifications of the JPL procurements, as described in Section II. Therefore the two panel support frames are very similar.

E. Extended Aluminum Heat Sinks

For convenience and for comparison purposes, the same extruded aluminum heat sink material was used for modules in both panels. This was not necessarily optimum for the hollow CPC panel, because its modules would have more heat losses from the front surface that would tend to make an extended-surface heat sink less necessary. The tops of the heat sinks were machined to provide for alignment of the circuit sheets and the reflectors. Figure CE-C6929 in Appendix B shows the heat sink design with alignment slots and a groove around the sides provided for the cover box. The back sides of the module heat sinks were degreased, undercoated with zinc chromate primer, and sprayed with flat black Krylon paint.

F. Acrylic Covers

Each module was protected by its own acrylic cover box. The boxes were made of 0.318-cm acrylic sheet cut to size and glued with PS-30. Grooves machined in the heat sinks held the boxes in place, and they were sealed with a single-component RTV adhesive. The grooves were oversize to allow for the differences in thermal expansion of acrylic and aluminum. The modules were vented to prevent pressure changes from displacing the cover boxes. Long partially crimped copper vent tubes run from north to south under the module heat sinks. Entry of water into the modules due to rain or washing is unlikely with this venting technique; however, the modules are not hermetically sealed.

G. Packing Factors

In some applications of photovoltaic power, array efficiencies are important, as well as the effective use of solar cells by concentrating sunlight on them. Therefore, it is appropriate to examine the panel's packing factor of 0.737 to determine to what extent the various area losses in this prototype panel could be reduced to increase the packing factor and thereby the array efficiency. There are three broad categories of area losses in the panel: the area of the flat tops of the reflector units, spaces between cells and reflectors, the areas within a module but outside the reflectors,

and areas between adjacent modules and/or the panel frame. These area losses are discussed below and are expressed as percentages of the panel area. A summary is presented in Table III-1.

TABLE III-1

Packing Factor Losses[a]
(As percentages of panel area)

Area	Prototype Panel, %	Optimized Modular Panel, %	Nonmodular Panel, %
Flat tops of reflectors	5.3	6.0[b] (2.0)	6.2[b] (2.0)
Spaces besides cells	2.9	3.3[b] (1.1)	3.4[b] (1.1)
Vacant half-rows at north and south ends of modules	6.5	0.0	0.0
Open ends of troughs	0.5	0.2	0.0
Module cover box walls	3.1	3.1	0.9
Heat sink area outside the cover walls	5.5	0.0	0.0
Areas between heat sinks	2.5	2.5	0.0
Total, %	26.3	15.1 (8.9)	10.5 (4.0)
Active Area, %	73.7	84.9 (91.1)	89.5 (96.0)

[a]Numbers in parentheses are based on a threefold increase in cell width and a corresponding decrease in the number of reflectors.

[b]The total areas of reflector tops and the spaces beside cells will increase as the other area losses are decreased.

The flat tops of the reflectors occupy 5.3% of the panel area. With the cell size and CPC design used in the panel, this loss could not be reduced significantly. The 0.127-cm-wide tops of reflectors cannot be significantly reduced for injection-molded plastics. One way of reducing the percentage of total area covered by the tops of the reflectors is to increase the cell size; this would also result in a corresponding increase in reflector size. This would reduce the number of reflectors and hence the total area of their tops. As noted in the section on reflectors, larger cell and CPC sizes could favor thermoforming in preference to injection-molding. Depending on the reflector design, the loss of area due to the tops could be reduced to about one to three percent of the total panel area.

There is also space between the cells (at the exit aperture) and the reflectors to prevent electrical shorting to the aluminized plastic. These spaces accounted for a 2.9% area loss, which could be reduced by design changes. This loss would become less significant if the cell width were increased.

In a module, there are three types of area losses other than the reflector tops. The most obvious are the vacant areas at the north and south ends of the modules. If special half-reflector units were molded for the north and south ends and if the cells and reflectors were shifted north by one-half row width on the heat sinks, these vacant areas would be combined at the south end and would nearly accommodate a thirteenth row. Making half-reflector units was judged unnecessary for the prototype panel, although it could be done to utilize an additional 6.5% of the panel area.

The second area loss within a module is along the east and west sides, where neither the CPC's nor the cells cover the full area out to the cover box. This is a consequence of using a single cell design for both the hollow CPC and the DCPC panels. By appropriately adjusting the cell and reflector dimensions, this loss of 0.5% could be virtually eliminated.

The third loss within each module was the area of the cover box walls. If a modular design is used in which each module is protected separately, this area (3.1% of the panel) cannot be saved. However, if the modular concept were abandoned or used in a modified version with a single cover box over all the modules on a common heat sink, the savings would be approximately 2.2% of the panel area.

Optimizing the modular design but still using the same CPC design and cells could increase the packing factor of the prototype panel by 15%, from 0.75 to 0.85. A nonmodular panel using the same cells and reflector design could have a packing factor of 0.90, an increase of 21% over the prototype panel. In both of these cases, the main loss of panel area would be at the tops of the reflectors. If the cell size were increased with a corresponding increase in reflector size, the number of reflectors would decrease, along with the area loss for their tops. A threefold increase in cell size would increase the packing factors of the optimized modular panel and the nonmodular panel to 0.91 and 0.96, respectively. These would be increases of 23% and 30% over the packing factor of the prototype panel.

There are two types of area loss between modules. The first is the area of the modules' heat sinks out beyond the acrylic cover boxes. This area loss is 5.5% of the panel area and could be eliminated in a second-generation panel. The second loss is the space between heat sinks and is 2.5% of the panel area. This spacing would not be changed if the modular design were retained with separately covered, interchangeable, and replaceable modules; however, with a one-piece heat sink for the panel, this loss could also be eliminated.

Table III-1 summarizes the packing factor losses for the prototype panel, estimated losses for an optimized modular panel with separately protected modules, and losses for a panel which uses a single heat sink and cover box with or without internal modular construction.

H. Cell-Concentrator Alignment

The Mylar substrates of the circuit sheets buckled slightly when the cells were soldered down. This contributed to a shrinkage of the circuit sheets, which consequently required a compromise in positioning the cells beneath the concentrators. As a result, rows of cells at the north and south ends of the modules have been pulled slightly toward the center of the modules. One effect of this misalignment was a decrease in short circuit current with an accompanying increase in the fill factor, characteristic of nonuniform illumination of the panel. Another result of the misalignment was narrowing of the acceptance angle. This problem could be minimized by using double-sided circuit sheet material to provide greater dimensional stability.

I. Panel Performance

Preliminary testing of each reflective CPC module was performed at Argonne National Laboratory on January 21, 1977. Prior to shipment of the CPC panel to Sandia Laboratories, the complete panel was tested on January 31, 1977. This test data is summarized in Figs. III-6 and III-7. The peak output power was 81 W (3.175 A at 25.6 V). This represents a conversion efficiency of 7.1% of the 844 W/m^2 within the acceptance angle of the panel, which is a factor of 5.7 times the power output of cells in the absence of concentration. This power concentration ratio is approximately what one should expect for the performance of this particular CPC design. The array efficiency could be increased by design modifications to increase the packing

factor. If the insolation within the acceptance angle is scaled to 1 kW/m^2, the peak power scales up to 97 W. The manner in which efficiencies are scaled up to 1 kW/m^2 is described in Appendix D.

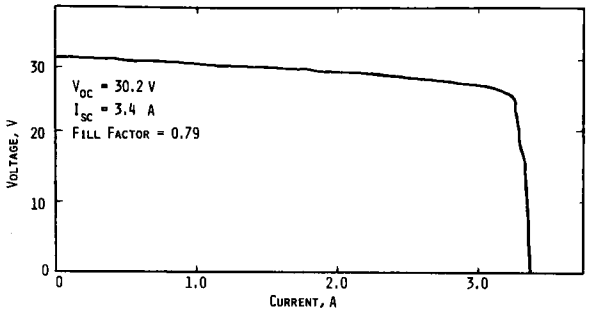

Fig. III-6.

Performance of CPC Panel

Insolation:	952 W/m^2 Total 829 W/m^2 Direct
Power Output:	81 W (97 W When Scaled to 1 kW/m^2 Direct)

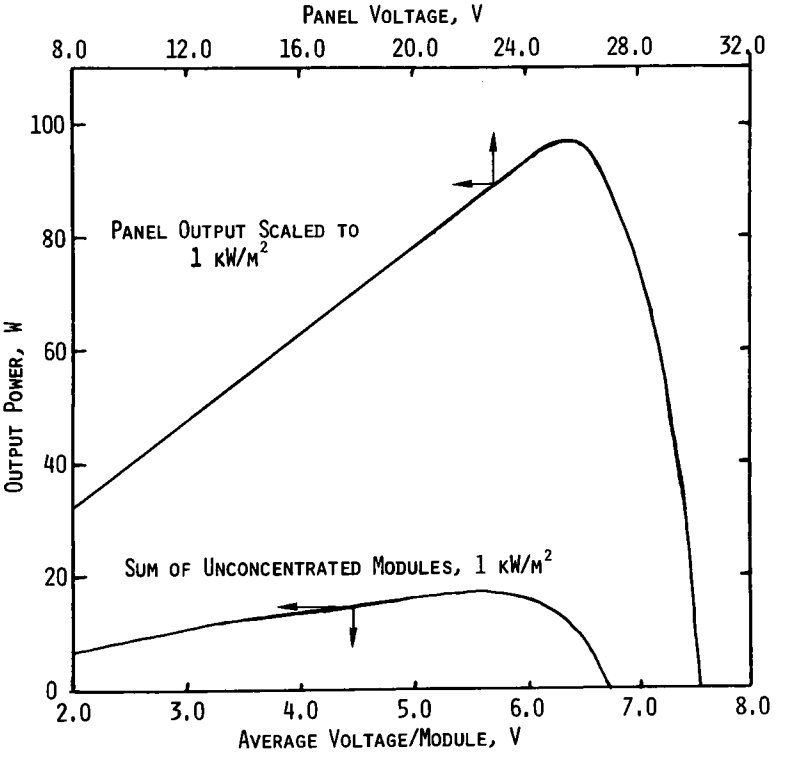

Fig. III-7. CPC Panel Output Power

The geometrical concentration ratio, defined as the entrance area divided by the active cell area, for the CPC reflectors is 6.9:1, but there are losses to be considered. Transmissivity of the acrylic cover box was measured, using a solar cell, and was 0.918 for normal incidence. The average reflectivity in the solar spectrum of the aluminized CPC walls is approximately 0.85. The average number of reflections is 0.9; therefore, the optical

transmission is $(0.85)^{0.9} = 0.86$. Another 4% loss due to reflections at the RTV-air interface near the surface of the cell also reduces the theoretically possible concentration ratio. The result of these losses is to reduce the expected concentration ratio from 6.9:1 to approximately 5.25:1. If the measured power concentration ratio of 5.7:1 is corrected by the increased cell performance under concentration (1.17), the concentration ratio achieved is 4.87:1, which is approximately 93% of the theoretical value. The 7% loss could be reduced by better alignment of the cells.

The hollow CPC panel has an efficiency of 7.1% over the panel area, yet an efficiency of 9.64% over its active area. As discussed previously, the packing factor of the panel could be increased by as much as 30% by design changes. Projecting the active area efficiency over a 0.96 packing factor would give a 9.25% panel efficiency. Figure III-8 shows the short-circuit current, I_{sc}, measured as a function of north-south tilt away from the normal to the sun. Theoretically, this curve should have a flat top out to ±6.25°, at which point it should drop abruptly to approximately one-eighth the peak value and continue to fall off at still larger tilt angles. The measured curve is flat for approximately ±4° from the normal (≥95% of peak), and has a full width at half maximum of approximately 14°. With better alignment of cells beneath the concentrators, both the short circuit current (and peak output power) and the acceptance angle would improve. The tilt adjustment schedule is given in Appendix C.

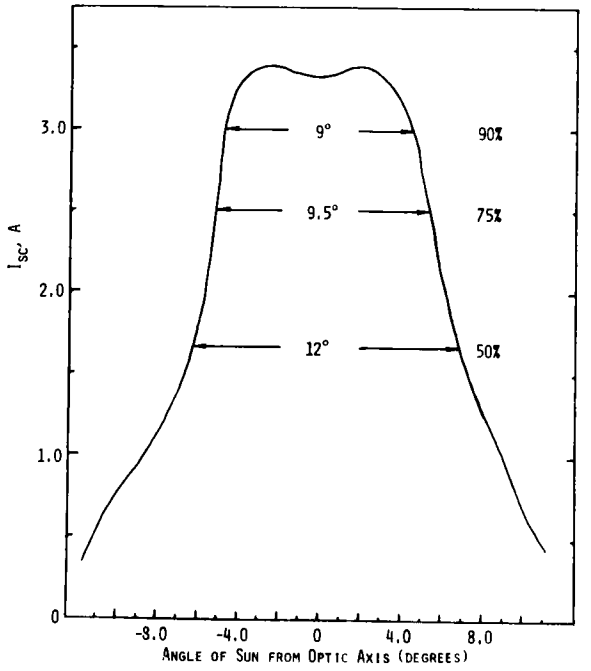

Fig. III-8.

Angular Acceptance of CPC Panel

IV. COST ANALYSIS

A. Introduction

The cost of electricity created by a photovoltaic panel of CPC's has been estimated for four types of CPC's. They are: (1) the dielectric (DCPC) trough; (2) the hollow CPC (HCPC) trough; (3) the DCPC cone;* and (4) the hollow CPC cone.* The cost estimates are compared with the work of Burgess[11] for collectors located at Albuquerque.

The estimates are based, where possible, on detailed analyses performed by others such as Mobil-Tyco[4] and Chamberlain Manufacturing Corp.[12] Where that is not possible, costs are based on material costs, with allowances for fabrication. A range of estimated costs is indicated from this work; more precise estimates of the cost would require a much more detailed analysis.

B. Formulation of the Cost Analysis

The cost estimates of the photovoltaic CPC array are consistent with the analysis performed by Burgess.[11] In particular, the array cost, K, is

$$K = \frac{24T}{W\eta_{cpc}\eta_{cell}}$$

where T = total cost per unit of aperture ($\$/m^2$),

W = average daily solar energy on the collector entrance aperture, taken from Table 2 of Ref. 11, $kWh/(m^2)(day)$,

η_{cpc} = optical efficiency of the CPC,

and η_{cell} = conversion efficiency of the cell.

The array cost, K, is the cost based on a 24-hr average power produced (avg kW), not on peak power produced (peak kW), which is often quoted. Basing the cost on average power produced gives a more realistic comparison of different collector types and different tracking schemes. Cost based on average power gives a realistic estimate of the power that can be produced under field conditions, but the cost is sensitive to geographic location. All cost estimates in this report are for Albuquerque, New Mexico.

---

*As a logical extension of the work on trough-type concentrators, cone-type concentrators were considered as possibly being more cost-effective. A few prototype cones were fabricated and preliminary measurements made on their concentration ratios.

The cost of a CPC panel per unit area of entrance aperture is the sum of the costs of several components, each having a different functional relationship to the total cost. The cost of silicon, C_{Si}, is divided by the concentration ratio, C'. In some situations, the cell will be larger than the exit aperture of the CPC and the cost of silicon must be multiplied by R, the ratio of cell area to exit aperture area. This situation arises when a small (2.5-mm-square) chip is to be mated to the round exit aperture (2.3-mm-dia) of a conical CPC.

The cost of reflector material, C_R, in $\$/m^2$ for the hollow CPC must be multiplied by a shape factor, f, that relates the area of the reflector to the exit aperture area as a function of collector geometry, and is then divided by the concentration ratio to base the cost on the entrance-aperture area. The shape factor for the DCPC's is similar, except that the cost of the reflector material, C_R, is in $\$/m^3$, and the shape factor, f, relates the volume of the dielectric material to the area of the exit aperture. The shape factor for the DCPC must then be divided by the concentration ratio to base the cost on the entrance-aperture area.

The shape factor, f, is defined as the amount of material used in the reflector divided by the exit aperture area. The shape factor is determined by approximating the CPC as either a trapezoidal prism (trough-type CPC) or a frustrum of a cone (conical CPC). The amount of material used by a hollow CPC is approximately equal to the area of the slanted sides of the trapezoid or the frustrum. The amount of material used in a dielectric CPC is approximately equal to the volume of the trapezoidal prism or the frustrum of a cone. The shape factors used in this analysis are summarized in Table IV-1.

The ratio h'/d_2, used in calculating the shape factor is derived from formulas in Refs. 4 and 13. For a trough-type CPC, the ratio is

$$\frac{h'}{d_2} = \left(1 + \sin\theta_m\right)\left[\frac{1}{2}\cos\theta_m + \frac{\cos^3\theta_m}{2\sin^2\theta_m} - \left(\frac{1}{\sin^2\theta_m}\right)\sqrt{\frac{1 - C'\sin\theta_m}{1 + \sin\theta_m}}\right.$$

$$\left. + \left(\frac{\cos\theta_m}{2\sin^2\theta_m}\right)\left(\frac{1 - C'\sin\theta_m}{1 + \sin\theta_m}\right)\right].$$

The result for a conical CPC is obtained by replacing C' with $\sqrt{C'}$.

TABLE IV-1. Shape Factors

Hollow trough	$f = 2\sqrt{\left(\frac{C' - 1}{2}\right)^2 + \left(\frac{h'}{d_2}\right)^2}$
Dielectric trough	$f = d_2\left(\frac{C' + 1}{2}\right)\left(\frac{h'}{d_2}\right)$
Hollow cone	$f = 2\left(\sqrt{C'} + 1\right)\sqrt{\left(\frac{\sqrt{C'} - 1}{2}\right)^2 + \left(\frac{h'}{d_2}\right)^2}$
Dielectric cone	$f = \frac{d_2}{3}\left(\frac{h'}{d_2}\right)\left(C' + \sqrt{C'} + 1\right)$

Lastly, the support and tracking costs, $(C_S + C_T)$, add directly to the cost of the panel. The total cost per unit area of panel is, therefore,

$$T = \frac{C_{Si}R}{C'} + \frac{C_R f}{C'} + C_S + C_T \ .$$

The optical efficiency of the CPC differs according to the type of optics used. For dielectric CPC's, the optical losses are reflection from the front surface and attenuation in the dielectric material. Because the dielectric CPC uses the principle of total internal reflection, the number of reflections does not enter into efficiency. Thus, the optical efficiency of the dielectric CPC (DCPC) is

$$\eta_{(dcpc)} = \tau_c e^{-\alpha h'}$$

Values of cover transmissivity,[14] $\tau_c = 0.96$, and extinction coefficient,[15] $\alpha = 1.02\ m^{-1}$, representing acrylic plastic have been used in this analysis.

For the hollow CPC's, the optical losses are reflections from the front cover (two surfaces) and absorption and scattering at the mirror surfaces. The optical efficiency for a hollow CPC is

$$\eta_{cpc} = \tau_c \rho^{<n>}$$

Values of cover transmissivity, $\tau_c = 0.92$, and reflectivity, $\rho = 0.88$, have been used in this analysis. Rabl[13] has calculated the average number of reflections, <n>, for hollow troughs at various values of θ_m and C'. The average number of reflections for a hollow cone can be conservatively estimated from Fig. 6 of Ref. 13 by using $\sqrt{C'}$ instead of C' as the abscissa and adding one to the number of reflections thereby obtained.

Mobil-Tyco[4] has determined empirically that the conversion efficiency of a silicon cell is a function of its temperature and the intensity of light falling on it. The empirical relationship, slightly modified for the application to this analysis, is

$$\eta_{cell} = 0.14 \left(\frac{C' \eta_{cpc}}{R} \right)^{0.1} \left(1 - 0.005T \right)$$

where T = cell temperature (°C). The cell temperature used in this analysis is 60°C.

A prototype DCPC trough panel has been built with a packing factor of 0.96 and a measured efficiency of 10.3% (10.7%, based on active aperture). This compares reasonably well with the efficiency of 10.9% with a packing factor of 1.00 used for the comparable collector in the cost analysis. In volume production, automated assembly methods will improve the panel efficiency by improving cell alignment with the exit aperture, the clarity of the dielectric material, the packing factor, and the bonding between the cells and the dielectric material. The cell temperature was not measured, but the temperature is believed to be well under the 60°C used in the cost analysis. The 60°C temperature is considered a worst-case condition.

Similarly, a prototype hollow CPC trough panel with a packing factor of 0.74 and a measured efficiency of 7.1% has been built (9.6% efficiency based on active aperture). This compares reasonably well with the efficiency of 9.6% with a packing factor of 1.00 used for the comparable collector in the cost analysis. Automated assembly methods will improve the panel efficiency by improving the

cell alignment, the mirror alignment, and the packing factor. As for the DCPC panel, the cell temperature is believed to be well under the 60°C assumed in the cost analysis. Thus, the prototype panels confirm the efficiency model used in the cost analysis.

C. Cost of Silicon

Burgess[11] has assumed alternative silicon costs of $\$2{,}000/m^2$, $\$200/m^2$ and $\$50/m^2$ for his cost estimates. The $\$2{,}000/m^2$ figure agrees reasonably well with current silicon costs. Spectrolab[16] has published an estimate for 1977 of $\$256/m^2$, but with current prices around $\$2{,}000/m^2$, their figure should be considered to be further in the future. Moore[17] indicates that $\$250/m^2$ is close to the ultimate limit for Czochralski crystals. Technological advances such as ribbon film growth, polycrystalline materials, thin-film semiconductors, and new materials may bring the cost of silicon below the Czochralski limit.

In this work, costs of $C_{Si} = \$2{,}000/m^2$ and $\$200/m^2$ are assumed to represent present and future costs in a manner consistent with Burgess.[11]

D. Cost of Dielectric Reflector Material

Acrylic is the material currently being used for dielectric CPC's. Its present cost in 40,000-lb lots is \$0.57/lb ($\$1{,}492/m^3$).[18] The cost of injection-molding and assembly labor would approximately double the cost of the acrylic to $\$2{,}984/m^3$.

Lower cost materials such as polystyrene (PS) could be used. The present cost of PS in 40,000-lb lots is \$0.28/lb ($\$660/m^3$).[19] Since PS has a higher index of refraction than does acrylic (1.6 vs 1.5), less PS is required to achieve a given concentration. PS is also easier to injection-mold than is acrylic. However, PS is slightly less transparent than acrylic, and it must be stabilized against exposure to ultraviolet light.

A transparent shell filled with a transparent liquid is another potential means of reducing cost. The liquid must not have severe freezing problems or large changes of volume with changing temperature; alternatively, the design must compensate for the expansion.

Alternative dielectric material costs used in this analysis are $C_R = \$1{,}492/m^3$, $\$2{,}984/m^3$, and $\$298/m^3$. The last number might be achievable using a liquid-filled shell.

E. Cost of CPC Reflector Material

Chamberlain Manufacturing Corp., after building prototype 3x CPC reflectors, did a detailed cost analysis of a 3x CPC panel using Kinglux reflectors.[12] In lots of 10,000 m^2, the cost of the reflector is \$12.18/m^2 of reflector, including assembly labor. Mobil-Tyco[4] did a similar analysis for a 5x CPC using 0.06-cm-thick polished aluminum reflectors. The cost of Mobil-Tyco's reflector was \$3.55/m^2 of reflector (\$11.98/m^2 of aperture). The Mobil-Tyco reflector cost appears to be optimistic since the current price of similar reflective material (Coilzak) is at least \$5/m^2 in large quantity.[20]

Another approach is to use vacuum-formed reflectorized plastic. A price of \$1.16 each in lots of 10,000 has been quoted to ANL[21] for 45.72 cm x 60.96 cm aperture CPC's formed of 0.08 cm clear PVC (\$4.173/m^2 of aperture). Metallization adds \$1.076/m^2, for a total of \$5.25/m^2 of aperture. Since the units are molded in one piece, little labor is required to assemble them. Larger sizes can be molded for greater savings in large quantities.

Costs of C_R of \$12.18/m^2 of reflector, \$5/m^2 of reflector, and \$5/m^2 of aperture are used for the hollow CPC calculations.

F. Cost of Support and Tracking

Costs of support and tracking are more difficult to determine because published data on the subject are vague or incomplete and subject to large variations. Burgess[11] indicates a cost of \$15/m^2 for a fixed flat-plate array. ANL has designed a solar collector support of 0.030-in.-thick aluminum capable of holding 4.2 m^2 of photovoltaic panel and weighing 30 kg. At a price of \$0.28/kg, the material cost is \$2.00/m^2. Allowing for labor (1 hr/m^2 at \$4/hr) and a 1/8-in. glass cover (\$5/m^2), the total cost of the support would be \$11/m^2.

Chamberlain Mfg. Corp.[12] indicates a cost of \$2.06/m^2 for their substrate plus tooling costs of \$0.22/m^2 for a total of \$2.28/m^2 to cover the cost of supports. Made of rolled sheet aluminum, the Chamberlain collector is nearly self-supporting and thus requires little additional support. Chamberlain lumped labor costs together with reflector cost, and the cost of a transparent cover is not included in the Chamberlain estimate.

Mobil-Tyco[4] estimates a cost of \$50.88/m^2 for supports for an unoptimized collector that is similar to Chamberlain's collector. Included in the

estimate for supports are aluminum ribs (two types), 0.32 cm glass cover, 1.59 cm plywood, adhesives, coatings, and screws. Labor is estimated at $\$16.39/m^2$ additional.

The trough-type CPC with an east-west orientation requires only seasonal adjustments. Support and tracking costs of a trough-type CPC would be only slightly more than support and tracking costs for a flat-plate collector.

Because of its total acceptance angle of 9°, a conical CPC can use a relatively crude 2-axis tracking system having the same geometry as the equatorial mount for astronomical telescopes. Astronomical telescopes use a simple clock drive for tracking, but a conical CPC does not require such continuous tracking. The conical CPC requires adjustment in the equatorial plane at 20 to 30-min intervals. The second axis adjustment (in the plane of the zenith) requires only 8 to 12 manual adjustments per year to account for the declination of the sun. A focusing system with an acceptance angle of about 1/2° requires more accurate tracking.

American Science Center, Inc. sells telescope clock drives for $69.50 and $89.50, retail.[22] If protection from wind is provided and if the collector is well balanced, such a clock drive could power 2-4 m^2 of solar panel. Allowing for retail markup, the cost would be $\$5\text{-}15/m^2$ plus the cost of bearings and the cost of enclosing the collector. Enclosing the collector in a transparent hemisphere eliminates the need for a cover attached to the collector, but requires about twice as much transparent material.

With the costs indicated above, the lower limit for support and tracking cost, $C_S + C_T$, appears to be about $\$15/m^2$. Support and tracking costs $(C_S + C_t)$ as large as $\$50/m^2$ have also been calculated to indicate a range of costs.

G. Discussion of Numerical Calculations

1. DCPC Trough

Calculated electricity costs per average kW vs concentration ratio are plotted in Figs. IV-1 and IV-2 for silicon costs of $\$2{,}000/m^2$ and $\$200/m^2$, respectively. A total acceptance angle of 19° with east-west trough

alignment and seasonal adjustment of tilt are assumed. No attempt was made to determine the optimum combination of acceptance angle and truncation.

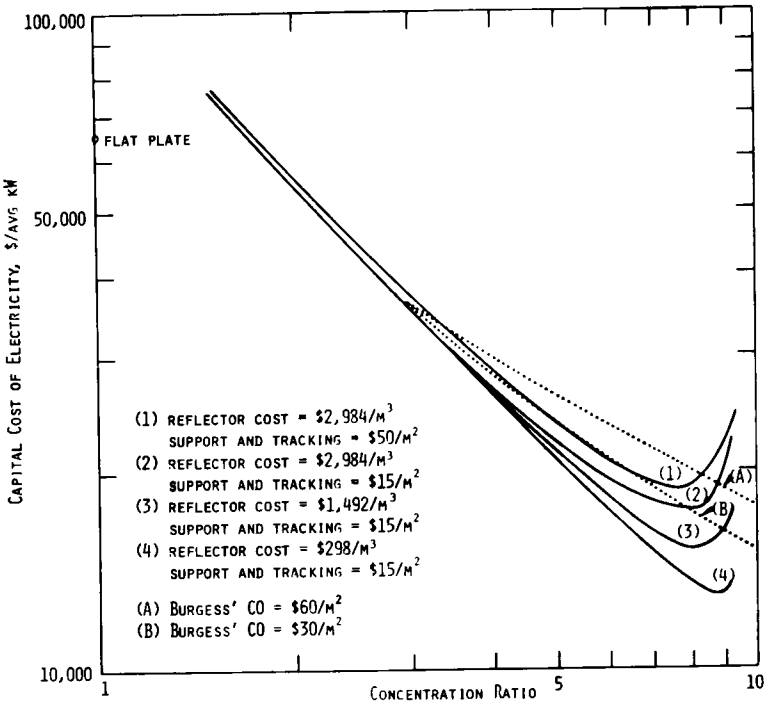

Fig. IV-1. Estimated Cost of Electricity for a DCPC Trough at Albuquerque, NM, with a Silicon Cost of $\$2,000/m^2$. CO = Cost of Optics.

A prototype panel of DCPC troughs having a small concentration ratio at right angles to the main concentration has been built, but the small concentration ratio was not included in this calculation.

Assuming a silicon cost of $\$2,000/m^2$, the electricity cost estimates are comparable to Burgess' lower estimate.[11] Even the worst case (C_R = $\$2,984/m^3$ and $C_S + C_T$ = $\$50/m^2$) is comparable to Burgess' estimate for combined cost of optics, support, and tracking of $\$30/m^2$. The reason for the improved performance estimate is that the DCPC trough has a higher optical efficiency than the 75% assumed by Burgess. At present silicon prices, the cost of electricity using a DCPC trough is estimated to be \$13,000-20,000/avg kW, compared with about \$65,000/avg kW for a flat-plate collector.

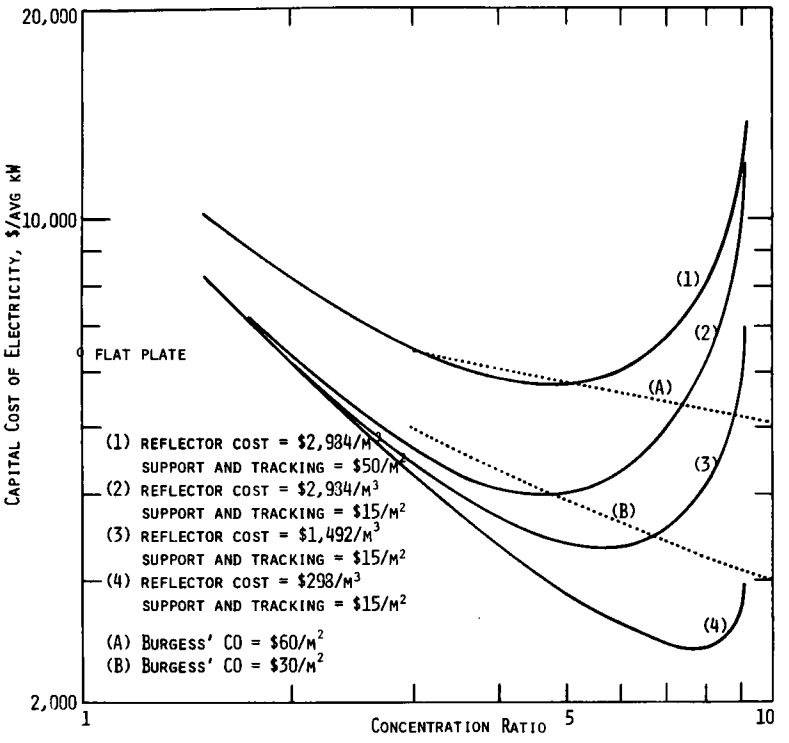

Fig. IV-2. Estimated Cost of Electricity for a DCPC Trough at Albuquerque, NM, with a Silicon Cost of $\$200/m^2$. CO = Cost of Optics.

2. Hollow CPC Trough

Calculated electricity costs per kW vs concentration ratio are plotted in Figs. IV-3 and IV-4 for silicon costs of $\$2,000/m^2$ and $\$200/m^2$, respectively. A total acceptance angle of 12° was assumed, but other assumptions are similar to those for the DCPC trough.

As shown in Figs. IV-3 and IV-4, the electricity cost estimates for the hollow CPC trough are comparable to Burgess' estimates,[11] but they are slightly higher than the estimated cost for the DCPC trough. This is because the optical efficiency of the hollow CPC trough is less than the optical efficiency of the DCPC trough. With present silicon prices, the cost of electricity produced by the hollow CPC trough is estimated to be in the $14,000-20,000/avg kW range compared with about $65,000/avg kW for a flat-plate collector.

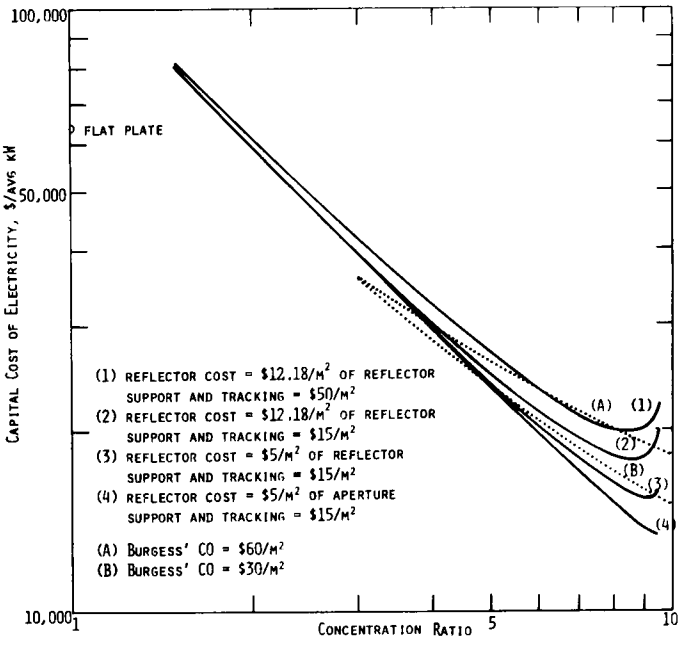

Fig. IV-3. Estimated Cost of Electricity for a HCPC Trough at Albuquerque, NM, with a Silicon Cost of $\$2,000/m^2$. CO = Cost of Optics.

3. DCPC Cone

Calculated electricity costs per average kW vs concentration ratio for the DCPC cone are plotted in Figs. IV-5 and IV-6 for silicon costs of $\$2,000/m^2$ and $\$200/m^2$, respectively. As shown, the cost estimates for the DCPC cone are comparable to Burgess' lower estimates,[11] although no attempt to optimize the combination of acceptance angle and truncation of the DCPC has been made. The cost advantage of the DCPC cone improves with declining silicon cost.

There are several reasons for the excellent cost performance of the DCPC cone. (1) The wide acceptance angle of the DCPC, in comparison to that of a parabolic dish, gives the performance of 2-axis tracking at the cost of 1-axis tracking. A tracking accuracy of ±4.5° is required for the conical CPC, compared with a tracking accuracy of ±0.25° for the parabolic dishes and troughs. (2) The dielectric CPC has a high optical efficiency in comparison with other collectors. Typical optical efficiencies are above 90%. Only one

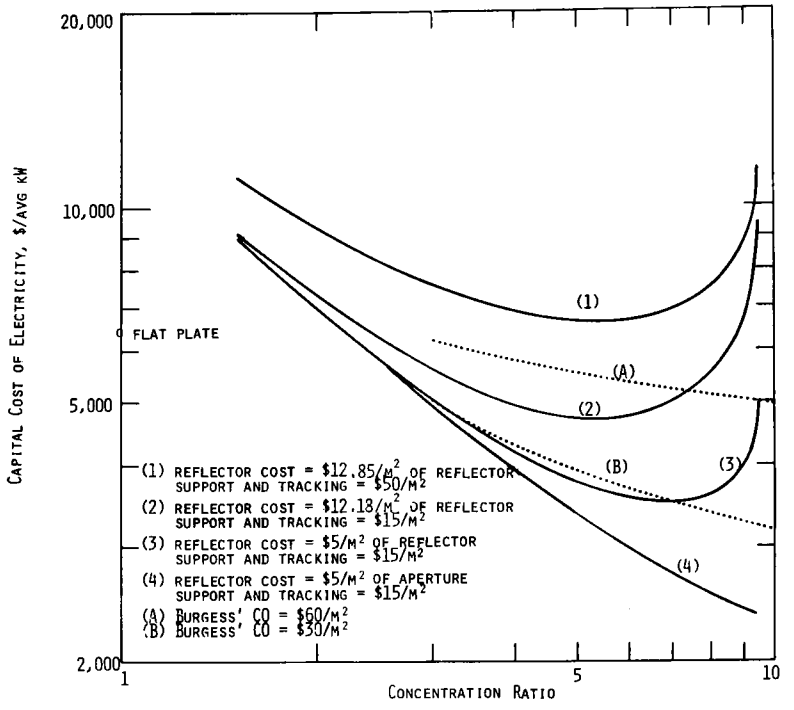

Fig. IV-4. Estimated Cost of Electricity for a HCPC Trough at Albuquerque, NM, with a Silicon Cost of $\$200/m^2$. CO = Cost of Optics.

air-dielectric interface is encountered by the light beam, the reflectivity of the walls is effectively 1.00 due to total internal reflection, and acrylic is an extremely transparent material. (3) As indicated by Mobil-Tyco,[4] the power output of the cell increases to the 1.1 power of light intensity. With a high concentration ratio, cell efficiency can be more than 12%, even at 60°C. At present silicon prices, the cost of electricity using a DCPC cone is estimated to be in the $1,000-3,000/avg kW range.

4. Hollow CPC Cone

Calculated electricity costs per average kW vs concentration ratio are plotted in Figs. IV-7 and IV-8 for silicon costs of $\$2,000/m^2$ and $\$200/m^2$, respectively. Most of the comments regarding the DCPC cone are applicable to the hollow CPC cone.

The hollow CPC cone has slightly higher estimated electricity costs than does the DCPC cone. The material costs of the hollow CPC cone are slightly higher and the optical efficiency is lower than are corresponding parameters for the DCPC cone.

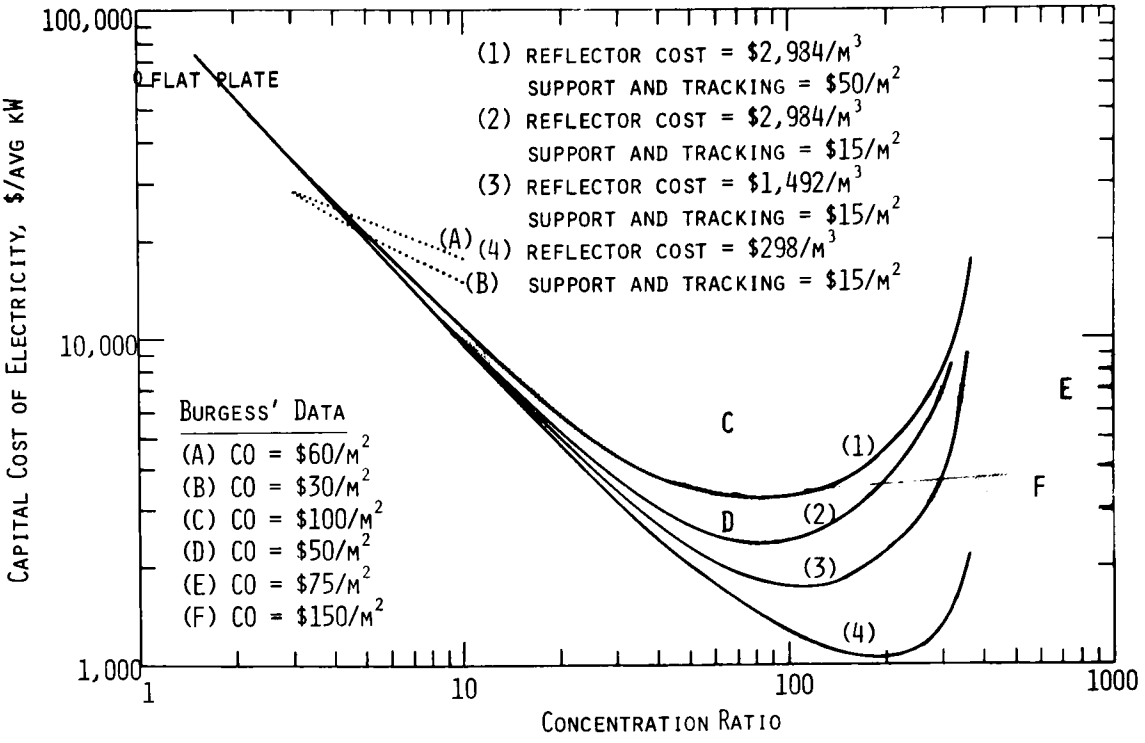

Fig. IV-5. Estimated Cost of Electricity for a DCPC Cone at Albuquerque, NM, with a Silicon Cost of $\$2,000/m^2$. CO = Cost of Optics.

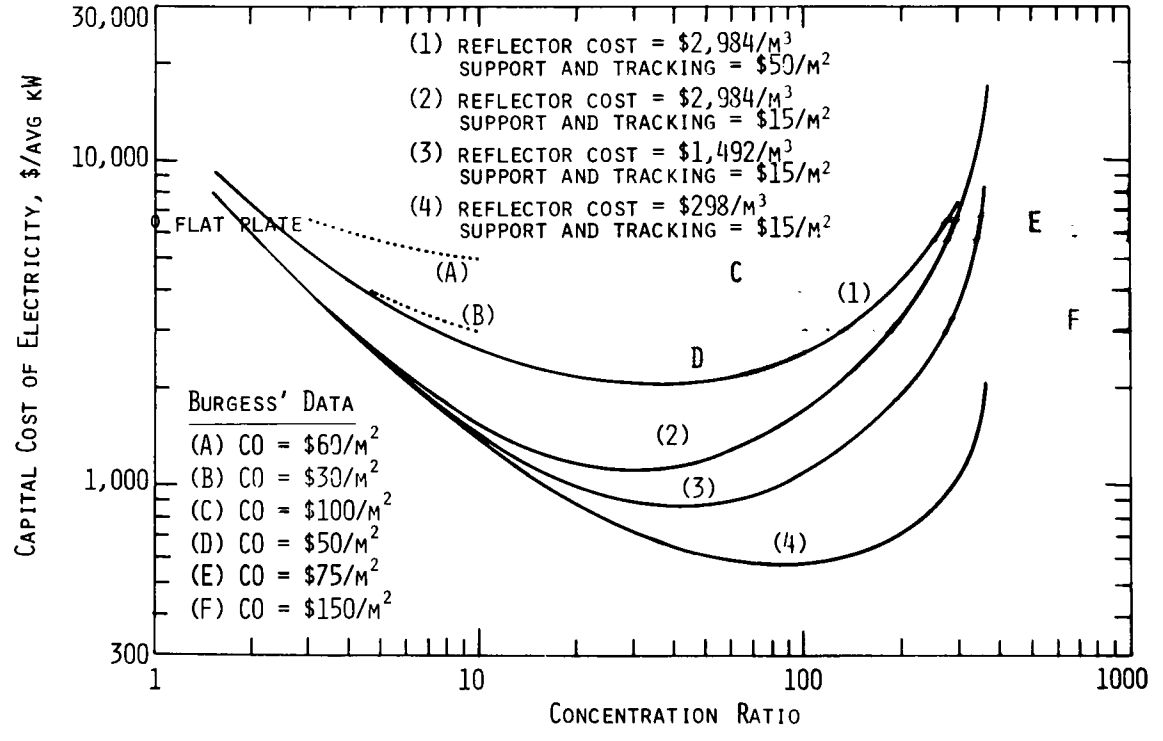

Fig. IV-6. Estimated Cost of Electricity for a DCPC Cone at Albuquerque, NM, with a Silicon Cost of $\$200/m^2$. CO = Cost of Optics.

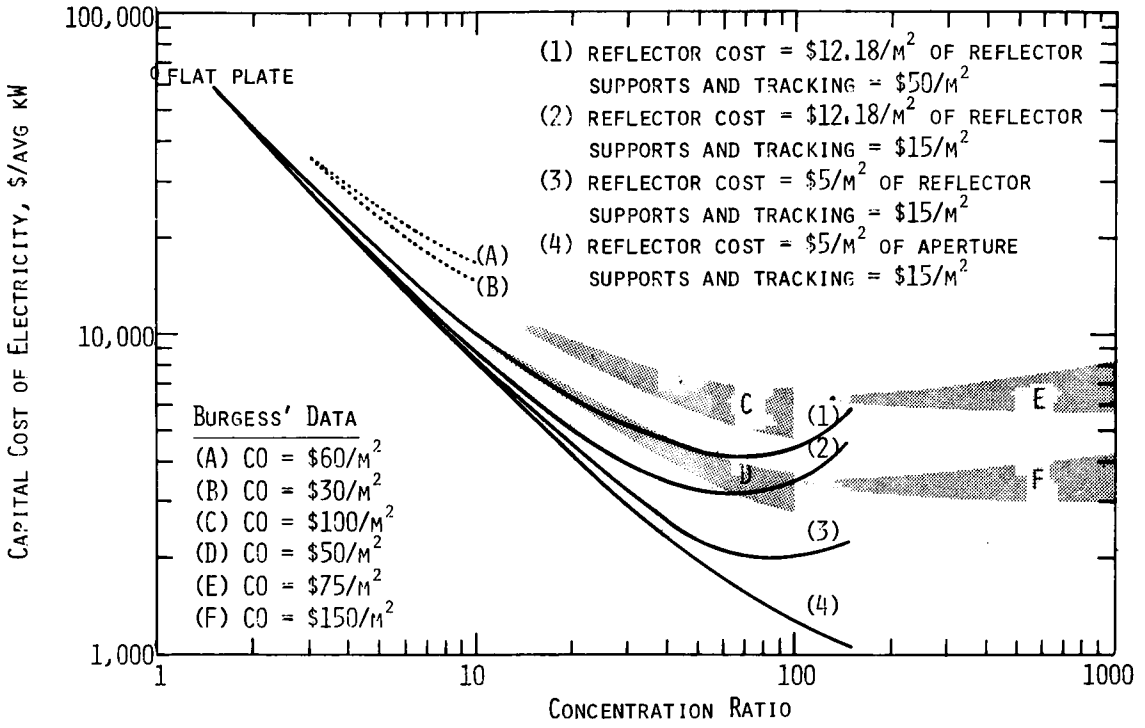

Fig. IV-7. Estimated Cost of Electricity for a Hollow CPC Cone at Albuquerque, NM, with a Silicon Cost of $\$2,000/m^2$. CO = Cost of Optics.

The cost curve of the hollow CPC cone, based on vacuum-formed sheet plastic (C_R = $\$5/m^2$ of aperture), does not show the minimum in the cost curve characteristic of other methods of manufacture. That is because the cost of the vacuum-formed reflector is based on aperture area rather than reflector area or volume. In practice, the maximum concentration ratio that can be vacuum-formed is limited by tearing of the plastic as it is stretched in the mold. Lower concentration ratios require less stretching.

At present silicon prices, the cost of electricity using a hollow CPC cone is estimated to be in the $1,500-4,000/avg kW range.

5. Cost of Electricity per Peak Watt

The cost of electricity per peak watt has been estimated, and the results are shown in Figs. IV-9 and IV-10. The curves in Figs. IV-9 and IV-10 correspond to corresponding curves labeled "(1)" in Figs. IV-1 through IV-8. The cost of energy per peak watt, K_p, is

$$K_p = \frac{T}{I\,\eta_{cpc}\eta_{cell}}$$

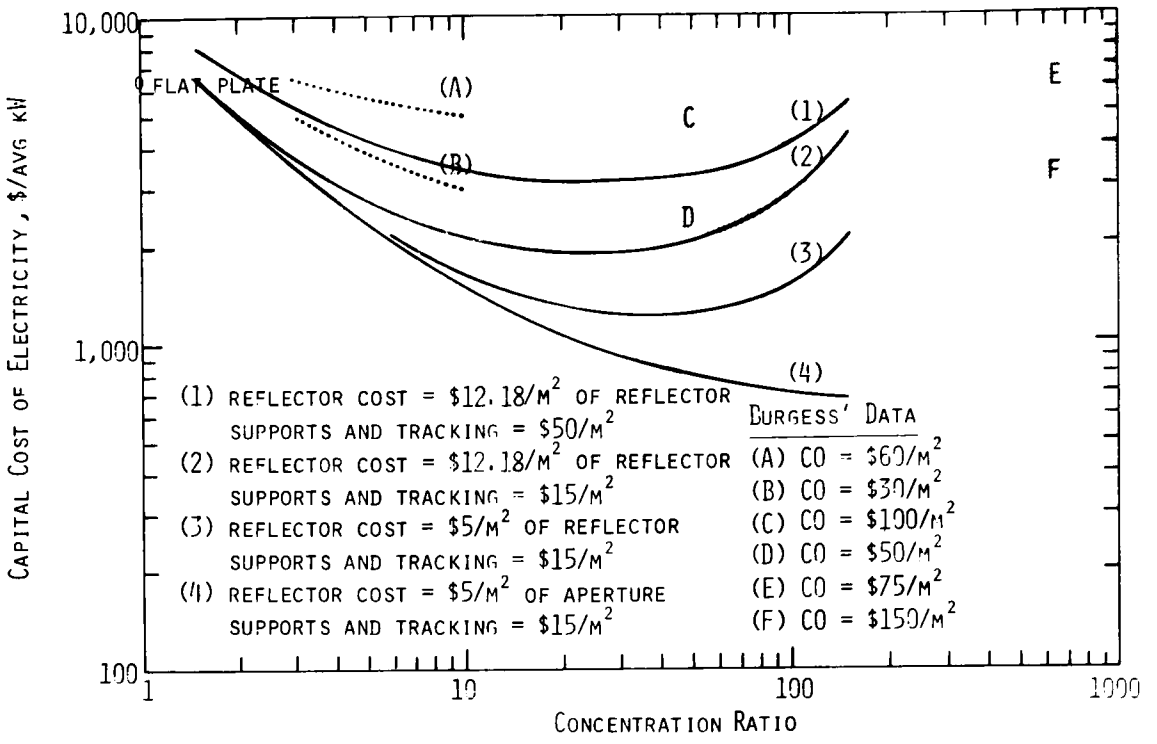

Fig. IV-8. Estimated Cost of Electricity for a Hollow CPC Cone at Albuquerque, NM, with a Silicon Cost of $\$200/m^2$. CO = Cost of Optics.

where T, η_{cpc}, and η_{cell} have been previously defined and I = 1000 W/m^2 is the peak intensity of sunlight. The reader is cautioned that comparing the cost of electricity produced by different collectors can be misleading if the cost is based on peak wattage.

H. Summary

Based on the efficiency model that has been confirmed by the two prototype panels and on material and component cost data, photovoltaic Compound Parabolic Concentrators (CPC's) can produce electricity at lower cost than flat-plate photovoltaic arrays. The cost reductions are significant in comparison to a flat-plate array, even if the cost of silicon should be decreased by one order of magnitude. The value of the DCPC concept was recognized by the Industrial Research magazine review committee (Appendix E).

If electricity cost figures are to be used for comparing different collectors, the cost figures should be based on 24-hr average power produced (avg kW), not peak power produced (peak kW). The cost per average power

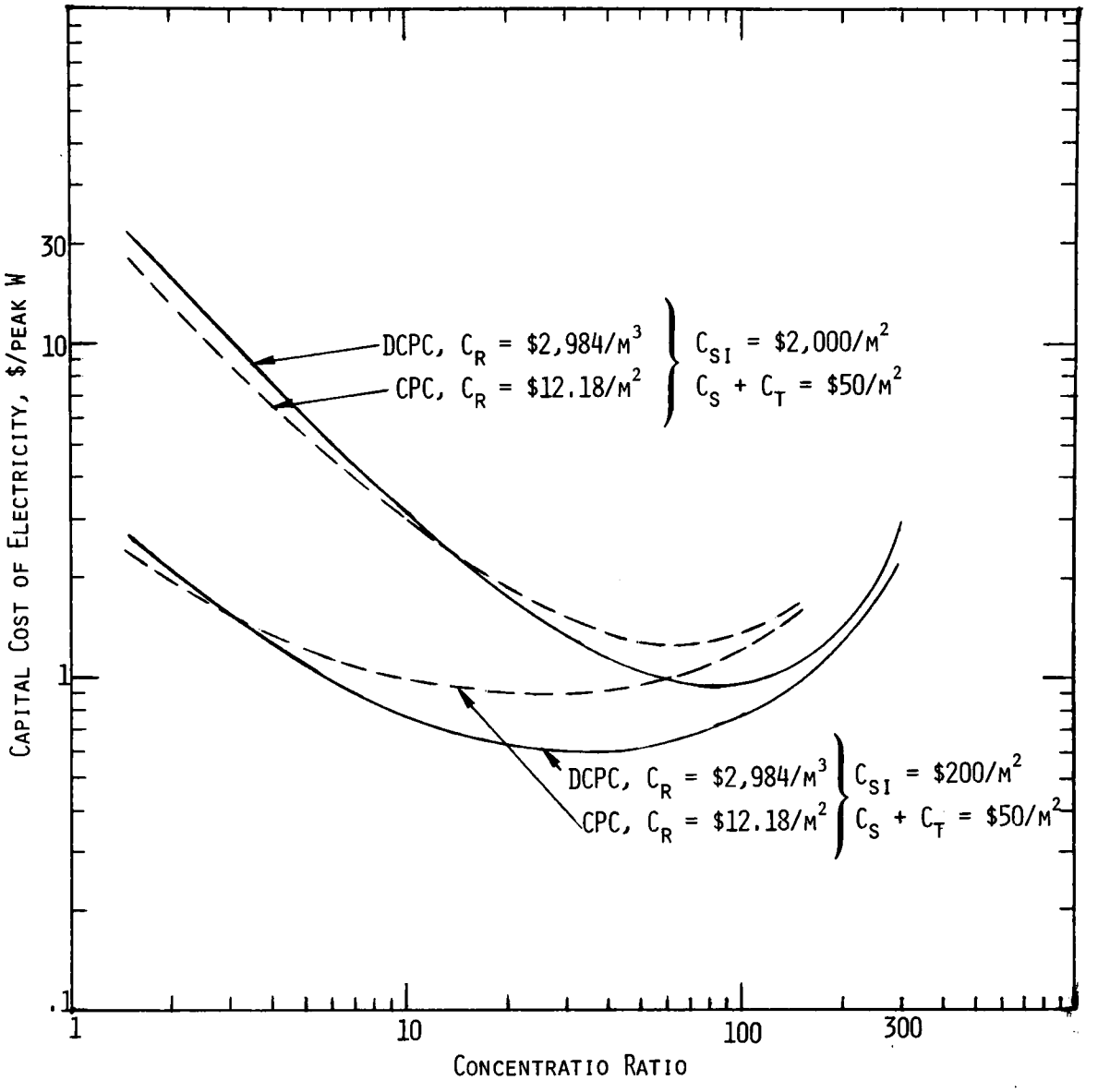

Fig. IV-9. Cost (Per Peak Watt) of Electricity for DCPC and HCPC Cones. I = 1000 W/m^2.

produced gives a more realistic comparison of different collector types than does cost per peak power. It is, however, dependent on geographic location. All cost figures in this work are for Albuquerque, New Mexico.

At current silicon prices, the estimated cost of electricity produced with a DCPC trough is in the $13,000-20,000/avg kW range at Albuquerque, New Mexico, and the estimated cost of electricity produced by the hollow CPC trough is in the $14,000-20,000 avg kW range. A flat-plate photovoltaic array would cost about $65,000/avg kW at Albuquerque.[11] If silicon cost is decreased

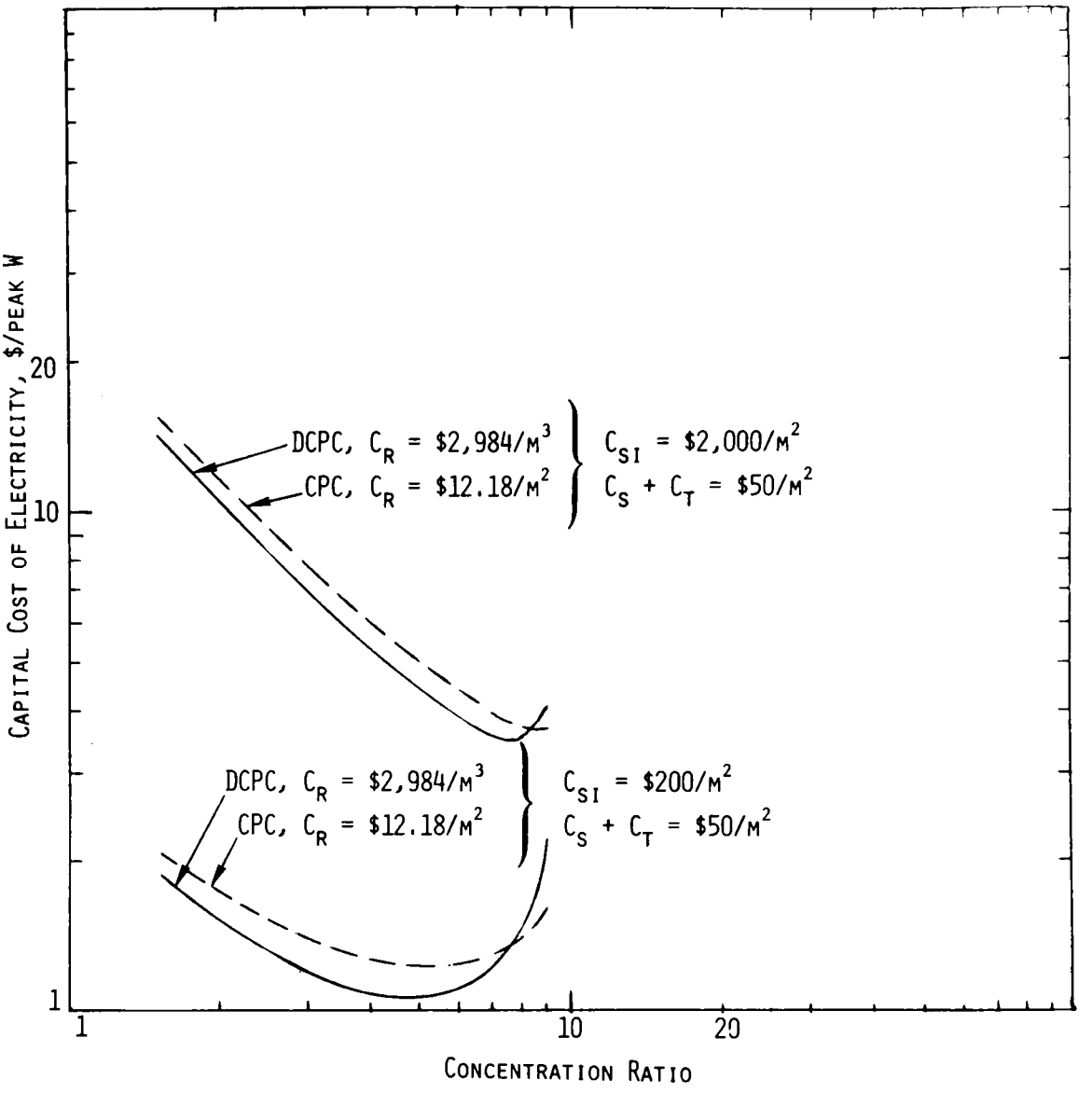

Fig. IV-10. Cost (Per Peak Watt) of Electricity for DCPC and HCPC Troughs. I = 1000 W/m^2.

by one order of magnitude, the estimated costs of electricity will be \$2,400-4,000/avg kW, \$2,400-4,700/avg kW, and about \$6,500/avg kW for the DCPC trough, the hollow CPC trough, and the flat-plate photovoltaic array, respectively.

Although the trough-type CPC's offer significant cost savings compared to a flat-plate photovoltaic array, the conical CPC's offer an even greater cost saving. At current silicon prices, the estimated cost of electricity produced by the DCPC cone is in the \$1,000-3,000/avg kW range, and the estimated cost of electricity produced by the hollow CPC cone is in the \$1,500-4,000/avg

kW range. The cost for a flat photovoltaic array is about $65,000/avg kW. If silicon cost is decreased by one order of magnitude, the estimated costs of electricity are $600-2,000/avg kW, $700-3,000/avg kW, and about $6,500/avg kW for the DCPC cone, the hollow CPC cone, and the flat photovoltaic array, respectively.

APPENDIX A

DCPC Panel Assembly Drawings

PART NO.	DRAWING NO.	PART NAME OR DESCRIPTION	REMARKS	FOR PURCH. PARTS ONLY MATERIAL	QTY.
	CE-EG912	SILICON SOLAR CELL MODULE-LAYOUT	SHT. 1 OF 5		
	CE-DG912	MODULE SECTIONS	SHT. 2 OF 5		
	CE-CG912	MODULE SECTIONS	SHT. 3 OF 5		
	CE-CG912	MODULE SECTIONS	SHT. 4 OF 5		
	CE-CG912	COLLECTOR ATTACHMENT LAYOUT	SHT. 5 OF 5		
	CE-CG912-1	HEAT SINK MODIFICATION	(REPLACES DWG CE-BG912-1)		
	CE-BG912-2	FRAME DRILL JIG		C1020 CRS	1
	CE-AG912-3	HEAT SINK DRILL JIG ADAPTER		AL 6061-T6	1
	CE-CG912-4	ACRYLIC COLLECTOR DRILL JIG ADAPTER	(SHOPS OPTION TO USE)	PLEXIGLASS	1
1		CHANNEL 3U 1.42 x 49" LG.		AL 6061-T6	4
2		SUPPORT T 2 x 1 x .421# x 49 3/8 LG.		AL 6061-T6	3
		OR SUBSTITUTE: 2 ANGLES L 1 x 1 x 1/8 x 49 3/8 BACK TO BACK			(6)
3		SUPPORT L 3 x 2 x 1/4 x 46 1/8 LG.		AL 6061-T6	2
4		GUARD ANGLE L 2 x 1 1/2 x 1/4 x 47 5/8 LG		AL 6061-T6	2
5		ANGLE, CLIP (WELD TO PT. NO 2) L 3/4 x 3/4 x 1/8 x 1 1/4" LG.		AL 6061-T6	12
6		ANGLE, CLIP L 1 1/4 x 1 1/4 x 1/4 x 2 LG.		AL 6061-T6	4

SYM.	CHANGE	BY	CK.	DATE

THIS PARTS LIST IS THE PROPERTY OF
ARGONNE NATIONAL LABORATORY

ASSEMBLY SILICON SOLAR CELL MODULE

SHEET 1 OF 5

APP'D	RMG 4-30-76	ASSEMBLY NO.
CHECKED	RMG 4-30-76	CE-EG912
DRAWN	JM 4-28-76	

ANL-146 (4-62) ENGINEERING PARTS LIST

PART NO.	DRAWING NO.	PART NAME OR DESCRIPTION	REMARKS	FOR PURCH. PARTS ONLY MATERIAL	QTY.
		SILICON SOLAR CELL MODULE			
7		SOLAR COLLECTOR, DCPC		ACRYLIC	240
		PHOTOVOLTAIC CELL			
8	CE-C6912-1	HEAT SINK - "WAKEFIELD" ALUMINUM EXTRUSION #4471 - MODIFY PER DWG.		AL	20

SYM.	CHANGE	BY	CK.	DATE

THIS PARTS LIST IS THE PROPERTY OF
ARGONNE NATIONAL LABORATORY

ASSEMBLY SILICON SOLAR CELL MODULE

SHEET 2 OF 5

APP'D	RMG	7.30.76
CHECKED	RMG	7.30.76
DRAWN	JM	7.29.76

ASSEMBLY NO. CE-E6912

ANL-146 (4-62) ENGINEERING PARTS LIST

PART NO.	DRAWING NO.	PART NAME OR DESCRIPTION	REMARKS	FOR PURCH. PARTS ONLY MATERIAL	QTY.
		SILICON SOLAR CELL MODULE			
9	CE-AG925-2	STAND, SUPPORT		304S.STL	80
10		SCREW - HEX HD CAP - 1/4-20 x 7/8" LG (ANGLES TO CHANNELS)		6.STL	32
11		SCREW-SHOULDER-1/4 DIA x 1/4 LG - NYLOK		S.STL.	80
12		SCREW - FL. HD. SOC. CAP - #10-24 x 1/2 LG. - NYLOK		S.STL.	80
13		SCREW - HEX. HD. CAP - 1/4-20 x 1/2 LG. NYLOK (IN CLIP ANGLES)		S.STL.	8
14		SCREW - HEX. HD. CAP - 1/4-20 x 3/4 LG (IN CLIP ANGLES)		S.STL.	20

SYM.	CHANGE	BY	CK.	DATE

THIS PARTS LIST IS THE PROPERTY OF
ARGONNE NATIONAL LABORATORY

ASSEMBLY SILICON SOLAR CELL MODULE — SHEET 3 OF 5

APP'D	RMG	7.30.76	ASSEMBLY NO. CE-E6912
CHECKED	RMG	7.30.76	
DRAWN	GM	7.29.76	

ANL-146 (4-62) ENGINEERING PARTS LIST

PART NO.	DRAWING NO.	PART NAME OR DESCRIPTION	REMARKS	FOR PURCH. PARTS ONLY MATERIAL	QTY.
		SILICON SOLAR CELL MODULE			
15		NUT, HEX - 1/4-20 (ON CLIP ANGLES)		S. STL	20
16		LOCKWASHER - 1/4 STD. (ON CLIP ANGLES)		S. STL	20
17		SPRING - "LEE" COMPRESSION - PT. Nº LC-042D-1		S. STL.	80
18		CONTAINER - SPRING.		S. STL.	80
19		ROD, THREADED - .094 DIA. x 2 5/8" LG.		S. STL	80
20		WASHER 1/4" O.D. x 9/64 I.D. x 1/32 THK.		S. STL	80

SYM.	CHANGE	BY	CK.	DATE

THIS PARTS LIST IS THE PROPERTY OF
ARGONNE NATIONAL LABORATORY

ASSEMBLY SILICON SOLAR CELL MODULE — SHEET 4 OF 5

APP'D	RMG	7.30.76
CHECKED	RMG	7.30.76
DRAWN	JM	7.29.76

ASSEMBLY NO. CE-EG012

ANL-146 (4-62) ENGINEERING PARTS LIST

PART NO.	DRAWING NO.	PART NAME OR DESCRIPTION	REMARKS	FOR PURCH. PARTS ONLY MATERIAL	QTY.
		SILICON SOLAR CELL MODULE			
21		CAP-"CAPLUG" #7		POLYETH-YLENE	80
22		PLASTIC SHEET		PLASTIC	1
		2 1/2" WIDE x " THK. x 75 FT LG.			
23		ALUMINUM SHEET		AL.	20
		2 WIDE x 24 GA. THK x 44 1/2 LG.			
24		RTV ADHESIVE		AS REQUIRED	
25		1/4-20 HEX NUT		S.STL.	32
26		1/4 STD. LOCKWASHER		S.STL.	32
27		Ph. V CELL 0.112 x .012 x 1.012 LG.			240
28		HEAT SINK .600 x .010 x 1.065 LG.			240
29		INSULATING SHEET - 9 7/8 x . x 11 3/4 LG.			20

SYM.	CHANGE	BY	CK.	DATE

THIS PARTS LIST IS THE PROPERTY OF
ARGONNE NATIONAL LABORATORY

ASSEMBLY SILICON SOLAR CELL MODULE — SHEET 5 OF 5

APP'D	RMC	4.30.76
CHECKED	RMC	4.30.76
DRAWN		4.29.76

ASSEMBLY NO. CE-E 6912

ANL-146 (4-62) ENGINEERING PARTS LIST

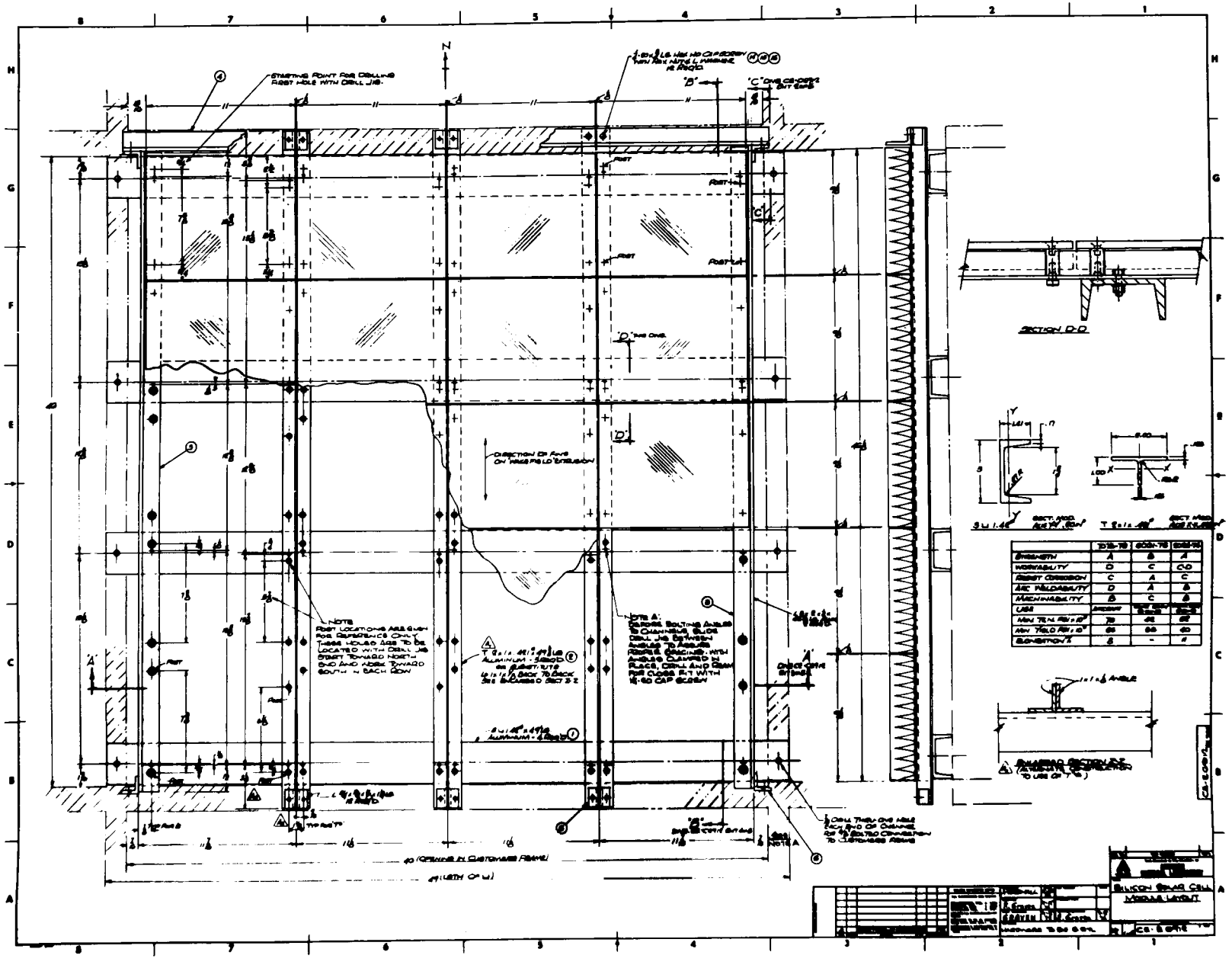
SECTION D-D
SILICON SOLAR CELL MODULE LAYOUT

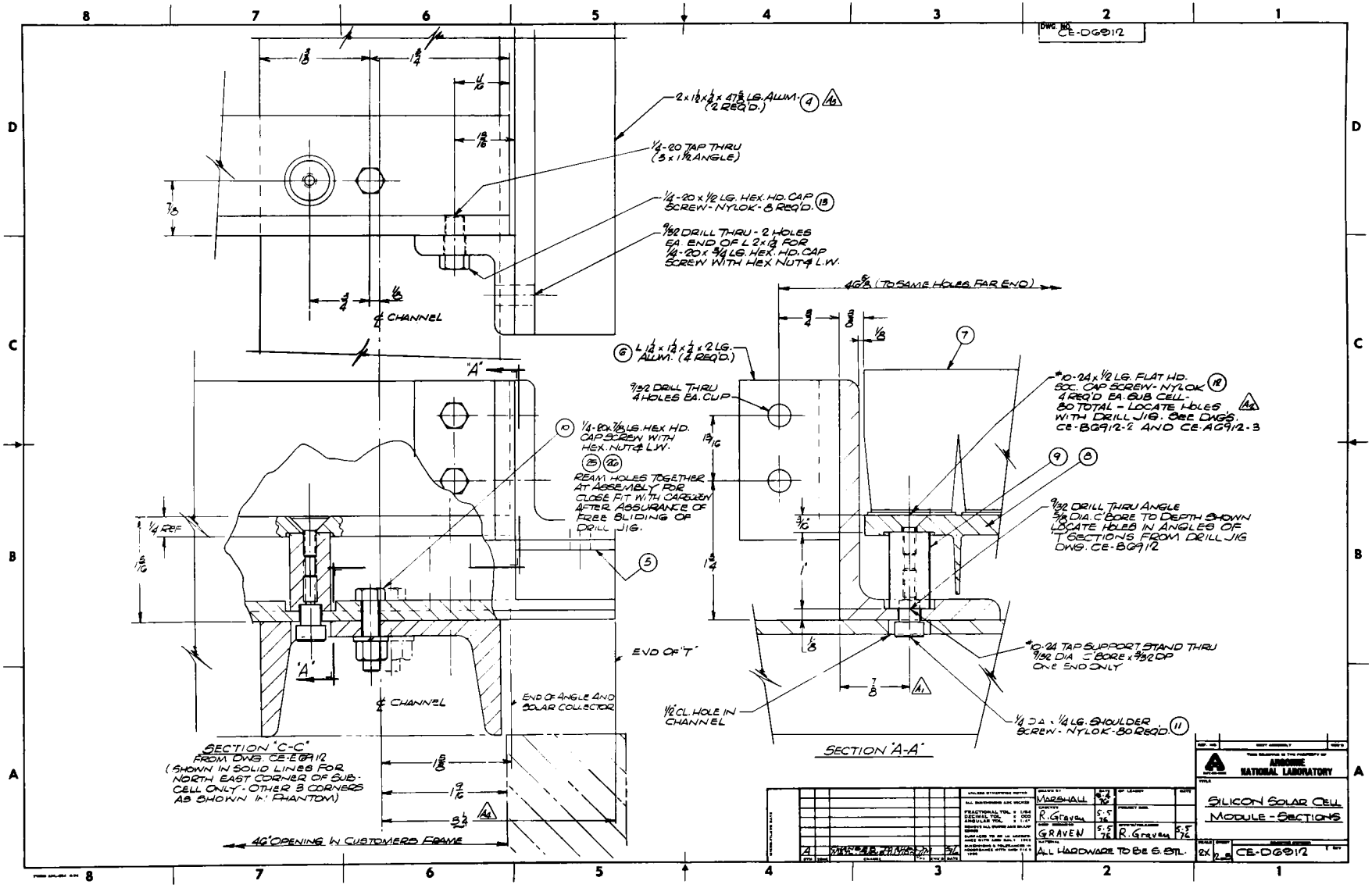
DWG NO. CE-DG912
2 x 1⅛ x ⅛ x 47⅝ LG. ALUM. (4) (2 REQ'D.)
¼-20 TAP THRU (3 x 1½ ANGLE)
¼-20 x ½ LG. HEX. HD. CAP SCREW - NYLOK - 8 REQ'D. (13)
9/32 DRILL THRU - 2 HOLES EA. END OF L 2 x ⅛ FOR ¼-20 x ¾ LG. HEX. HD. CAP SCREW WITH HEX NUT & L.W.
℄ CHANNEL
"A"
46⅝ (TO SAME HOLES FAR END)
(6) L 1½ x 1½ x ⅛ x 2 LG. ALUM. (4 REQ'D.)
(7)
9/32 DRILL THRU 4 HOLES EA. CUP
#10-24 x ½ LG. FLAT HD. SOC. CAP SCREW - NYLOK (18) 4 REQ'D EA. SUB CELL - 80 TOTAL - LOCATE HOLES WITH DRILL JIG. SEE DWGS. CE-BG912-2 AND CE-AG912-3
(10) ¼-20 x ⅞ LG. HEX HD. CAP SCREW WITH HEX. NUT & L.W. (25) (26)
REAM HOLES TOGETHER AT ASSEMBLY FOR CLOSE FIT WITH CARBURN AFTER ASSURANCE OF FREE SLIDING OF DRILL JIG.
(9) (8)
9/32 DRILL THRU ANGLE 5/8 DIA. C'BORE TO DEPTH SHOWN LOCATE HOLES IN ANGLES OF "T" SECTIONS FROM DRILL JIG DWG. CE-BG912
¼ REF
(5)
"A"
END OF "T"
℄ CHANNEL
END OF ANGLE AND SOLAR COLLECTOR
#10-24 TAP SUPPORT STAND THRU 9/32 DIA C'BORE x 9/32 DP ONE END ONLY
½" CL. HOLE IN CHANNEL
¼ DIA x ¼ LG. SHOULDER SCREW - NYLOK - 80 REQ'D. (11)
SECTION "C-C" FROM DWG. CE-EB912 (SHOWN IN SOLID LINES FOR NORTH EAST CORNER OF SUB-CELL ONLY - OTHER 3 CORNERS AS SHOWN IN PHANTOM)
46" OPENING IN CUSTOMERS FRAME
SECTION "A-A"
ARGONNE NATIONAL LABORATORY
SILICON SOLAR CELL MODULE - SECTIONS
MARSHALL
R. GRAVEN
ALL HARDWARE TO BE S. STL.
CE-DG912

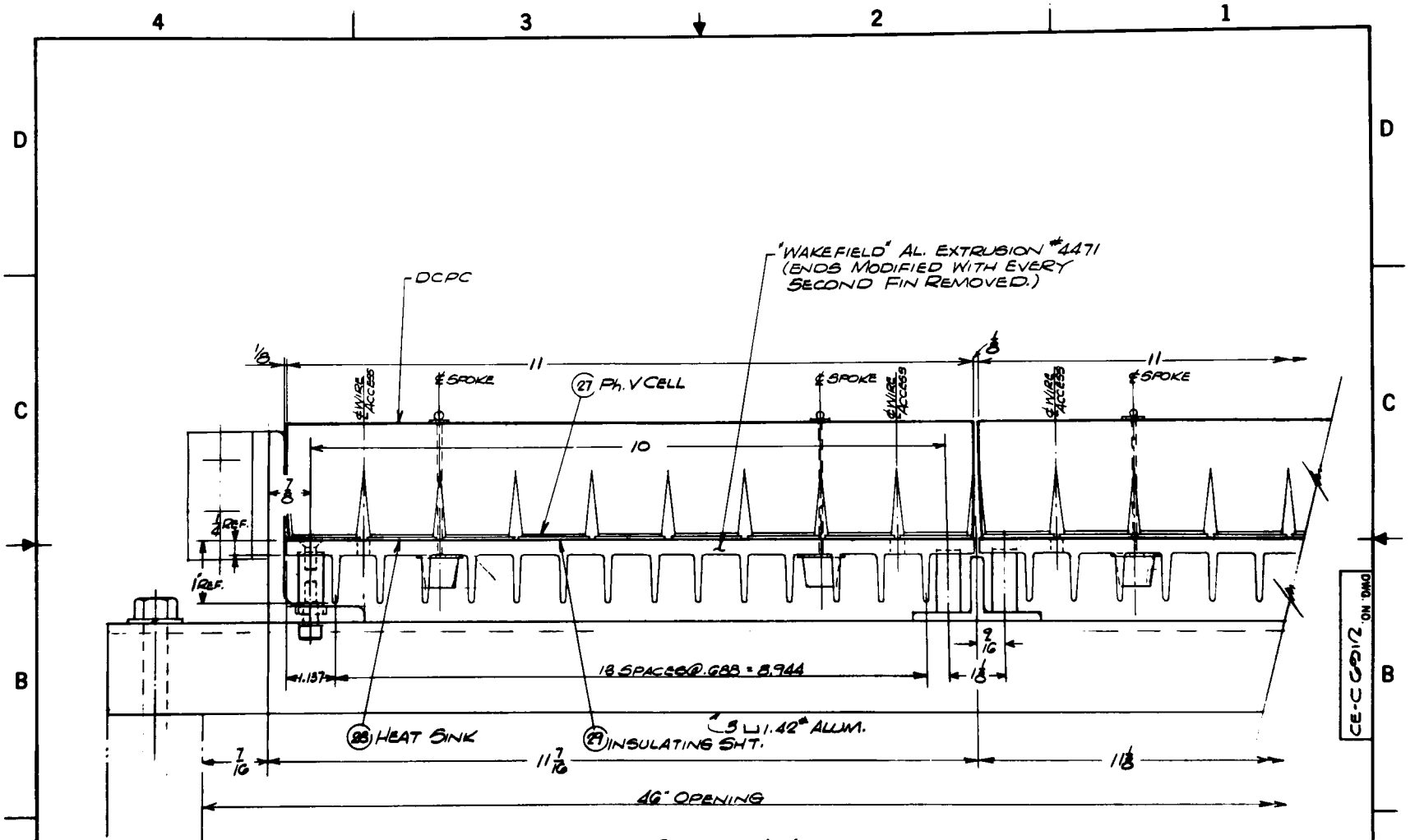
'WAKEFIELD' AL. EXTRUSION #4471
(ENDS MODIFIED WITH EVERY
SECOND FIN REMOVED.)
DCPC
℄ WIRE ACCESS
℄ SPOKE
27 PH. V CELL
10
11
1/8
7/8
1/2 REF.
1 REF.
1.157
18 SPACES @ .688 = 8.944
9/16
1/8
28 HEAT SINK
29 INSULATING SHT.
3 LU 1.42# ALUM.
7/16
11 7/16
40" OPENING
SECTION A-A
FROM DWG. CE-EGOI2
CE-CGOI2
DWG. NO.
ARGONNE
NATIONAL LABORATORY
SILICON SOLAR CELL
MODULE - LAYOUT
CE-CGOI2
HARDWARE TO BE 6-STL.
MARSHALL
R. GRAVEN
GRAVEN
4-26-76
4-30-76
4-30-76
4-30-76

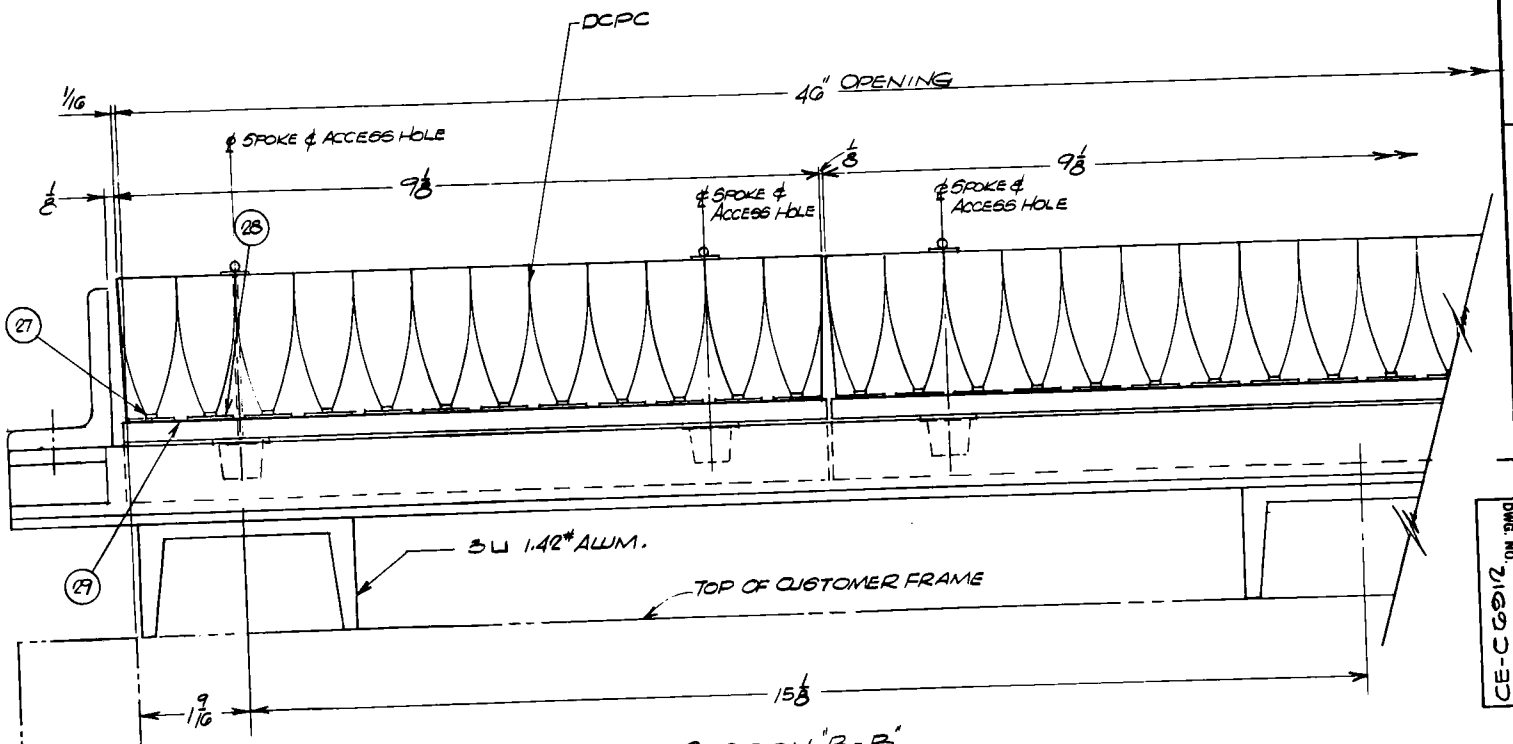

SECTION "B-B"
FROM DWG. CE-EG912

DRAWN BY	MARSHALL	2-26-76
CHECKED	R. Graven	4-20-76
RESP. ENGINEER	GRAVEN	4-20-76
GP. LEADER		DATE
PROJECT MGR		
APPR'D/RELEASED	R. Graven	4-20-76

UNLESS OTHERWISE NOTED
ALL DIMENSIONS ARE INCHES
FRACTIONAL TOL ± 1/64
DECIMAL TOL ± .005
ANGULAR TOL ± 1/4°
REMOVE ALL BURRS AND SHARP EDGES
SURFACES TO BE IN ACCORDANCE WITH ANSI B46.1 - 1962
DIMENSIONS & TOLERANCES IN ACCORDANCE WITH ANSI Y14.5 1966

MATERIAL: HARDWARE TO BE S.STL.

REF. NO. | NEXT ASSEMBLY | REQ'D

THIS DRAWING IS THE PROPERTY OF
ARGONNE NATIONAL LABORATORY

TITLE
SILICON SOLAR CELL MODULE-LAYOUT

SCALE: FULL | SHEET: 4-5 | DRAWING NUMBER: CE-CG912 | REV

SYM	ZONE	CHANGE	BY	CHK'D	DATE

MICROFILMED DATE

67

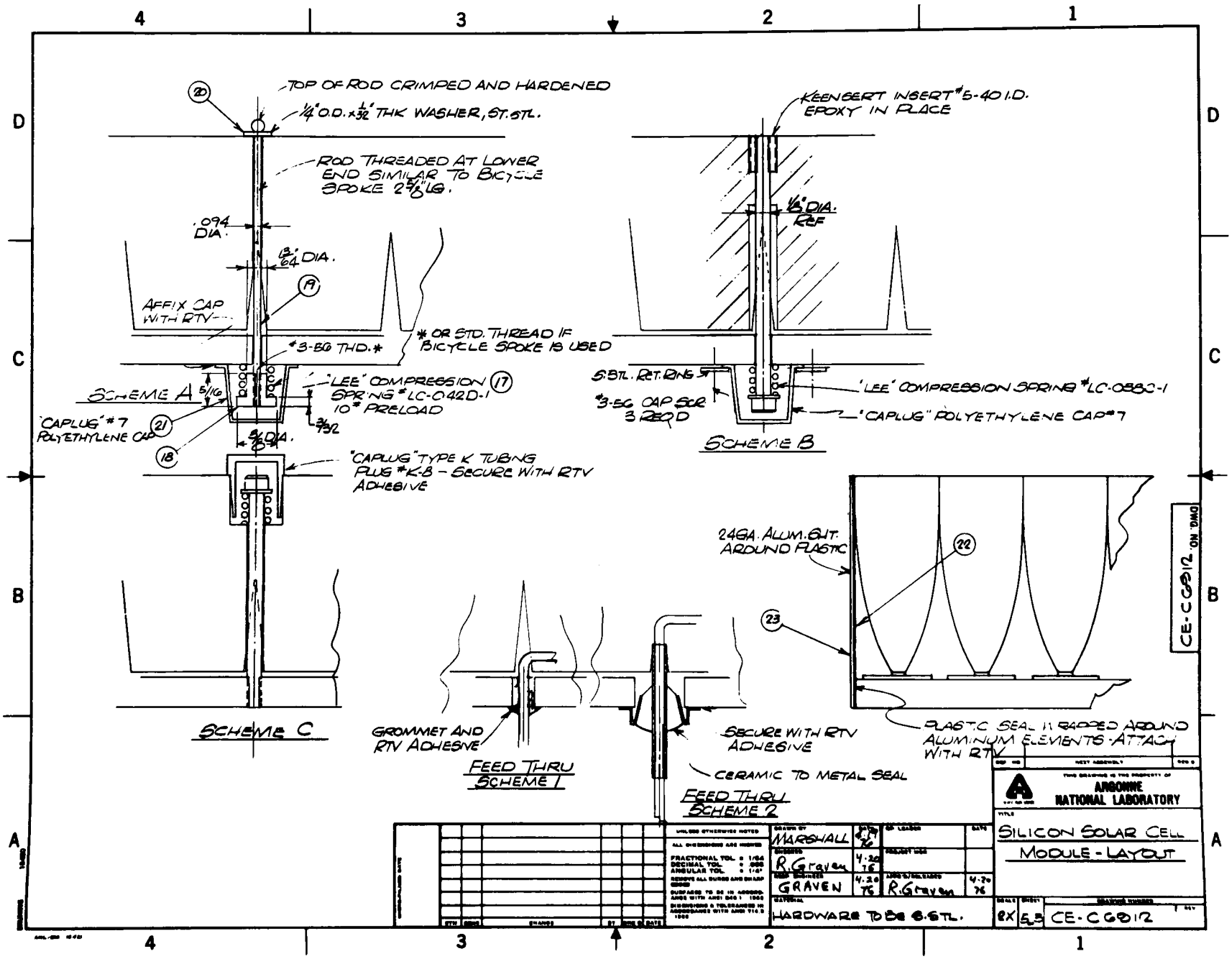
TOP OF ROD CRIMPED AND HARDENED
1/4" O.D. x 1/32" THK WASHER, ST. STL.
ROD THREADED AT LOWER END SIMILAR TO BICYCLE SPOKE 2 5/8" LG.
.094 DIA.
13/64 DIA.
AFFIX CAP WITH RTV
#3-80 THD.*
* OR STD. THREAD IF BICYCLE SPOKE IS USED
'LEE' COMPRESSION SPRING #LC-042D-1 10# PRELOAD
5/16
3/32
5/8 DIA.
'CAPLUG' #7 POLYETHYLENE CAP
'CAPLUG' TYPE K TUBING PLUG #K-8 - SECURE WITH RTV ADHESIVE
SCHEME A
KEENSERT INSERT #5-40 I.D. EPOXY IN PLACE
1/8" DIA. REF
S.STL. RET. RING
#3-56 CAP SCR 3 REQ'D
'LEE' COMPRESSION SPRING #LC-0880-1
'CAPLUG' POLYETHYLENE CAP #7
SCHEME B
24GA. ALUM. SHT. AROUND PLASTIC
SCHEME C
GROMMET AND RTV ADHESIVE
FEED THRU SCHEME 1
SECURE WITH RTV ADHESIVE
CERAMIC TO METAL SEAL
FEED THRU SCHEME 2
PLASTIC SEAL WRAPPED AROUND ALUMINUM ELEMENTS ATTACH WITH RTV
CE-CG812 ON DWG
ARGONNE NATIONAL LABORATORY
SILICON SOLAR CELL MODULE - LAYOUT
MARSHALL 4-7-76
R.G Graven 4-20-76
GRAVEN 4-20-76
R.G Graven 4-20-76
HARDWARE TO BE S.STL.
8X 5.5
CE-CG812

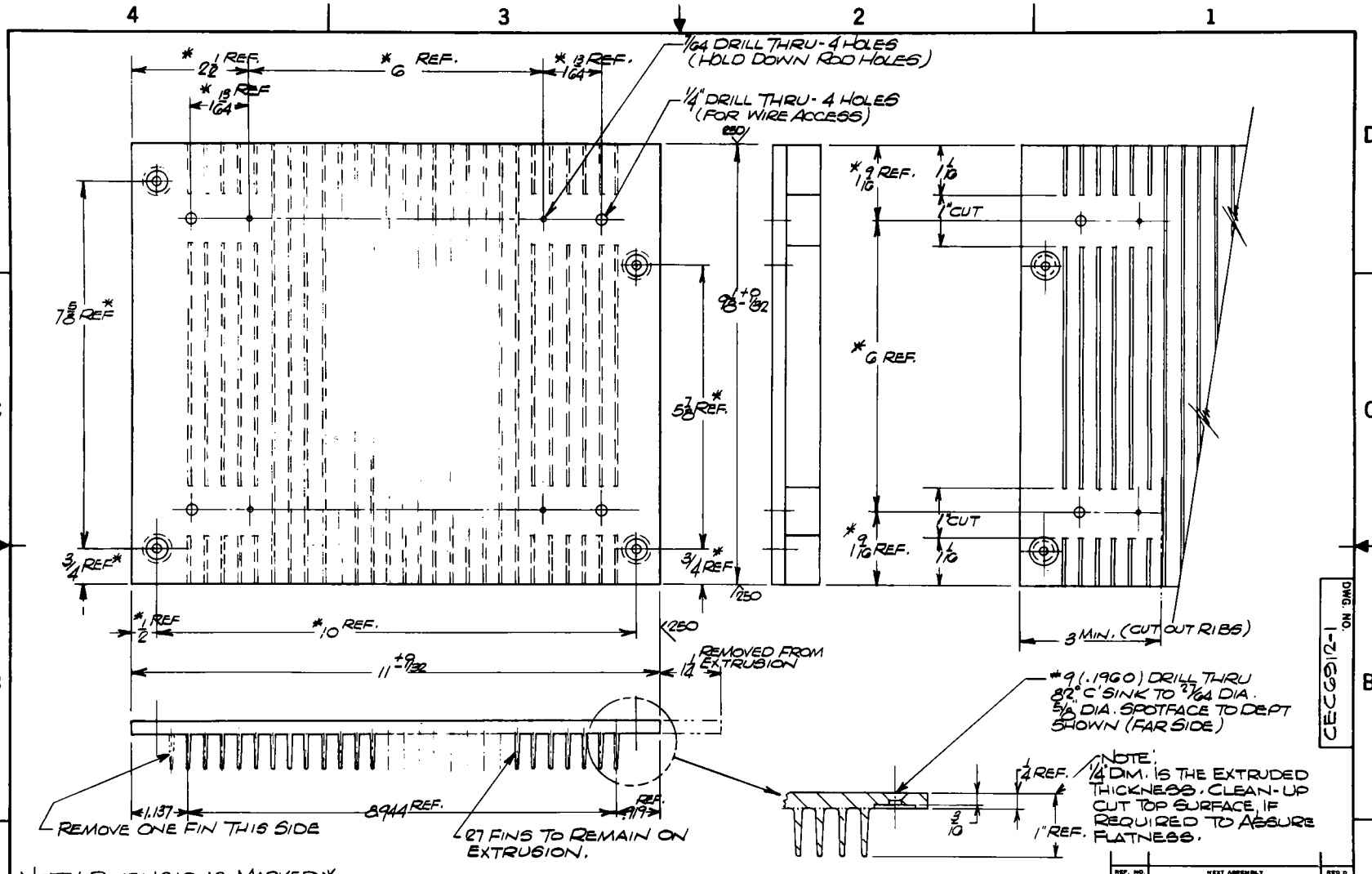

NOTE: DIMENSIONS MARKED * ARE GIVEN FOR REFERENCE ONLY. ACTUAL HOLE LOCATIONS ARE DETERMINED BY DRILL JIG.

NOTE: THIS DWG. SUPERCEEDS DWG. CE-BG912-1

DWG. NO. CE-CG912-1

UNLESS OTHERWISE NOTED	DRAWN BY MARSHALL	DATE 7-26-76	GP LEADER
ALL DIMENSIONS ARE INCHES	CHECKED R. Graven	7-30-76	PROJECT DES
FRACTIONAL TOL. ± 1/64	RESP. ENGINEER GRAVEN	7-30-76	APPR'D/RELEASED R. Graven
DECIMAL TOL. ± .020	MATERIAL MAKE FROM "WAKEFIELD" AL. EXTRUSION Nº 4471		
ANGULAR TOL. ± 1/4°			
REMOVE ALL BURRS AND SHARP EDGES			
SURFACES TO BE IN ACCORDANCE WITH ANSI B46.1 - 1962			
DIMENSIONING & TOLERANCES IN ACCORDANCE WITH ANSI Y14.5 1966			

REF. NO.	NEXT ASSEMBLY	REQ'D

THIS DRAWING IS THE PROPERTY OF ARGONNE NATIONAL LABORATORY

TITLE: HEAT SINK

SCALE	SHEET	DRAWING NUMBER	REV
1/4" = 1"		CE-CG912-1	

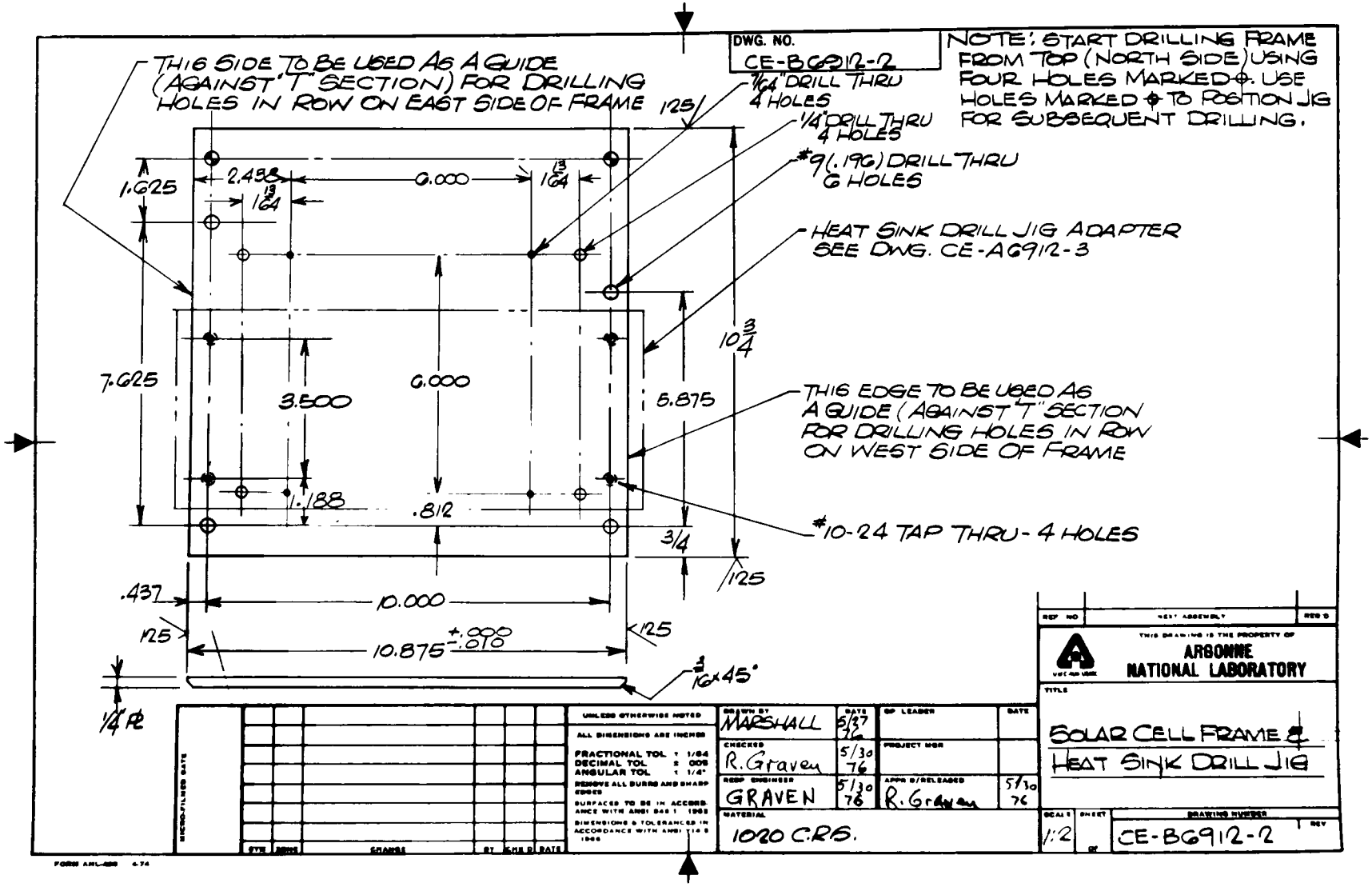
DWG. NO.
CE-BG912-2
NOTE: START DRILLING FRAME FROM TOP (NORTH SIDE) USING FOUR HOLES MARKED ⊕. USE HOLES MARKED ⊕ TO POSITION JIG FOR SUBSEQUENT DRILLING.
THIS SIDE TO BE USED AS A GUIDE (AGAINST "T" SECTION) FOR DRILLING HOLES IN ROW ON EAST SIDE OF FRAME
1/4" DRILL THRU 4 HOLES
1/4" DRILL THRU 4 HOLES
*9(.196) DRILL THRU 6 HOLES
HEAT SINK DRILL JIG ADAPTER SEE DWG. CE-AG912-3
THIS EDGE TO BE USED AS A GUIDE (AGAINST "T" SECTION FOR DRILLING HOLES IN ROW ON WEST SIDE OF FRAME
*10-24 TAP THRU - 4 HOLES
1.625
2.438
13/64
6.000
13/64
7.625
3.500
6.000
6.875
10 3/4
1.188
.812
3/4
.437
10.000
.125
10.875 +.000 -.010
3/16 x 45°
1/4 R
UNLESS OTHERWISE NOTED
ALL DIMENSIONS ARE INCHES
FRACTIONAL TOL ± 1/64
DECIMAL TOL ± .005
ANGULAR TOL ± 1/4°
REMOVE ALL BURRS AND SHARP EDGES
SURFACES TO BE IN ACCORDANCE WITH ANSI B46.1 1962
DIMENSIONS & TOLERANCES IN ACCORDANCE WITH ANSI Y14.5 1966
DRAWN BY MARSHALL 5/27/76
CHECKED R. Graven 5/30/76
DESIGN ENGINEER GRAVEN 5/30/76
APPR'D/RELEASED R. Graven 5/30/76
DP LEADER
PROJECT MGR
MATERIAL 1020 C.R.S.
THIS DRAWING IS THE PROPERTY OF ARGONNE NATIONAL LABORATORY
TITLE
SOLAR CELL FRAME & HEAT SINK DRILL JIG
SCALE 1:2
SHEET
DRAWING NUMBER CE-BG912-2
REV
MICROFILMED DATE

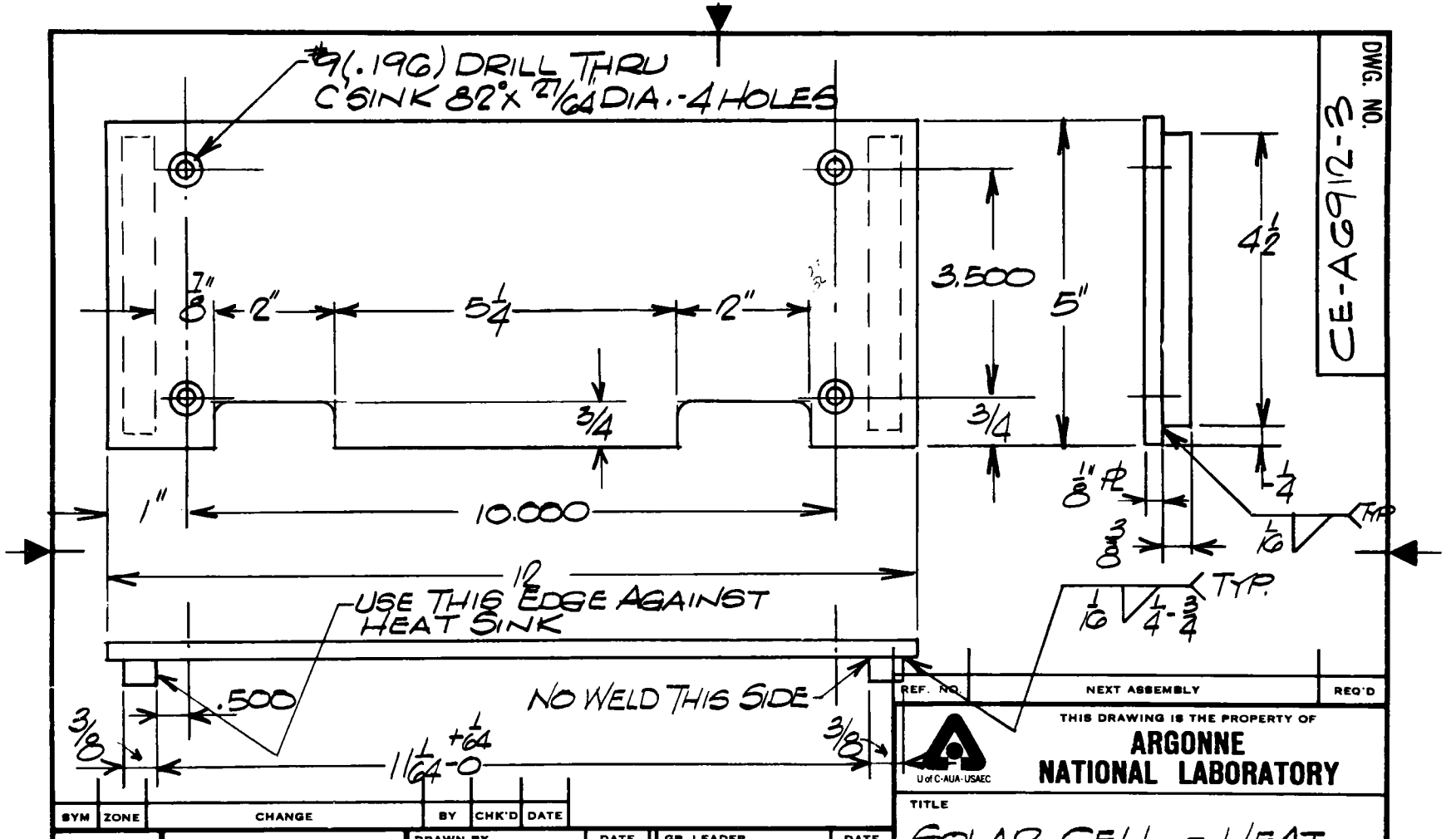

DWG. NO. CE-A6912-3

REF. NO.	NEXT ASSEMBLY	REQ'D

THIS DRAWING IS THE PROPERTY OF
U of C-AUA-USAEC
ARGONNE NATIONAL LABORATORY

SYM	ZONE	CHANGE	BY	CHK'D	DATE

UNLESS OTHERWISE NOTED

ALL DIMENSIONS ARE INCHES

FRACTIONAL TOL. ± 1/64
DECIMAL TOL. ± .005
ANGULAR TOL. ± 1/4°

REMOVE ALL BURRS AND SHARP EDGES

SURFACES TO BE IN ACCORDANCE WITH ANSI B46.1 - 1962

DIMENSIONS & TOLERANCES IN ACCORDANCE WITH ANSI Y14.5 1966

DRAWN BY	MARSHALL	DATE	5/27/76	GP. LEADER	DATE
CHECKED	R. Graven	DATE	5/30/76	PROJECT MGR.	
RESP. ENGINEER	GRAVEN	DATE	5/30/76	APPR'D/RELEASED	R. Graven 5/30/76
MATERIAL	6061-T6 ALUM.				

TITLE
SOLAR CELL - HEAT SINK DRILL JIG ADAPTER

SCALE	SHEET	DRAWING NUMBER	REV.
1:2	OF	CE-A6912-3	

BRUNING MICRO-FILMED DATE 18450

ANL-292 (5-72)

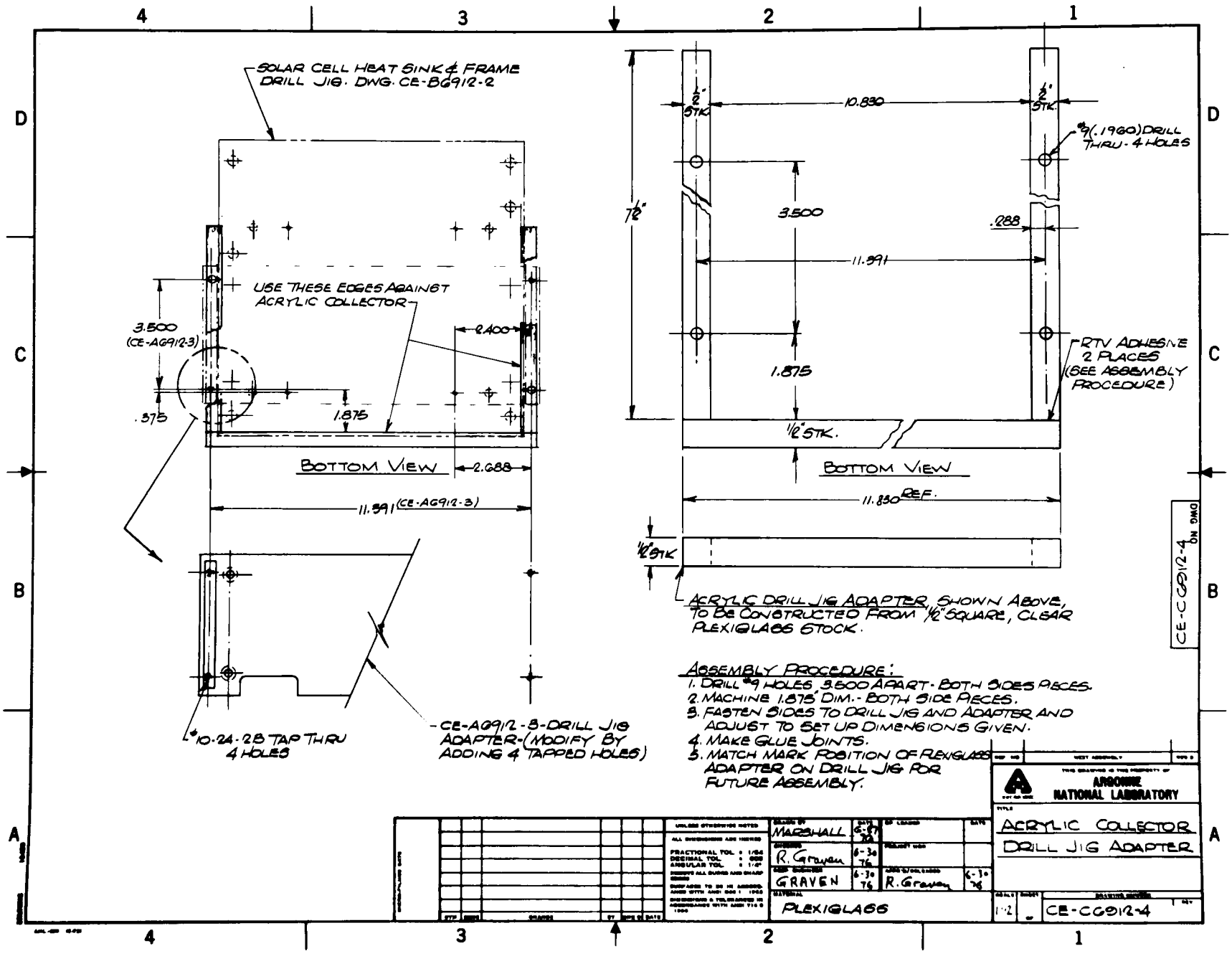
SOLAR CELL HEAT SINK & FRAME DRILL JIG. DWG. CE-BG912-2
USE THESE EDGES AGAINST ACRYLIC COLLECTOR
3.500 (CE-AG912-3)
.375
1.875
2.000
2.088
BOTTOM VIEW
11.591 (CE-AG912-3)
#10-24-2B TAP THRU 4 HOLES
-CE-AG912-8-DRILL JIG ADAPTER-(MODIFY BY ADDING 4 TAPPED HOLES)
1/2" STK.
10.830
#9(.1960) DRILL THRU-4 HOLES
7/8"
3.500
.288
11.591
1.875
RTV ADHESIVE 2 PLACES (SEE ASSEMBLY PROCEDURE)
1/2" STK.
BOTTOM VIEW
11.830 REF.
1/2" STK
ACRYLIC DRILL JIG ADAPTER, SHOWN ABOVE, TO BE CONSTRUCTED FROM 1/2" SQUARE, CLEAR PLEXIGLASS STOCK.
ASSEMBLY PROCEDURE:
1. DRILL #9 HOLES 3.500 APART - BOTH SIDES PIECES.
2. MACHINE 1.875" DIM. - BOTH SIDE PIECES.
3. FASTEN SIDES TO DRILL JIG AND ADAPTER AND ADJUST TO SET UP DIMENSIONS GIVEN.
4. MAKE GLUE JOINTS.
5. MATCH MARK POSITION OF REXIGLASS ADAPTER ON DRILL JIG FOR FUTURE ASSEMBLY.
CE-CG912-4 ON DWG
ARGONNE NATIONAL LABORATORY
ACRYLIC COLLECTOR
DRILL JIG ADAPTER
MARSHALL 6-27-76
R. Graven 6-30-76
GRAVEN 6-30-76
R. Graven 6-30-76
PLEXIGLASS
1:2
CE-CG912-4

APPENDIX B

CPC Panel Assembly Drawings

PART NO.	DRAWING NO.	PART NAME OR DESCRIPTION	REMARKS	FOR PURCH. PARTS ONLY MATERIAL	QTY.
		HOLLOWS SCHEME			
	CE-E6925	SILICON SOLAR CELL - MODULE LAYOUT	SHT. 1 OF 4		
	CE-C6925	MODULE SECTIONS	SHT. 2 OF 4		
	CE-C6925	MODULE SECTIONS	SHT. 3 OF 4		
	CE-D6925	MODULE SECTIONS	SHT. 4 OF 4		
	CE-D6935	CIRCUIT SHEET ASSEMBLY			
1	CE-C6925-1	COVER			16
2	CE-A6925-2	STAND, SUPPORT			64
3	CE-C6929	HEAT SINK, MODIFICATION			16
4	CE-B6929-1	DRILL JIG			1
5	CE-A6929-2	DRILL JIG ADAPTER			1
6	CE-D6935-1	CIRCUIT SHEET			16

SYM.	CHANGE	BY	CK.	DATE

THIS PARTS LIST IS THE PROPERTY OF
ARGONNE NATIONAL LABORATORY

ASSEMBLY SILICON SOLAR CELL (HOLLOWS SCHEME)

APP'D	RMG	8-30-76	ASSEMBLY NO. CE-E6925
CHECKED	RMG	"	
DRAWN	[signature]	7-30-76	

SHEET 1 OF 3

*46 14-623 ENGINEERING PARTS LIST

PART NO.	DRAWING NO.	PART NAME OR DESCRIPTION	REMARKS	FOR PURCH. PARTS ONLY MATERIAL	QTY.
7	CE-C6935-2	CELL ASSEMBLY			16 ·
8		CHANNEL 3" L 1.42 x 49" LG.		AL 6061-T6	4 ·
9		ANGLE L 1" x 1" x 1/8" x 49 3/8" LG.		AL 6061-T6	6 ·
10		ANGLE L 1 3/4" x 1 3/4" x 1/4" x 46 1/8" LG.		AL 6061-T6	2 ·
11		GUARD ANGLE L 2 1/2" x 1 1/2" x 1/4 x 48 7/8" LG		AL 6061-T6	2 ·
12		CLIP ANGLE L 1 1/4" x 1 1/4 x 1/4 x 3 1/2" LG		AL 6061-T6	4 ·
13		ACRYLIC GUARD 3 1/2 x 1/4 x 43 7/8 LG		ACRYLIC	2 ·
14		CLIP ANGLE L 3/4 x 3/4 x 1/8 x 1" LG.		AL 6061 | T6	12 ·
15		SOLAR COLLECTOR, DCPC, PHOTOVOLTAIC CELL			205 ·

SYM.	CHANGE	BY	CK.	DATE

THIS PARTS LIST IS THE PROPERTY OF
ARGONNE NATIONAL LABORATORY

ASSEMBLY SILICON SOLAR CELL (HOLLOWS SCHEME) — SHEET 2 OF 3

APP'D	RMG	8/30/76
CHECKED	RMG	11
DRAWN	[signature]	7/30/76

ASSEMBLY NO. CE-E6925

ANL-146 (4-62) ENGINEERING PARTS LIST

PART NO.	DRAWING NO.	PART NAME OR DESCRIPTION	REMARKS	FOR PURCH. PARTS ONLY MATERIAL	QTY.
16		SCREW - HEX. HD. CAP - 1/4-20 x 7/8 LG		S.STL	32.
17		NUT, HEX 1/4-20		S.STL	52.
18		LOCKWASHER - 1/4" STD.		S.STL	52.
19		SCREW, SHOULDER 1/4" DIA x 1/4" LG. NYLOK		S.STL	64.
20		SCREW - FL. HD. SOC CAP #10-24 x 1/2 LG - NYLOK		S.STL	64.
21		SCREW - FL. HD. CAP - 1/4-20 x 1/2 LG (FOR ACRYLIC)		S.STL	14.
22		SCREW - HEX. HD. CAP. 1/4-20 x 1/2 LG. (IN CLIP ANGLE)		S.STL.	8.
23		SCREW - HEX HD. CAP 1/4-20 x 3/4" LG. (IN CLIP ANGLES)		S.STL.	20.
24		RTV ADHESIVE		AS REQUIRED	.

SYM.	CHANGE	BY	CK.	DATE

THIS PARTS LIST IS THE PROPERTY OF
ARGONNE NATIONAL LABORATORY

ASSEMBLY SILICON SOLAR CELL (HOLLOWS SCHEME) SHEET 3 OF 3

APP'D	RMG	8/30/76
CHECKED	RMG	"
DRAWN	[signature]	7/30/76

ASSEMBLY NO. CE-E6925

ANL-146 (4-62) ENGINEERING PARTS LIST

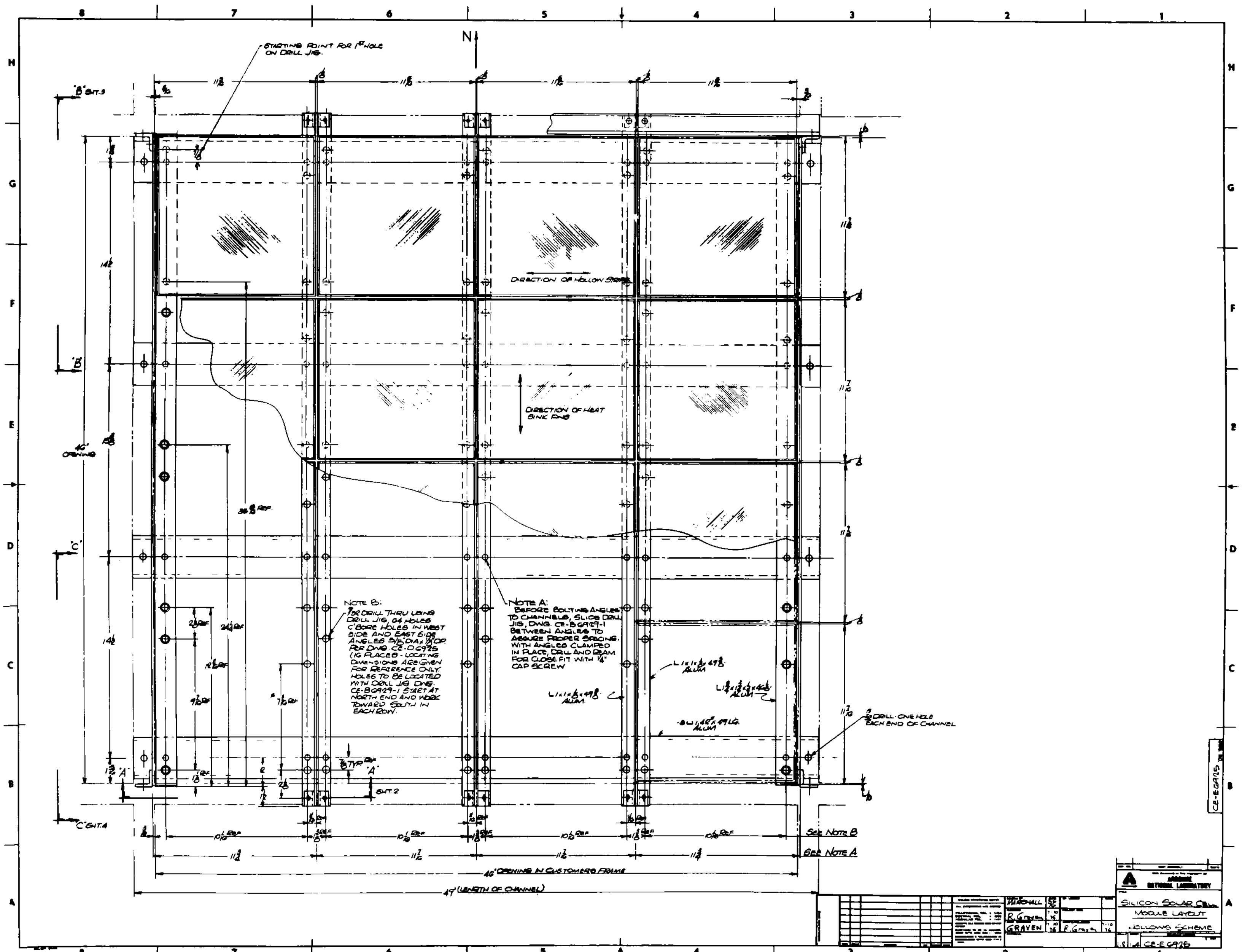
STARTING POINT FOR 1ST HOLE ON DRILL JIG.
DIRECTION OF HOLLOW STRIPS
DIRECTION OF HEAT SINK FINS
46" OPENING
NOTE B:
9/32 DRILL THRU USING DRILL JIG, 04 HOLES C'BORE HOLES IN WEST SIDE AND EAST SIDE ANGLES 5/16" DIA x 1/16 DP. PER DWG. CE-D6925 (16 PLACES) - LOCATING DIMENSIONS ARE GIVEN FOR REFERENCE ONLY. HOLES TO BE LOCATED WITH DRILL JIG DWG. CE-B6929-1 START AT NORTH END AND WORK TOWARD SOUTH IN EACH ROW.
NOTE A:
BEFORE BOLTING ANGLES TO CHANNELS, SLIDE DRILL JIG, DWG. CE-B6929-1 BETWEEN ANGLES TO ASSURE PROPER SPACING. WITH ANGLES CLAMPED IN PLACE, DRILL AND REAM FOR CLOSE FIT WITH 1/4" CAP SCREW
DRILL - ONE HOLE EACH END OF CHANNEL
SEE NOTE B
SEE NOTE A
46" OPENING IN CUSTOMERS FRAME
49" (LENGTH OF CHANNEL)
ARGONNE NATIONAL LABORATORY
SILICON SOLAR CELL MODULE LAYOUT HOLLOWS SCHEME
GRAVEN
CE-E6925

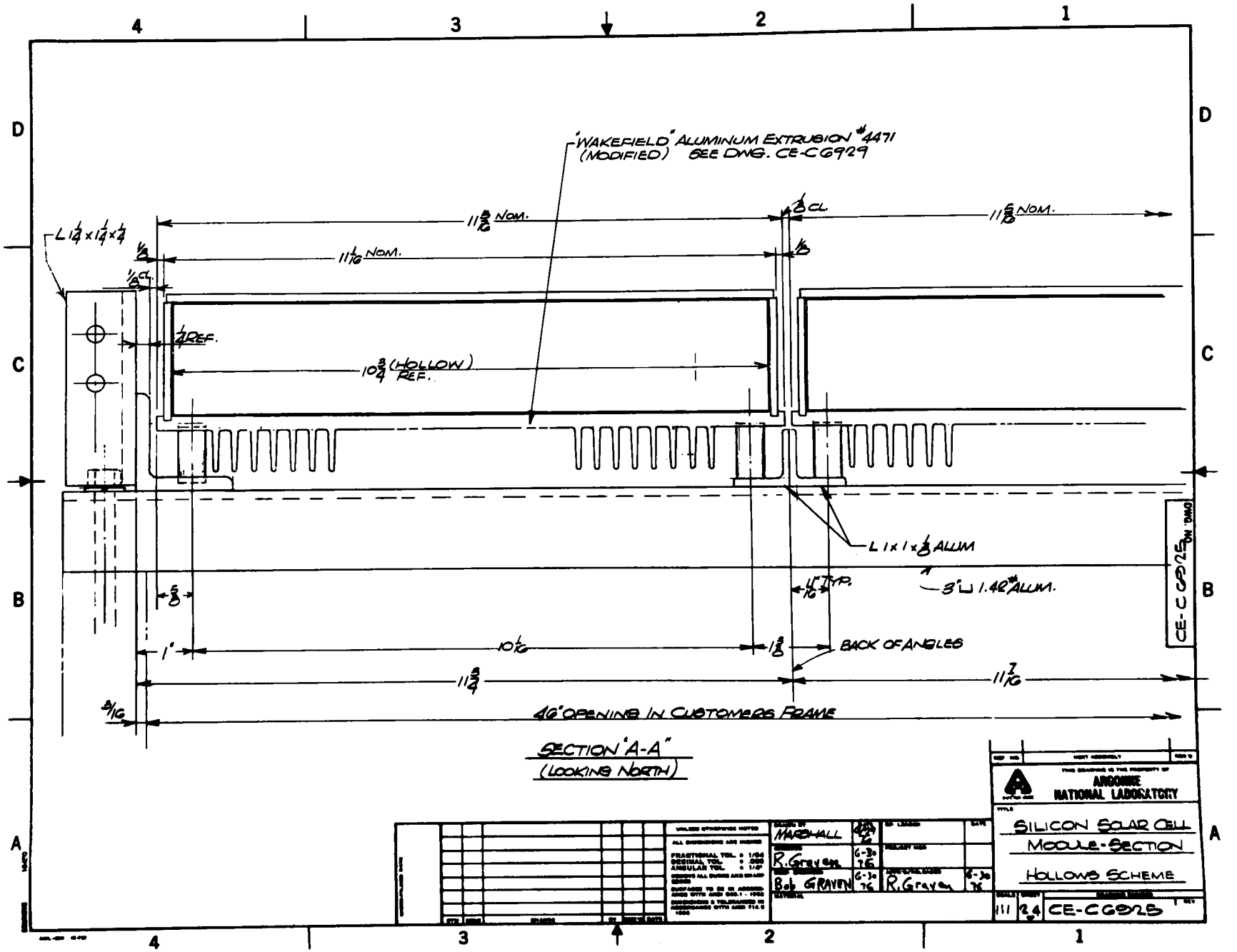
"WAKEFIELD" ALUMINUM EXTRUSION #4471 (MODIFIED) SEE DWG. CE-CG929
L 1¼ x 1¼ x ¼
11⅝ NOM.
11 1/16 NOM.
10¾ (HOLLOW) REF.
L 1 x 1 x ⅛ ALUM
3" L 1.42# ALUM.
BACK OF ANGLES
46" OPENING IN CUSTOMERS FRAME
SECTION "A-A" (LOOKING NORTH)
CE-CG925 DWG
ARGONNE NATIONAL LABORATORY
SILICON SOLAR CELL MODULE-SECTION
HOLLOWS SCHEME
CE-CG925
MARSHALL
R. Graven
Bob GRAVEN
R. Graven

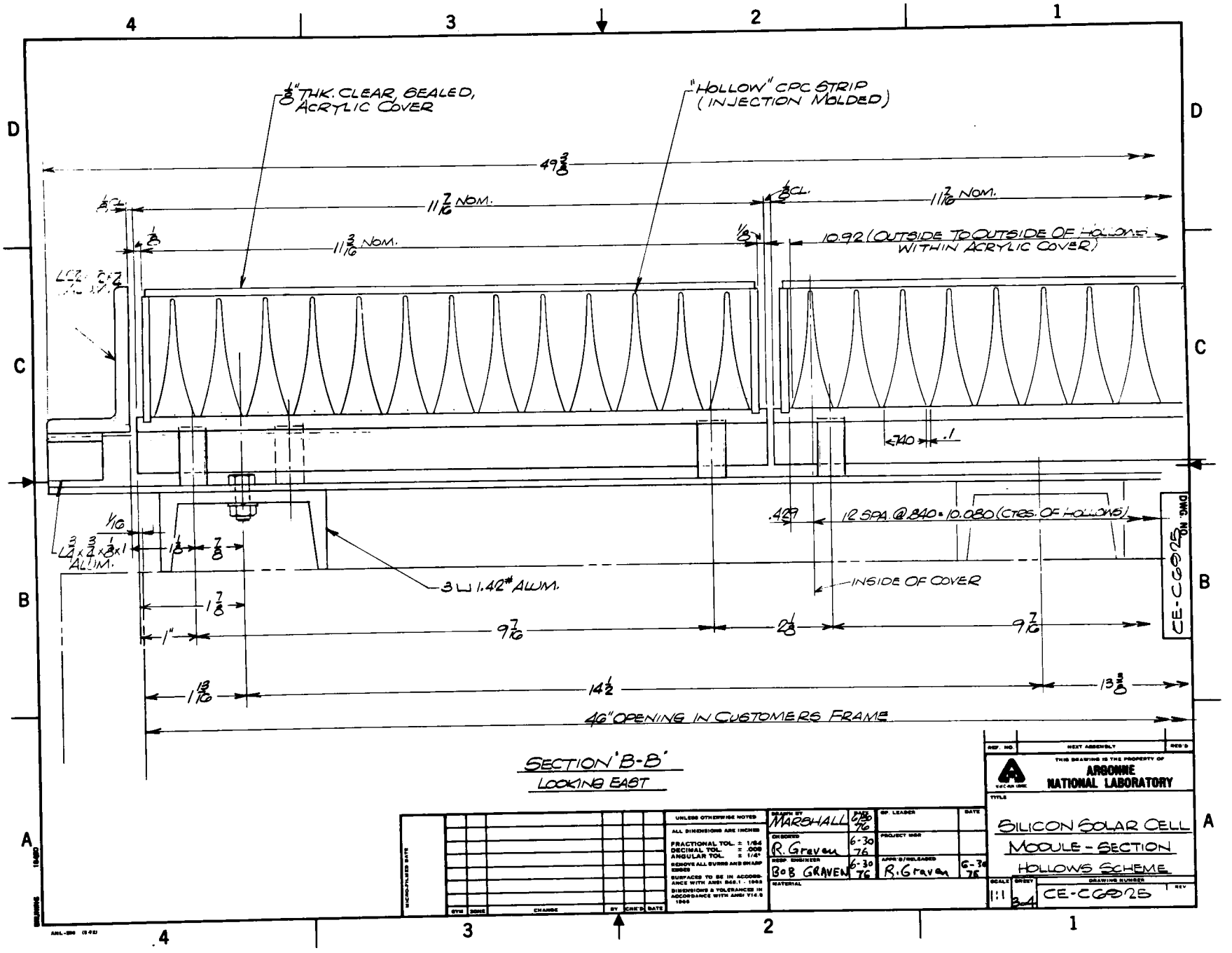

SECTION 'B-B'
LOOKING EAST

UNLESS OTHERWISE NOTED: ALL DIMENSIONS ARE INCHES; FRACTIONAL TOL. ± 1/64; DECIMAL TOL. ± .005; ANGULAR TOL. ± 1/4°; REMOVE ALL BURRS AND SHARP EDGES; SURFACES TO BE IN ACCORDANCE WITH ANSI B46.1 - 1962; DIMENSIONS & TOLERANCES IN ACCORDANCE WITH ANSI Y14.5 1966	DRAWN BY MARSHALL 6/28/76	GP. LEADER	DATE
	CHECKED R. Graven 6-30 76	PROJECT MGR.	
	RESP. ENGINEER Bob GRAVEN 6-30 76	APPR. & RELEASED R. Graven 6-30 76	
	MATERIAL		

THIS DRAWING IS THE PROPERTY OF ARGONNE NATIONAL LABORATORY

TITLE: SILICON SOLAR CELL MODULE - SECTION HOLLOWS SCHEME

SCALE 1:1 | SHEET 3 of 4 | DRAWING NUMBER CE-CG025 | REV

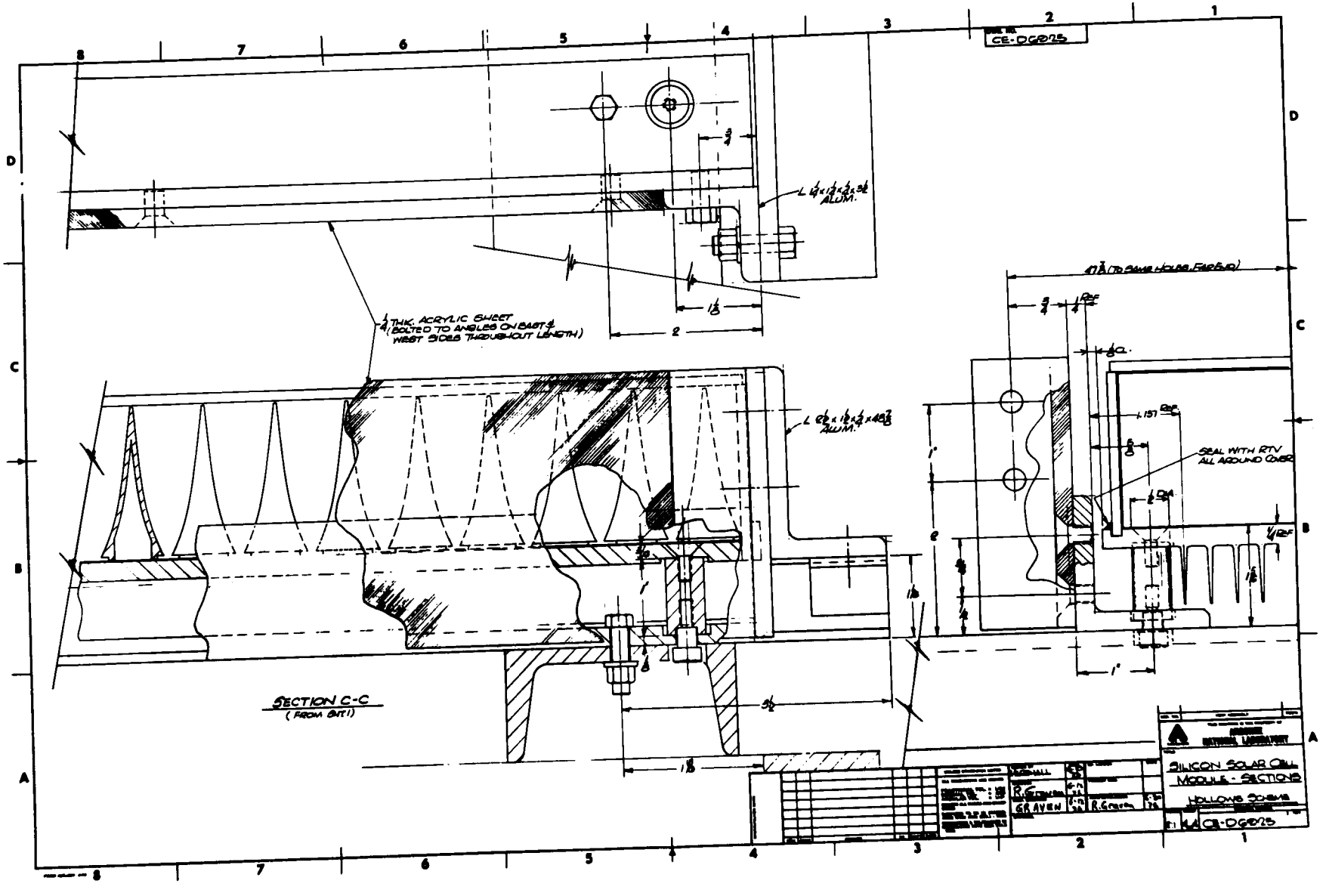
CE-DG0025
1/4 THK. ACRYLIC SHEET (BOLTED TO ANGLES ON EAST & WEST SIDES THROUGHOUT LENGTH)
SEAL WITH RTV ALL AROUND COVER
SECTION C-C
(FROM SHT 1)
SILICON SOLAR CELL MODULE - SECTIONS
HOLLOWS SCHEME
CE-DG0025
GRAVEN

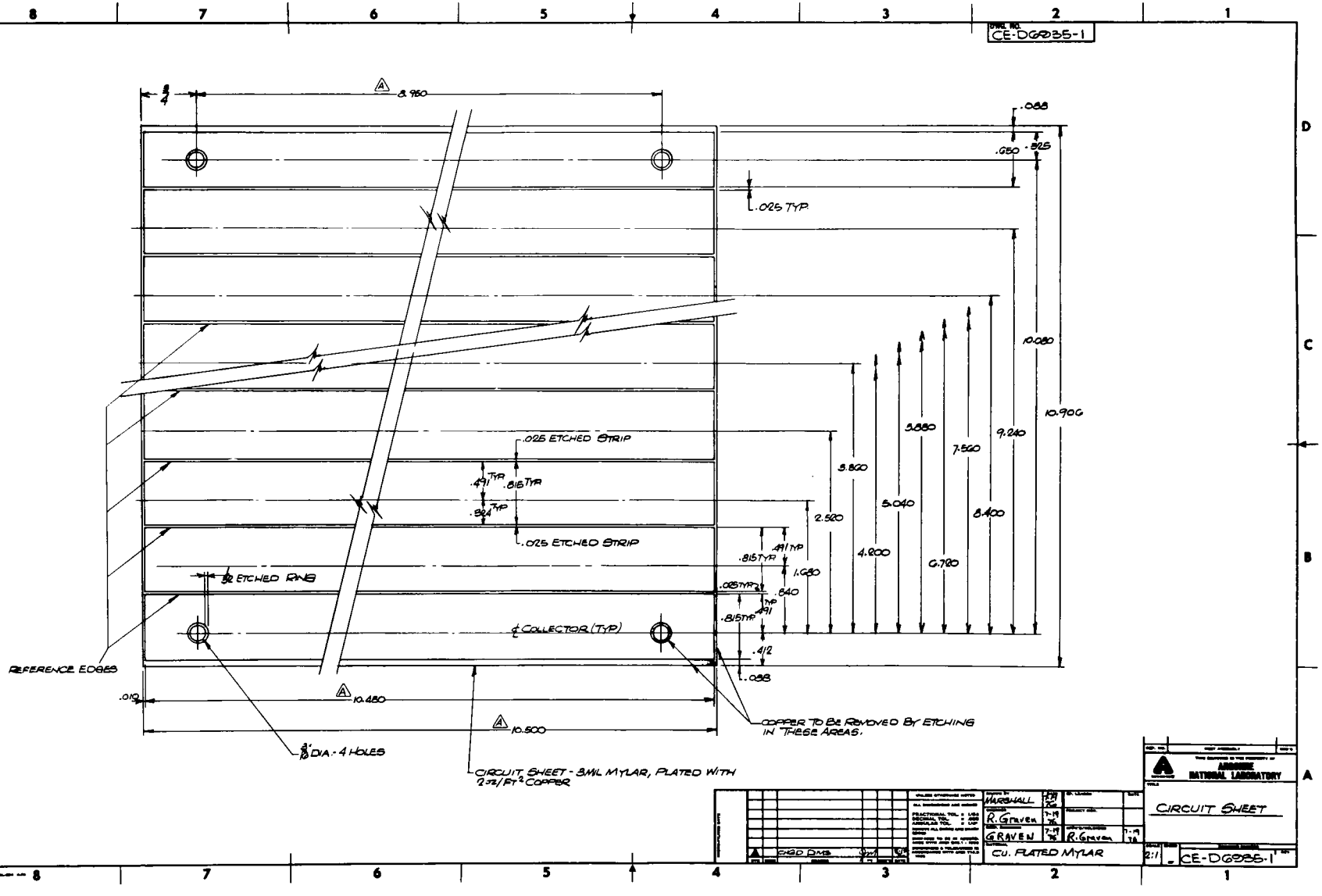
DWG NO. CE-DG835-1
8.980
.088
.650
.525
.025 TYP.
10.080
10.906
9.240
7.560
5.880
5.880
5.040
4.200
2.520
8.400
6.720
1.680
.025 ETCHED STRIP
.491 TYP
.815 TYP
.840 TYP
.025 ETCHED STRIP
.032 ETCHED RING
℄ COLLECTOR (TYP)
REFERENCE EDGES
.012
10.480
10.500
.412
.088
⅛" DIA - 4 HOLES
COPPER TO BE REMOVED BY ETCHING IN THESE AREAS.
CIRCUIT SHEET - 3 MIL MYLAR, PLATED WITH 2 oz/Ft² COPPER
MARSHALL
R. GRAVEN
GRAVEN
R. GRAVEN
CU. PLATED MYLAR
ARGONNE NATIONAL LABORATORY
CIRCUIT SHEET
2:1
CE-DG835-1

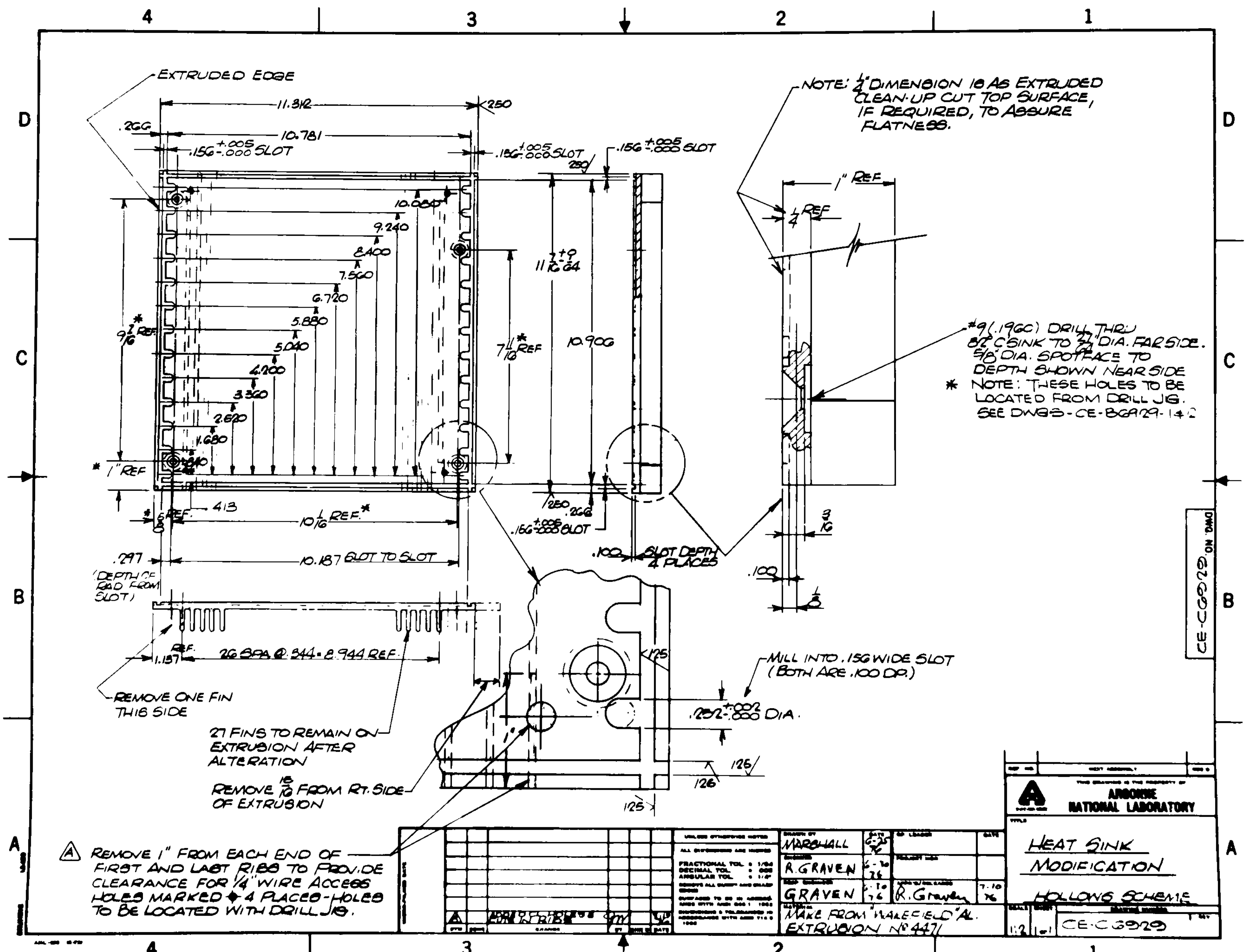

EXTRUDED EDGE
11.312
.250
10.781
.266
.156 +.005 -.000 SLOT
NOTE: 1/2" DIMENSION IS AS EXTRUDED CLEAN-UP CUT TOP SURFACE, IF REQUIRED, TO ASSURE FLATNESS.
1" REF
1/4 REF
10.080
9.240
8.400
7.560
6.720
5.880
5.040
4.200
3.360
2.520
1.680
10.906
7 11/16 REF
9 1/16 REF
1" REF
10 1/16 REF.
.413
.297
(DEPTH OF RAD FROM SLOT)
10.187 SLOT TO SLOT
SLOT DEPTH 4 PLACES
#9 (.1960) DRILL THRU 82° C'SINK TO 3/4" DIA. FAR SIDE. 5/8" DIA. SPOTFACE TO DEPTH SHOWN NEAR SIDE
* NOTE: THESE HOLES TO BE LOCATED FROM DRILL JIG. SEE DWGS-CE-BG929-1 & 2
3/16
.100
1/8
1.137
26 SPA @ .344 = 8.944 REF.
REMOVE ONE FIN THIS SIDE
27 FINS TO REMAIN ON EXTRUSION AFTER ALTERATION
REMOVE 15/16 FROM RT. SIDE OF EXTRUSION
MILL INTO .156 WIDE SLOT (BOTH ARE .100 DP.)
.252 +.002 -.000 DIA.
.125
.126
REMOVE 1" FROM EACH END OF FIRST AND LAST RIBS TO PROVIDE CLEARANCE FOR 1/4" WIRE ACCESS HOLES MARKED ◆ 4 PLACES - HOLES TO BE LOCATED WITH DRILL JIG.
MARSHALL
R. GRAVEN
GRAVEN
MAKE FROM "WAKEFIELD" AL. EXTRUSION No 4471
ARGONNE NATIONAL LABORATORY
HEAT SINK MODIFICATION
HOLLOWS SCHEME
CE-C 63929

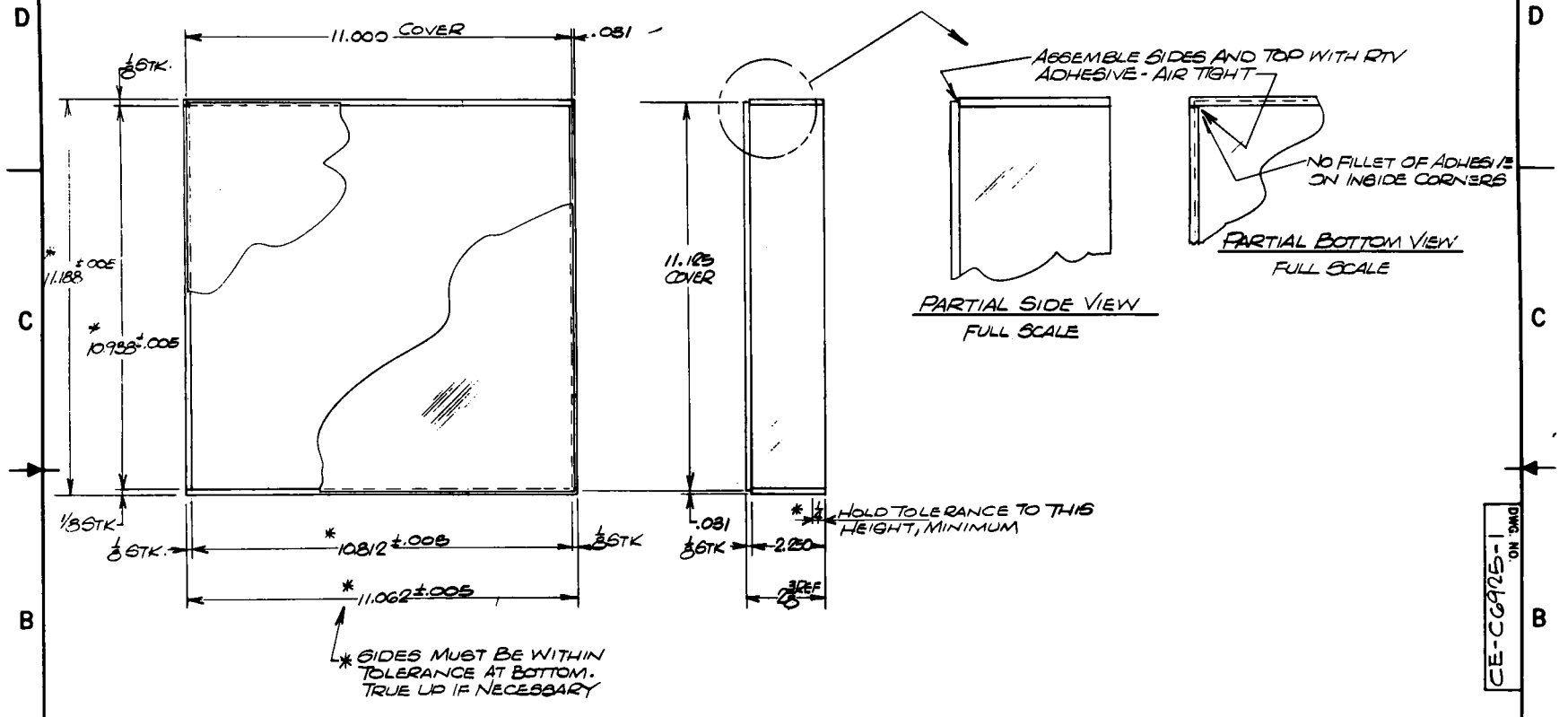

DWG. NO. CE-C6925-1

UNLESS OTHERWISE NOTED
ALL DIMENSIONS ARE INCHES
FRACTIONAL TOL. ± 1/64
DECIMAL TOL. ± .005
ANGULAR TOL. ± 1/4°
REMOVE ALL BURRS AND SHARP EDGES
SURFACES TO BE IN ACCORD. ANCE WITH ANSI B46.1 - 1962
DIMENSIONS & TOLERANCES IN ACCORDANCE WITH ANSI Y14.5 1966

	BY	DATE
DRAWN	MARSHALL	7-9-76
CHECKED	R. Graven	7-10-76
DESIGN ENGINEER	GRAVEN	7-10-76
APPR'D/RELEASED	R. Graven	7-10-76

MATERIAL: 1/8 THK. CLEAR ACRYLIC STK.

THIS DRAWING IS THE PROPERTY OF
ARGONNE NATIONAL LABORATORY

TITLE
COVER
HOLLOWS SCHEME

SCALE: 1:2 | SHEET | DRAWING NUMBER: CE-C6925-1 | REV

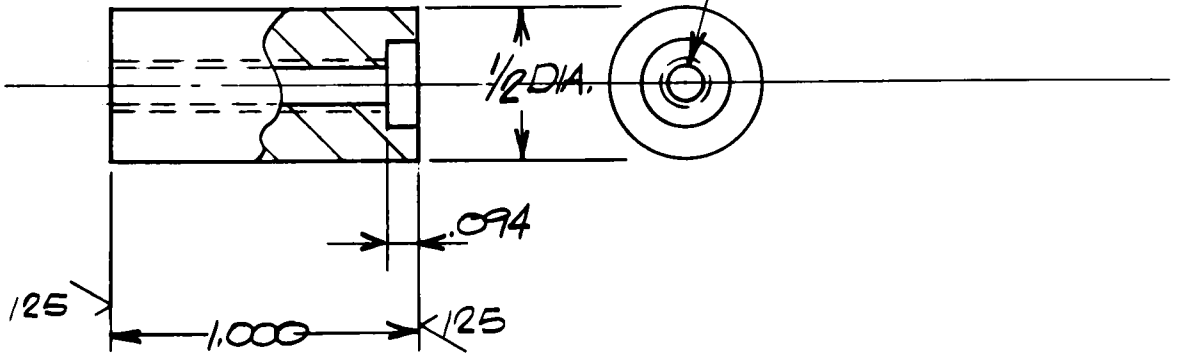

DWG. NO. CE-AG925-2

REF. NO.	NEXT ASSEMBLY	REQ'D

THIS DRAWING IS THE PROPERTY OF
U of C-AUA-USAEC
ARGONNE NATIONAL LABORATORY

SYM	ZONE	CHANGE	BY	CHK'D	DATE

UNLESS OTHERWISE NOTED

ALL DIMENSIONS ARE INCHES

FRACTIONAL TOL. ± 1/64
DECIMAL TOL. ± .005
ANGULAR TOL. ± 1/4°

REMOVE ALL BURRS AND SHARP EDGES

SURFACES TO BE IN ACCORD. ANCE WITH ANSI B46.1 - 1962

DIMENSIONS & TOLERANCES IN ACCORDANCE WITH ANSI Y14.5 - 1966

DRAWN BY MARSHALL	DATE 7-9 76	GP. LEADER	DATE
CHECKED R.H.G	7/10 76	PROJECT MGR.	
RESP. ENGINEER GRAVEN	7/10 76	APPR'D/RELEASED R. Graven	7/10 76

MATERIAL 304 S. STL.

TITLE: SUPPORT - HEAT SINK

SCALE	SHEET	DRAWING NUMBER	REV
2:1	OF	CE-AG925-2	

BRUNING 18450 MICRO-FILMED DATE

ANL 895 (6 72)

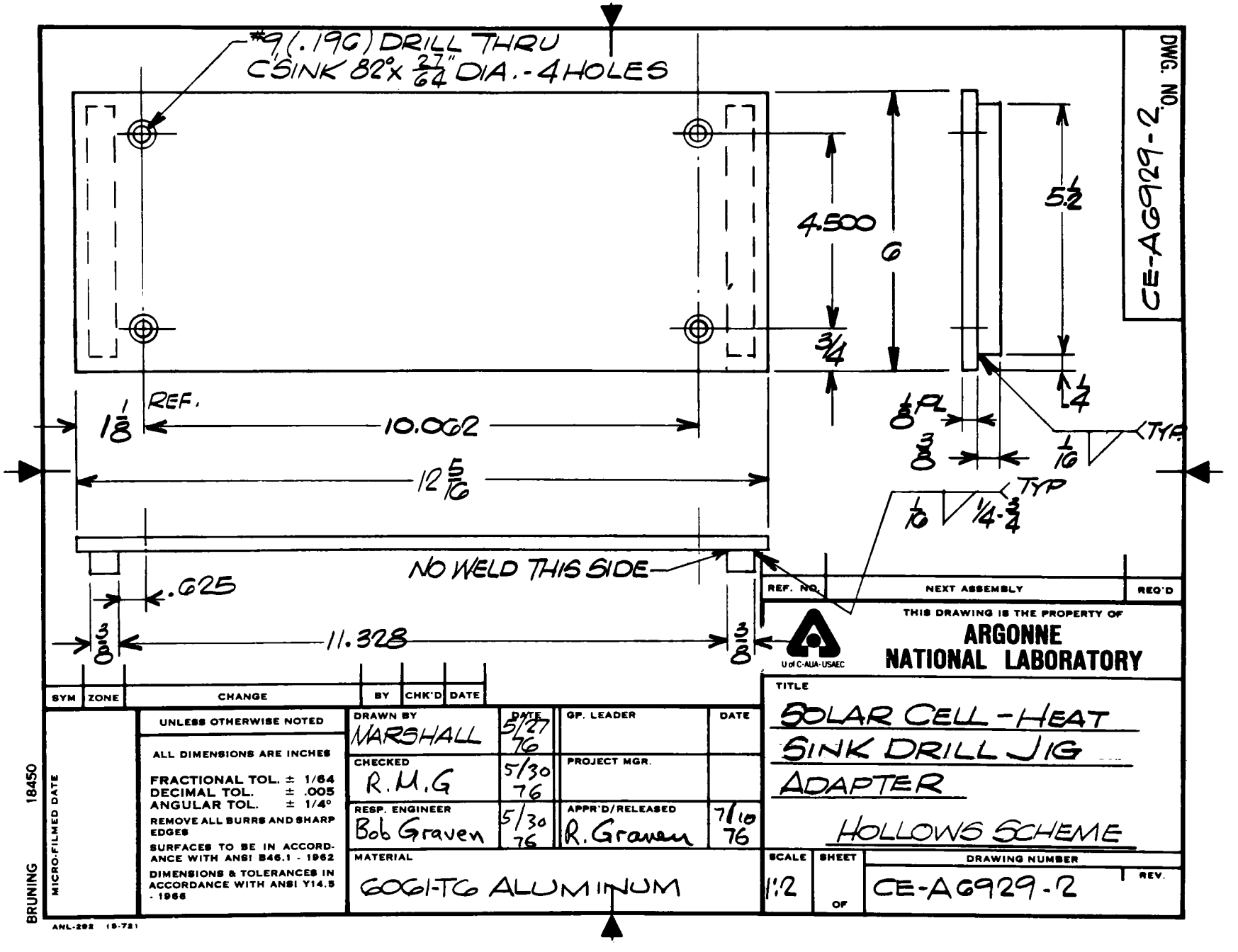
#9 (.196) DRILL THRU
CSINK 82° x 27/64" DIA. - 4 HOLES
4.500
6
5 1/2
3/4
1/4
1/8 REF.
10.062
12 5/16
1/8 PL
TYP
3/8
1/16
1/16
1/4-3/4
TYP
NO WELD THIS SIDE
.625
3/8
11.328
3/8
DWG. NO. CE-A6929-2
REF. NO.
NEXT ASSEMBLY
REQ'D
THIS DRAWING IS THE PROPERTY OF
ARGONNE NATIONAL LABORATORY
U of C-ALIA-USAEC
SYM
ZONE
CHANGE
BY
CHK'D
DATE
UNLESS OTHERWISE NOTED
ALL DIMENSIONS ARE INCHES
FRACTIONAL TOL. ± 1/64
DECIMAL TOL. ± .005
ANGULAR TOL. ± 1/4°
REMOVE ALL BURRS AND SHARP EDGES
SURFACES TO BE IN ACCORDANCE WITH ANSI B46.1 - 1962
DIMENSIONS & TOLERANCES IN ACCORDANCE WITH ANSI Y14.5 - 1966
DRAWN BY MARSHALL 5/27/76
GP. LEADER
DATE
CHECKED R.M.G 5/30/76
PROJECT MGR.
RESP. ENGINEER Bob Graven 5/30/76
APPR'D/RELEASED R. Graven 7/10/76
MATERIAL 6061-T6 ALUMINUM
TITLE
SOLAR CELL - HEAT SINK DRILL JIG ADAPTER
HOLLOWS SCHEME
SCALE 1:2
SHEET
OF
DRAWING NUMBER CE-A6929-2
REV.
BRUNING 18450
MICRO-FILMED DATE
ANL-292 (5-72)

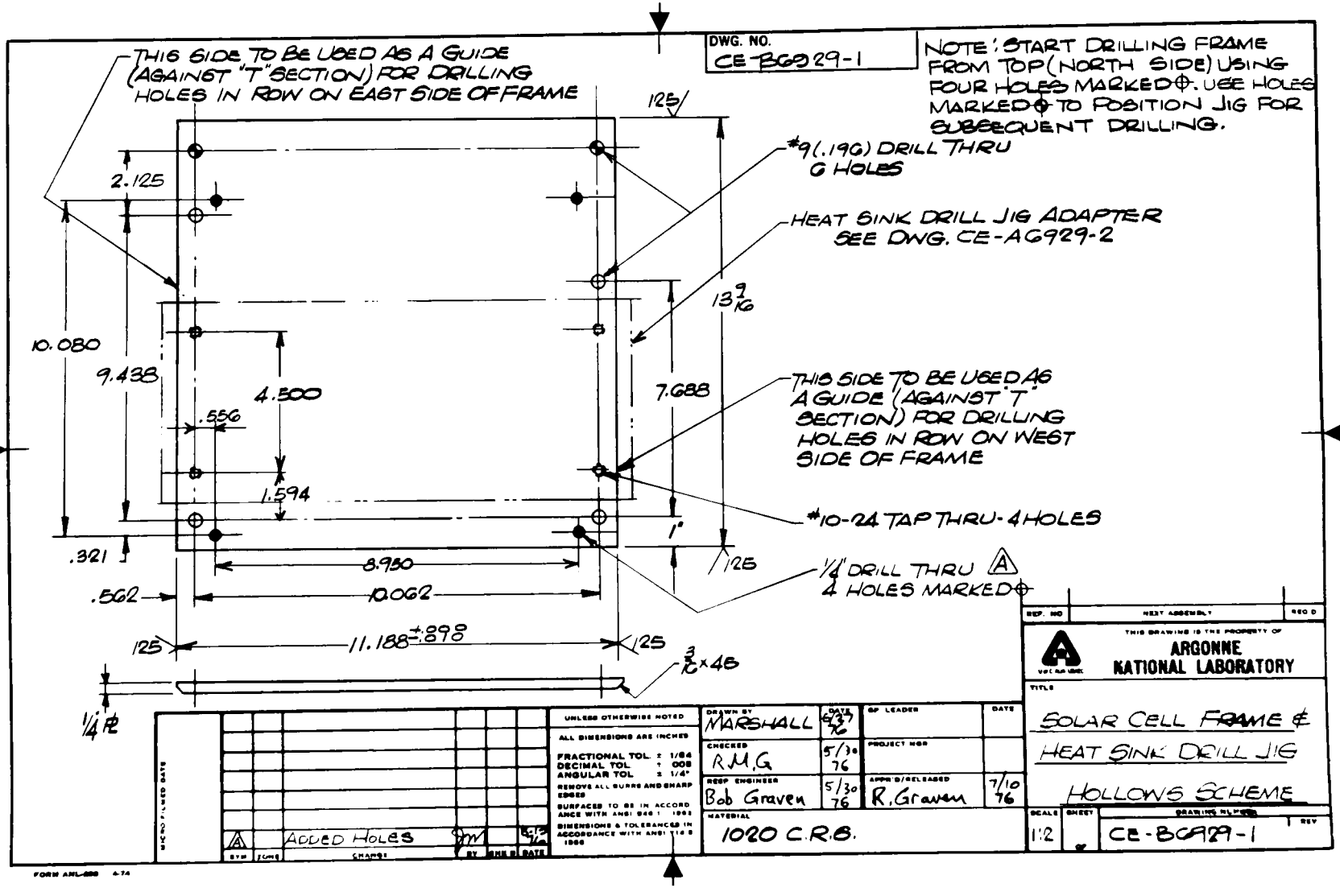
DWG. NO.
CE-BG929-1
NOTE: START DRILLING FRAME FROM TOP (NORTH SIDE) USING FOUR HOLES MARKED ⊕. USE HOLES MARKED ⊕ TO POSITION JIG FOR SUBSEQUENT DRILLING.
THIS SIDE TO BE USED AS A GUIDE (AGAINST "T" SECTION) FOR DRILLING HOLES IN ROW ON EAST SIDE OF FRAME
#9 (.196) DRILL THRU 6 HOLES
HEAT SINK DRILL JIG ADAPTER SEE DWG. CE-AG929-2
THIS SIDE TO BE USED AS A GUIDE (AGAINST T SECTION) FOR DRILLING HOLES IN ROW ON WEST SIDE OF FRAME
#10-24 TAP THRU - 4 HOLES
1/4" DRILL THRU (A) 4 HOLES MARKED ⊕
2.125
10.080
9.438
4.300
.556
1.594
.321
.562
8.950
10.062
11.188±.898
.125
13 9/16
7.688
1"
3/16 x 45
1/4 R
ADDED HOLES
UNLESS OTHERWISE NOTED
ALL DIMENSIONS ARE INCHES
FRACTIONAL TOL ± 1/64
DECIMAL TOL .008
ANGULAR TOL ± 1/4°
REMOVE ALL BURRS AND SHARP EDGES
SURFACES TO BE IN ACCORDANCE WITH ANSI B46.1 1962
DIMENSIONS & TOLERANCES IN ACCORDANCE WITH ANSI Y14.5 1966
DRAWN BY MARSHALL 6/27/76
CHECKED R.M.G 5/30/76
DESIGN ENGINEER Bob Graven 5/30/76
GP LEADER
PROJECT MGR
APPR'D/RELEASED R. Graven 7/10/76
MATERIAL 1020 C.R.S.
THIS DRAWING IS THE PROPERTY OF ARGONNE NATIONAL LABORATORY
TITLE
SOLAR CELL FRAME & HEAT SINK DRILL JIG HOLLOWS SCHEME
SCALE 1:2
SHEET
DRAWING NUMBER CE-BG929-1
REV

APPENDIX C

Tilt Adjustment Schedules

Tilt schedules for the prototype DCPC and hollow CPC panels are presented in this appendix. The DCPC panel, which has a theoretical half-angle of acceptance, $\theta_m = 9°$, requires ten adjustments per year for the six tilt positions shown in Table C-1. The minimum collection time is 7.14 hr/day, and the minimum time between tilt adjustments is 22 days. The maximum time between tilt adjustments is 77 days.

The hollow CPC panel, which has a theoretical half-angle of acceptance, $\theta_m = 6.25°$, requires 36 adjustments per year for the nineteen tilt positions shown in Table C-2. The minimum collection time is 7.0 hr/day, and the minimum time between tilt adjustments is four days. The maximum time between tilt adjustments is 22 days.

If different minimum collection times per day or different half-angles of acceptance should be specified, the tables would have to be recomputed.

Table C-1. Theoretical Tilt Schedule for DCPC Panel, $\theta_m = 9°$

Minimum Collection Time of 7.14 hr/day

Days After Winter Solstice	Latitude - Tilt (Degrees)
326-38	-27.2
39-61, 303-325	-19.9
62-90, 274-302	-9.0
91-119, 245-273	+9.0
120-143, 222-244	+19.9
144-221	+27.2

Table C-2. Theoretical Tilt Schedule for Hollow CPC Panel, $\theta_m = 6.25°$

Minimum Collection Time of 7 hr/day

Days After Winter Solstice	Latitude - Tilt (Degrees)
354-10	-29.2
11-16, 348-353	-28.6
17-22, 342-347	-27.8
23-28, 336-341	-26.7
29-34, 330-335	-25.3
35-42, 322-329	-23.3
43-52, 313-321	-20.5
53-64, 300-312	-16.3
65-81, 284-299	-10.0
82-100, 264-283	0.0
101-117, 247-263	+10.0
118-129, 235-246	+16.3
130-138, 226-234	+20.5
139-146, 218-225	+23.3
147-153, 211-217	+25.3
154-159, 206-210	+26.7
160-164, 200-205	+27.8
165-170, 194-199	+28.6
171-193	+29.2

APPENDIX D

Calculating Efficiencies and Scaling up of CPC Data to 1 kW/m^2 Direct Insolation

The performance of most photovoltaic panels can be measured at or scaled up to the equivalent of 1 kW/m^2 direct insolation. Flat panels can be illuminated evenly at 1 kW/m^2 with multiple light sources as at the NASA-Lewis Research Center, or can be tested outdoors with total insolation measured with a pyranometer. This is possible because flat panels accept all direct and diffuse radiation. To calculate efficiencies and to scale up outputs of focusing concentrators requires only a pyrheliometer to measure the direct insolation. Even for a focusing parabolic trough concentrator, which accepts light from a narrow north-south band, pyrheliometer data is a sufficient measure of insolation. The amount of diffuse radiation in that 1° or 2° wide band is usually insigificant. With any focusing concentrator, there is a question regarding how much circumsolar radiation is included in the pyrheliometer data.[23]

For nonimaging CPC's with moderate concentration ratios, a significant amount of diffuse radiation is collected, as well as all of the circumsolar and direct radiation. In order to compare data on modules in the two CPC panels and to calculate their efficiencies for light collection within their acceptance angles, one must calculate, from pyranometer and pyrheliometer insolation data, the total amount of sunlight (both direct and diffuse) within the acceptance angle of a collector.

Rabl[24] has shown that the total amount of sunlight within the acceptance angle of a CPC trough is given for CPC troughs.

$$\text{Accepted Insolation} = \text{"direct"} + \frac{1}{C}\,\text{diffuse},$$

where the term "direct" includes circumsolar as well as the direct beam, and C is the actual CPC geometric concentration ratio. This ratio is a characteristic of the concentrator. Unlike the geometric concentration ratios used in the text above, it does not involve the active areas of the photovoltaic cells. The diffuse light is not concentrated but merely collected; this collection efficiency depends only on the ratio of entrance aperture area to exit aperture area. For a DCPC trough, the index of refraction, n, of the concentrator must be considered and the accepted insolation is given approximately by (DCPC)

$$\text{Accepted Insolation} = \text{"direct"} + \frac{n}{C}\ \text{diffuse.}$$

The difference between total insolation as measured by a pyranometer and the "direct" insolation as measured by a pyrheliometer is the diffuse light, which is assumed to have a uniform distribution over the sky. Thus, the insolation within the acceptance angle of the reflective CPC units (C = 8.0) is given by

$$I_{CPC} = \text{"direct"} + \frac{1}{8.0}\ (\text{total} - \text{"direct"}).$$

The insolation accepted by the DCPC units (C = 9.2) is given by

$$I_{DCPC} = \text{"direct"} + \frac{1.49}{9.2}\ (\text{total} - \text{"direct"}).$$

For example, at a time when pyrheliometer and pyranometer readings are 865 W/m^2 and 985 W/m^2, respectively:

$$I_{CPC} = 865 + \frac{1}{8.0}\ (985 - 865)$$

$$= 880\ W/m^2$$

$$I_{DCPC} = 865 + \frac{1.49}{9.2}\ (985 - 865)$$

$$= 884\ W/m^2$$

These panel outputs could be scaled to 1 kW/m^2 direct insolation by the factors, 1.136 and 1.131, respectively.

In scaling up the output of the two panels to 1 kW/m^2 direct insolation, we have been quite conservative, scaling up only the current characteristics of the I-V plots. That is, we have used a linear scaling of power with insolation. If an assumption were made regarding the effect of increased insolation upon the voltage characteristics, the scaled panel output powers might be greater than the values given in the text.

APPENDIX E

I-R 100 Award

On September 23, 1976, one of three Industrial Research-100 (IR-100) awards awarded to Argonne National Laboratory by Industrial Research magazine was for the Dielectric Compound Parabolic Concentrator (DCPC). This award was shared with the University of Chicago. Industrial Research magazine works with a review committee to select the 100 most significant, new technical products each year and presents awards to the organizations that developed them. The award was presented at a banquet held in the main hall of the Museum of Science and Industry in Chicago. Dr. R. G. Sachs, Director of Argonne National Laboratory, received the award on behalf of ANL and the University of Chicago. An IR-100 display showing the main features of the DCPC module was on display at the museum during October 1976 for public viewing.

REFERENCES

1. A. Rabl et al, *"Use of Compound Parabolic Concentrator for Solar Energy Collection,"* Semi-Annual Progress Report for July-December, 1974, ANL-75-42.

2. R. M. Giugler et al, *"Compound Parabolic Concentrators for Solar-Thermal Power,"* Semi-Annual Progress Report for January-June, 1975, ANL-75-52.

3. G. Thodos, *"Predicted Heat-Transfer Performance of an Evacuated Glass-Jacketed CPC Receiver: Countercurrent Flow Design,"* May 1976, ANL-76-67.

4. R. O. Bell, J. L. T. Ho, W. Kurth, and T. Surek, *"Photovoltaic Engineering Services Pertinent to Solar Energy Conversion,"* prepared by Mobil-Tyco Solar Energy Corp. for Argonne National Laboratory under Subcontract No. 31-109-38-3171 (June 1975).

5. Spectrolab, Inc., *"Preliminary Evaluation of Two-Element Optical Concentrators for Use in Solar Photovoltaic Systems,"* June 30, 1975, ANL-K-75-3191-1.

6. R. Winston, *"Dielectric Compound Parabolic Concentrators,"* Applied Optics 15, 291 (1976); N. B. Goodman, R. Ignatius, L. Wharton, and R. Winston, *"On the Use of Solid-Dielectric Compound Parabolic Concentrators with Photovoltaic Devices,"* Applied Optics 15, 2434 (1976).

7. A. Gorski, R. Graven, W. McIntire, W. W. Schertz, R. Winston and S. Zwerdling, *"Novel Versions of the Compound Parabolic Concentrator for Photovoltaic Power Generation,"* presented at 12th IEEE Photovoltaic Specialists Conference, Baton Rouge, Louisiana, November 1976, to be published in Proceedings of 12th IEEE Photovoltaic Specialists Conference.

8. *"Silicon Solar Cell Module Performance Environmental Test and Inspection Requirements,"* Document 5-342-1, Jet Propulsion Lab, Pasadena, California (October 1975).

9. N. B. Goodman, R. Ignatius, L. Wharton, and R. Winston, *"On the Use of Solid-Dielectric Compound Parabolic Concentrators with Photovoltaic Devices,"* Applied Optics 15, 2434 (1976).

10. L. W. Butterworth and R. K. Yanul, *"Structural Analysis of Silicon Solar Arrays,"* Technical Report JPL-32-1528, Nasa Jet Propulsion Laboratory, Pasadena, California (May 1971).

11. E. L. Burgess, *"Photovoltaic Energy Conversion Using Concentrated Sunlight,"* SPIE Vol. 85, Optics in Solar Energy Utilization II (1976).

12. T. J. Peters and W. A. Voly, *"Design and Development of Lightweight Reflectors for Compound Parabolic Concentrator Solar Panels - Final Summary Point,"* Chamberlain Manufacturing Corp., prepared for Argonne National Laboratory (November 29, 1976).

13. A. Rabl, *"Optical and Thermal Properties of Compound Parabolic Concentrators, SOL-75-01,"* Argonne National Laboratory (February 1975).

14. S. Gross (Ed.), *"Modern Plastic Encyclopedia 1973-1974,"* Vol. 50, No. 10A (October 1973).

15. Measured extinction coefficient for acrylic sheet.

16. Electronics, *"Probing the News,"* 75 (June 12, 1975).

17. R. M. Moore, *"Cost Predictions for Photovoltaic Energy Sources,"* Solar Energy 18, 225-234 (1976).

18. Private communication with Mr. Mays, Rohm and Haas (December 3, 1976).

19. Private communication with Bruce Kleinert, Monsanto (December 15, 1976).

20. Private communication with Ron Bean, Alcoa.

21. Private communication with Rich Davit, Plastofilm Industries, Inc. (December 2, 1975).

22. American Science Center, Inc., Chicago, Catalog (1976).

23. Lawrence Berkeley Laboratory, presentation at ERDA Semi-Annual Review, Albuquerque, NM (January 27, 1977).

24. A. Rabl, Solar Energy 18, 93 (1976).

Distribution of ANL-77-42

Internal:

J. P. Ackerman
J. W. Allen
J. Barghusen
J. E. Battles
E. C. Berrill
L. Burris
F. A. Cafasso
A. A. Chilenskas
P. Cunningham
J. G. Eberhart
R. Elliott
W. Frost
E. C. Gay
A. Gorski
F. Hornstra
R. O. Ivins
A. A. Jonke
R. Kampwirth
G. M. Kesser
R. W. Kessie
D. Knox
V. M. Kolba
M. L. Kyle
W. Lark
S. Lawroski
N. Levitz
L. Link
A. E. Martin
J. H. Martin
R. G. Matlock
A. Melton
W. E. Miller
F. Mrazek
K. M. Myles
P. A. Nelson
E. G. Pewitt
E. R. Proud
A. Rabl
K. Reed
M. F. Roche
J. Royal
R. Rush
W. W. Schertz (200)
V. Sevcik
H. Shimotake
R. K. Steunenberg
C. Stevenson
A. D. Tevebaugh
Z. Tomczuk
W. D. Tuohig
D. R. Vissers
G. J. Vogel
S. Vogler
P. Walker
W. J. Walsh
A. Wantroba
D. S. Webster
I. Winsch
R. Winston
R. Yamartino
N. P. Yao
S. Zwerdling
A. B. Krisciunas
ANL Contract Copy
ANL Libraries (5)
TIS Files (6)

External:

ERDA-TIC, for distribution per UC-63 (225)
Manager, Chicago Operations Office
Chief, Chicago Patent Group
President, Argonne Universities Association
Chemical Engineering Division Review Committee:
R. C. Axtmann, Princeton U.
R. E. Balzhiser, Electric Power Research Inst.
J. T. Banchero, U. Notre Dame
D. L. Douglas, Gould Inc.
P. W. Gilles, U. Kansas
R. I. Newman, Allied-General Nuclear Services
G. M. Rosenblatt, Pennsylvania State U.
R. W. Allen, U. Maryland
B. N. Anderson, Total Environmental Action, Harrisville, NH
L. B. Anderson, Lockheed Palo Alto Res. Lab.
C. Backus, Arizona State U.
D. Baker, East Lansing, Mich.
M. D. Balcomb, Los Alamos Scientific Lab.
R. M. Banks, Lawrence Berkeley Lab.
C. S. Barnaby, Berkeley Solar Group
T. R. Beck, Electrochemical Technical Corp.
W. A. Beckman, U. Wisconsin
J. A. Belding, CONRT, USERDA
R. F. Boehm, U. Utah
P. Bos, Electric Power Research Inst.

K. W. Boer, U. Delaware
P. S. Bringham, Lawrence Berkeley Lab.
H. Buchberg, U. California, Los Angeles
E. Buzzelli, Westinghouse Electric Corp., Pittsburgh
R. Caputo, Altadena, Calif.
I. Catton, U. California, Los Angeles
B. T. Chao, U. Illinois
B. Chen, U. Nebraska
W. Christensen, Asst. for Energy Resources, The Pentagon
F. Cornford, Shuron Continental, Rochester
G. Cramer, Southern California Edison
J. E. Cummings, Electric Power Research Inst.
E. S. Davis, Jet Propulsion Lab.
F. DeWinter, Atlas Corp.
J. L. Douglas, Gould Inc.
K. Drumheller, Richland, Wash.
F. Dubin, Dubin-Mindell-Bloome, Assoc.
W. S. Duff, Colorado State U.
D. K. Edwards, U. California, Los Angeles
J. A. Eibling, Battelle Columbus Lab.
R. P. Epple, BES, USERDA
G. Ervin, Rockwell International
F. Fachat, Kaiser Aluminum & Chemical Corp.
E. A. Farber, U. Florida
R. L. French, Jet Propulsion Lab.
J. H. B. George, Arthur D. Little, Inc.
S. F. Gilman, State College, Pa.
B. Gopler, Scientific Applications, Inc.
J. C. Grosskreutz, Black and Veatch Consulting Engs.
Y. P. Gupta, E-Systems, Dallas
W. Hassenzahl, Los Alamos Scientific Lab.
H. R. Hay, Skytherm Processors Eng.
A. F. Hildenbrandt, U. Houston
J. E. Hill, National Bureau of Standards
A. S. Hirshberg, Jet Propulsion Lab.
R. M. Holdredge, Utah State U.
Dr. Jardine, Colorado Springs, Colo.
P. O. Jarvinen, Masschusetts Institute of Technology
A. Jenkins, Systems, Science and Software
P. E. Jenkins, Texas A & M U.
G. R. Johnson, Colorado State U.
H. Kausman, New York State Energy Research and Development Authority
P. A. Kittle, Rohm and Haas Co.
W. H. Klein, Smithsonian Institution
J. F. Kreider, Environmental Consulting Services, Boulder
F. Kreith, U. Colorado
Z. Lavan, Illinois Institute of Technology
Civil Engineering Laboratory, Naval Construction Battalion Center, Port Hueneme
Energy Resources Conservation and Development Commission, Sacramento
G. O. G. Lof, Colorado State U.
J. D. MacKenzie, U. California, Los Angeles
K. N. Marshall, Lockheed Research Lab.
D. K. McDaniels, U. Oregon
J. McKeown, Jr. AC, USERDA

M. Merriam, U. California, Berkeley
A. C. Meyers, Technical Environmental Resources Research Associates, Ames
C. Miller, Chamberlain Mfg. Corp., Waterloo
J. E. Minardi, U. Dayton
F. H. Morse, U. Maryland
P. W. B. Niles, Calif. Polytechnic State U.
M. C. Noland, Midwest Research Inst.
F. Notaro, Union Carbide Corp., Tonawanda
P. G. Pabil, PPG Industries, Inc., Pittsburgh
B. A. Phillips, Phillips Engineering Co., St. Joseph
J. W. Ramsey, Honeywell, Inc., Minneapolis
D. R. Reese, Wyle Laboratories, Huntsville
G. T. Reynolds, Princeton U.
R. K. Sakhuja, Thermo Electron Corp. R & D Center, Waltham
A. T. Sales, Georgia Inst. Technology
R. L. San Martin, New Mexico State U.
H. J. Schwartz, NASA Lewis Research Center
R. I. Schoen, National Science Foundation
M. K. Selcuk, Jet Propulsion Laboratory
C. Sepsy, Ohio State U.
A. M. Severson, Minneapolis, Minn.
F. F. Simon, NASA Lewis Research Center
R. H. Smith, Solergy, San Francisco
D. L. Spencer, U. Iowa
O. Stephens, General Electric Co., Bellevue, Ohio
E. Streed, National Bureau of Standards
M. Telkes, U. Delaware
E. Thomas, International Silver Co., Meriden
L. Topper, National Science Foundation
L. Vant-Hull, U. Houston
H. Volkin, Los Alamos Scientific Lab.
M. Wahlig, Lawrence Berkeley Lab.
L-C. Wen, Jet Propulsion Lab.
D. H. White, U. Arizona
R. Williams, Georgia Inst. Technology
J. W. Williamson, Vanderbilt U.
M. Wolf, U. Pennsylvania
J. I. Yellot, Arizona State U.
K. Collier, U. Maryland
A. Heller, Bell Telephone Labs.
B. L. Youtz, Olympia, Wash.
B. Shelpuk, RCA Corp., Camden
D. Ludwig, Intertech Corp.
L. T. Fan, Kansas State U.
R. Humphries, NASA Marshall Space Flight Center
D. Moeller, Sun Trac Corp., Wheeling, Ill.
P. Call, Solar Energy Research Inst.
C. Mahrok, General Services Administration
C. E. Bond, U. Illinois
G. Thodos, Northwestern U.
R. Ashby, Ministry of Mining & Natural Resources, Kingston, Jamaica
P. I. Cooper, C.S.I.R.O., Victoria, Australia
R. L. Datta, Central Salt and Marine Chemicals Research Inst., Bhavnagar, India
R. V. Dunkle, C.S.I.R.O., Victoria, Australia

J. C. Francken, U. Groningen, The Netherlands
J. T. E. Gilbert, Commission for The Environment, Wellington North, New Zealand
N. K. Gopalkrishnan, Tata Energy Research Inst., Bombay, India
M. C. Gupta, Indian Inst. Technology, Madras, India
K. G. Hollands, U. Waterloo, Canada
C. J. Hoogendorn, Technical U. Delft, The Netherlands
R. Kersten, Philips Forschungslaboratorium Aachen GmbH, Aachen, W. Germany
K. Kimura, Waseda University, Tokyo, Japan
V. Korsgaard, Technical U. Denmark, DK-2800 Lyngby
T. A. Lawland, McGill University, Canada
R. N. Morse, C.S.I.R.O., Victoria, Australia
J. Mustoe, London, England
Y. Nakajima, Kojakuin U., Tokyo
K. S. Ong, U. Malaya, Kuala Lampur
D. Proctor, P.O.B. 26, C.S.I.R.O., Victoria, Australia
W. R. Read, C.S.I.R.O., Victoria, Australia
A. Roy, U. Negev, P.O.B. 2053, Beer-Sheva, Israel
K. Saito, Osaka Inst. Technology, Osaka, Japan
B. Sesolis, U. Paris, France
H. Tabor, The Scientific Research Foundation, Jerusalem, Israel
F. Trombe, Laboratoire de l'Energie Solaire, Font Romen, France
R. Bruno. Philips Forschungslaboratorium Aachen, GmbH, Germany
W. W. S. Charters, U. Melbourne, Victoria, Australia
Salah El-Ein Hedayat, Minister of State for Research and Development, Cairo, Egypt
R. Rigopoulos, U. Patras, Greece